CHALMERS

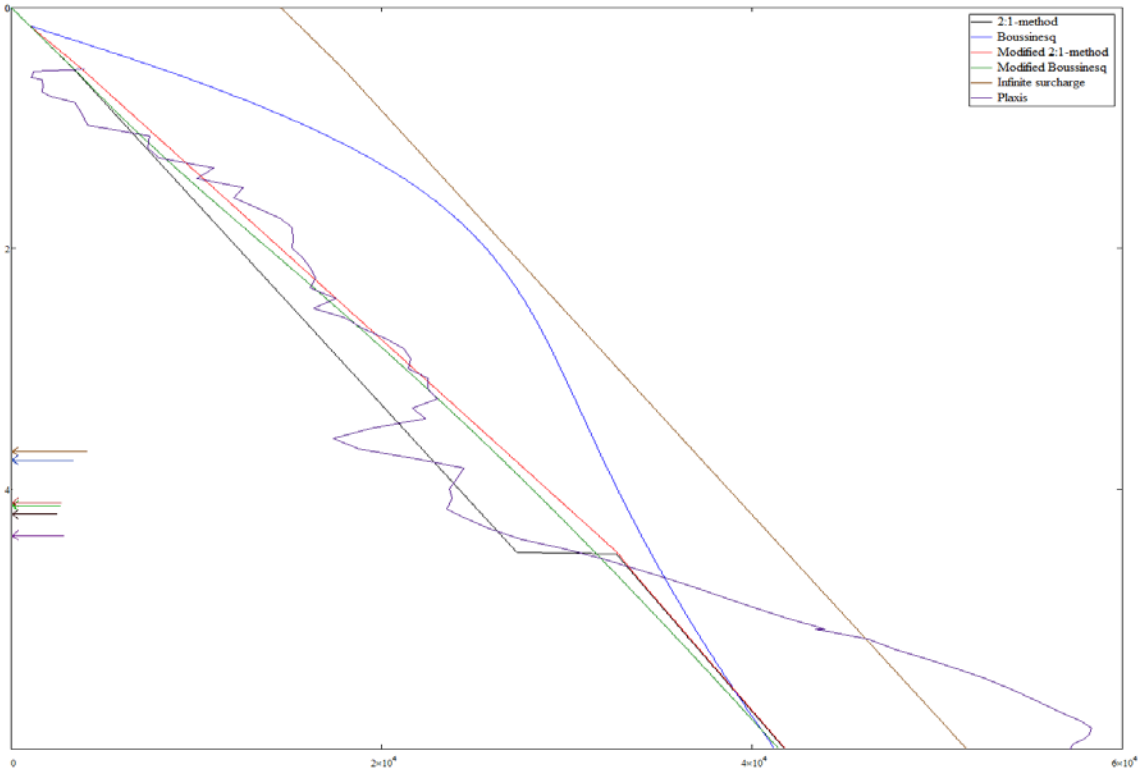

In depth study of lateral earth pressure

A comparison between hand calculations and PLAXIS

Master of Science Thesis in the Master's Programme Geo and Water Engineering

MATTIAS PETERSSON
MATHIAS PETTERSSON

Department of Civil and Environmental Engineering
Division of Geo Engineering

Geotechnical Engineering Research Group

CHALMERS UNIVERSITY OF TECHNOLOGY
Göteborg, Sweden 2012
Master's Thesis 2012:69

MASTER'S THESIS 2012:69

In depth study of lateral earth pressure

A comparison between hand calculations and PLAXIS

Master of Science Thesis in the Master's Programme Geo and Water Engineering

MATTIAS PETERSSON

MATHIAS PETTERSSON

Department of Civil and Environmental Engineering
Division of Geo Engineering
Geotechnical Engineering Research Group
CHALMERS UNIVERSITY OF TECHNOLOGY

Göteborg, Sweden 2012

In depth study of lateral earth pressure
A comparison between hand calculations and PLAXIS

Master of Science Thesis in the Master's Programme Geo and Water Engineering

MATTIAS PETERSSON
MATHIAS PETTERSSON

Examensarbete / Institutionen för bygg- och miljöteknik,
Chalmers tekniska högskola 2012:69

Department of Civil and Environmental Engineering
Division of GeoEngineering
Geotechnical Engineering Research Group
Chalmers University of Technology
SE-412 96 Göteborg
Sweden
Telephone: + 46 (0)31-772 1000

Cover:
Graph showing the different earth pressure models studied and the corresponding lateral earth pressure.

Chalmers Reproservice
Göteborg, Sweden 2012

In depth study of lateral earth pressure

A comparison between hand calculations and PLAXIS

Master of Science Thesis in the Master's Programme Geo and Water Engineering

MATTIAS PETERSSON

MATHIAS PETTERSSON

Department of Civil and Environmental Engineering

Division of Geo Engineering

Geotechnical Engineering Research Group

Chalmers University of Technology

ABSTRACT

In the field of geotechnical engineering there are several ways of calculating the horizontal pressures on retaining structures as well as a number of different methods of calculating how the stresses from a surcharge is distributed in the soil. For some of these methods the position of the resulting thrust on the retaining structure is unclear.

In Eurocode there are no clear guidelines on which methods that should be used. The aim of this master thesis is to investigate these methods and try to conclude which are the most suitable for a certain situation.

A conceptual model was made which was used for the different hand calculation methods, Rankine, Boussinesq, Coloumb, Culmann as well as for finite element calculations.

The results show that there is a clear difference between the load distribution methods in location of thrust, magnitude of thrust and therefore also in magnitude in bending moment. Sensitivity analyses indicate also that when the load is in the vicinity of the retaining wall the methods give approximately the same result in thrust. Further away from the retaining wall, the choice of distribution method becomes more important.

Comparing the pressure profiles between hand calculations to the FEM-program PLAXIS shows that the distribution is not interpreted in the same way. However, the resulting values still become relatively equal.

The difference between hand calculation methods could be reduced by adding a new η-value that concerns the ratio between self-weight and surcharge or one that affects each earth distribution method differently depending on how conservative it is.

Key words: Rankine, Coulomb, Boussinesq, Culmann, Lateral earth pressure, Earth pressure coefficient

Contents

Preface

In this thesis a number of different hand calculation models have been compared to the results of finite element model software. The work has taken place at Chalmers University of Technology and at REINERTSEN's head office in Gothenburg. Claes Alén at Chalmers Geotechnical Research Group and Nicholas Lusack from REINERTSEN have been supervising the project. Additional help and guidance with finite element modelling has been provided by Mats Olsson and Anders Kullingsjö at Chalmers.

Gothenburg May 2012

Mattias Petersson & Mathias Pettersson

Notations

Roman upper case letters

E	Young's modulus
G	Shear strength modulus
H	Wall height
K_0	Coefficient of at rest pressure
M_x	Moment around x-axis
P_a	Active thrust
P_{tot}	Total thrust
X_d	Variable notation for something
X_{mean}	Variable notation for something

Roman lower case letters

c'	Cohesion
q	Uniform surcharge
u	Pore pressure
z	Depth
z_w	Depth to water table

Greek upper case letters

α	Angle of wall inclination
α_f	Angle of failure plane
β	Angle of ground slope
δ	Angle of wall friction
ϵ	Strain
υ	Poisson's ratio
σ_0	Total vertical stress in the soil
σ'_0	Effective stress in the soil
σ'_1	Primary stress
σ'_3	Tertiary stress
σ'_a	Effective active pressure
σ'_h	Effective horizontal stresse
σ'_p	Effective passive pressure
σ'_v	Effective vertical stress
σ_{pn}	Passive pressure normal to the wall
τ_f	Shear strength

ϕ	Internal friction angle of soil
ψ	Dilatancy angle

Greek lower case letters

γ	Soil weight
γ_d	Partial factor depending on safety factor
γ_M	Partial factor found in the national options
η	Factor from Eurocode

1 Introduction

1.1 Background

In Södertälje a railroad bridge has been designed where there has been discussion around what calculation methods to use to retrieve the lateral earth pressure on a retaining wall. It is from this discussion that this master thesis has been inspired.

When designing a retaining structure, different standards recommend different calculation methods for load distribution, such as Culmann's graphical method, the 2:1-method or Boussinesq's. However the position of the resultant is not given by these methods. The design of the retaining structure is highly dependent on where the position of the resultant is since it changes the maximum bending moment of the structure.

1.2 Aim

The aim of this master thesis is to investigate and compare common calculation methods for modeling of soil pressure to give a conclusion on which methods are suitable during certain circumstances. In addition to this, the thesis will also evaluate and compare two FEM programs, ADINA and PLAXIS. PLAXIS is today the most commonly used finite element method (FEM) software in the geotechnical engineering area and is often considered to give the most accurate results. ADINA is a more general FEM software and can be applied to several fields of engineering. Therefore a comparison between the two is interesting.

To be able to evaluate the methods a literature study will be performed which will also result in a summary of the current regulations and norms considering earth pressure.

1.3 Method

A literature study within each calculation method will be performed. A conceptual model will be constructed and the different methods will be used to determine the lateral earth pressure in the model. The results from calculations will be the basis for the discussion. Different exercises and a literature study will be done to be able to apply PLAXIS and ADINA into the project.

1.4 Delimitations and assumptions

No partial factors have been used for soil strength or surcharges. This is motivated by the fact that this will lead to the same percental change of the resultant forces for the different methods and does not help in the evaluation of them. In this analysis of different methods frictional materials with drained conditions have been investigated.

In the Södertälje project front fill is used in front of the wall but in this thesis the front fill has been excluded since it does not contribute to the evaluation of the different calculation methods.

The earth pressure that is being evaluated is the lateral earth pressure that act upon the vertical segment of the cantilever wall. In some of the calculation methods, such as PLAXIS, the inclination of the wall has been neglected. This simplification has been made to reduce the risk of low quality mesh.

2 Norms

2.1 Eurocode summary

2.1.1 Geotechnical category and safety class

As in the Swedish standard BKR, the geotechnical category decides the extent of the needed investigations. The decision on which geotechnical category to use, is made considering the risk of failure and the risk of personal injuries.

As well as the geotechnical category the safety class remains, however it is due to the national options. It does not consider the material properties as it did in BKR, but refers, in Eurocode, to the unfavorable geotechnical loads. The safety class reduces the impact of the load the lower class which is used, see Table 1.

Table 1 Safety class values in Eurocode.

SC	γ_d
1	0.83
2	0.91
3	1.00

2.1.2 Design values

There are several methods that can be used according to Eurocode:

- Analytical models – use of partial factors, such as Coulomb.
- Semi-empirical models – use of partial factors.
- Numerical models, for example PLAXIS.
- Experienced measures.
- Tests by loading and modeling.
- Observational method.
- Probability based methods.

When deciding the material properties, they should be derived from geotechnical investigations which are modified in correlation to the liquid limit, the overconsolidation ratio and the plasticity index. The mean value of the data shall be adjusted with the national options factor eta, η, to decide the characteristic value of a parameter. To increase the safety margin, the characteristic value is also adjusted by γ_M, a partial factor that can be found in the national options (Geoteknik, 2010). When a low design value results in the worst case scenario equation 2.1 should be used or if a high value is more critical, use equation 2.2.

$$X_d = \frac{\eta \cdot X_{mean}}{\gamma_M} \tag{2.1}$$

$$X_d = \eta \cdot X_{mean} \cdot \gamma_M \tag{2.2}$$

The factor eta, η, depends on the extent of the geotechnical investigation and also the geometry of the geo construction. A large geotechnical field investigation with wisely chosen probe holes is rewarded with a higher safety factor. The result could be a shorter sheet pile wall and therefore an economical cost saving.

The factor eta is divided into several sub factors, see equation 2.3. For retaining walls the sub factors can be combined.

$$\eta = \eta_1 + \eta_2 + \eta_3 + \eta_4 + \eta_5 + \eta_6 + \eta_7 + \eta_8 \quad (2.3)$$

- η(1,2,3,4) Factors that consider site investigation:

η_1 The properties natural variation.

η_2 Number of independent investigation points.

η_3 Uncertainty related to the soil properties.

η_4 The geo constructions vicinity to the investigation points.

The factors depend on the extent of the field investigation, the spread and number of probe holes, the spread of the results and if the values correspond to empirical values. A probe hole that can be included should be within ten meters from the retaining wall or within the horizontal line made by a 45 degrees slope from the foot of the wall. A normal value for $\eta_{(1,2,3,4)}$ is 0.95 when an average ground investigation has been performed but $\eta_{(1,2,3,4)}$ may vary between 0.6 to 1.05.

- η(5, 6) Factors concerning the geometry of the geo construction:

η_5 The ratio of the ground that governs the behavior of the geo construction in the current limit state.

η_6 The ability of the geo construction to transfer loads from weak to strong parts of the soil.

For η_5 and η_6 the geometry of the construction is governing. If a local weak spot of the soil cannot be distributed by the retaining wall a low value should be chosen, normally 0.85. In comparison with good abilities to distribute the pressure the value 1.15 can be chosen.

η_7 Type of failure (brittle or ductile failure). Since the normal case is a ductile failure, it is given the value 1.0. For example when a layer or pore pressure can create a slip surface or if quick clay is present a lower value should be used.

η_8 The parameters importance compared to other load or resistance parameters. For frictional materials where tan Φ is of less importance, e.g. frictional soils with high pore pressures, a higher value may be used, maximum of 1.15.

η may not exceed 1.2

There are several ultimate limit states to consider (Standardization, 2004):

- EQU: loss of equilibrium of the structure or the ground. Strengths in materials and the ground are irrelevant in providing resistance e.g. foundation bearing on rock.
- STR: Internal failure or excessive deformation of the structure or structural elements. Strengths in materials are of importance in providing resistance.

- GEO: Internal failure or excessive deformation of the ground, in which strength of rock and soil is of importance in providing resistance.
- UPL: Vertical actions or water pressure that results in loss of equilibrium of the structure.
- HYD: hydraulic gradients that leads to heave, erosion and piping.

2.1.3 Ultimate limit state

The limit states decide different verifications needed for a safe structure. Eurocode's design approach determines which combinations of equations and factors to be used in that process. When designing retaining structures design approach number 3 (DA3) should be used, see Table 2. When designing piles DA2 is the correct approach.

Table 2 How to chose factors according to design approach 3.

DA3	Action loads	Soil parameters	Resistance
Factor	1(structural) 2(geotechnical)	2	3

For the resisting soil the surface level should be reduced when designing in the ultimate limit state. The amount is decided by the extent of the field investigation. For a "normal" extent the values decided by Eurocode are (Standardization, 2004):

- Cantilever wall: 10% of wall height above excavation level. Maximum 0.5 m.
- Supported wall: 10% of the distance between excavation level and lowest support. Max 0.5 m.
- 0-10% when surface level is certain to be correct during construction. The reduction is increased if the level is very uncertain.

When determining the earth pressure there is factors that should be considered:

- The surcharge and slope of the ground surface.
- The inclination of the wall to the vertical.
- Water table and seepage forces in ground.
- The amount and direction of the movement of the wall relative to the ground.
- Equilibrium: vertical and horizontal.
- The shear strength.
- The density of the ground.
- Rigidity of structural elements.
- Roughness of wall.

The earth pressure coefficient at rest is calculated as below if the surface is horizontal, or modified according to equation 2.5 if the ground is inclined.

$$\boldsymbol{K_0 = \left(1 - sin(\varphi') \cdot \sqrt{OCR}\right)} \tag{2.4}$$

$$\boldsymbol{K_{0,\beta} = K_0 \cdot (1 + sin(\beta))} \tag{2.5}$$

The resulting force should always be assumed to be parallel to the ground surface when the soil pressure is at rest (Standardization, 2004).

Backfill behind the wall shall be considered, also the procedure of compaction. Normally, only the upper part of the wall is affected by the additional stress by backfill and only when there is lateral yielding (Whitlow, 2001).

2.1.4 Serviceability limit state

Characteristic values shall be used in calculations for permanent surcharge and earth pressure. The value of eta, η, can differ from 1.0 in the defining of the characteristic value from the mean value.

3 Earth pressure - theories

Earth pressure is the force exerted by the soil in any direction, analogous with water pressure, on its surroundings. What this report will focus on is how the vertical earth pressure, both from self-weight and surcharges, is distributed in the soil and converted into lateral earth pressure, as illustrated in Figure 1.

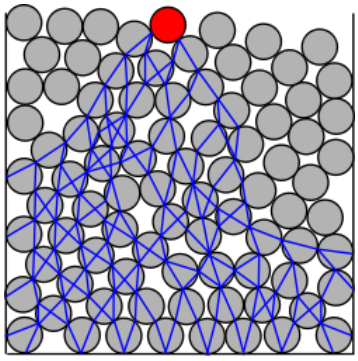

Figure 1 Stress distribution in soil

Earth pressure is determined by a number of factors, the weight of the soil, type of soil, depth of water table, soil depth and ground slope.

The effective stress principle which is one of the fundamental equations for soil mechanics is:

$$\sigma_0 = \sigma'_0 + u \tag{3.1}$$

where σ_0 is the total stress, σ'_0 is the effective stress and u is the pore pressure. The effective stress is the stress that is carried by the solid particles in the soil mass.

As listed earlier one of the contributors to the stress in the soil is the self-weight. The equation for vertical stress due to self-weight without any pore pressure is:

$$\sigma'_0 = z \cdot \gamma \tag{3.2}$$

To calculate the pore pressure for hydrostatic conditions equation 3.3 can be used, see Figure 2 for definitions.

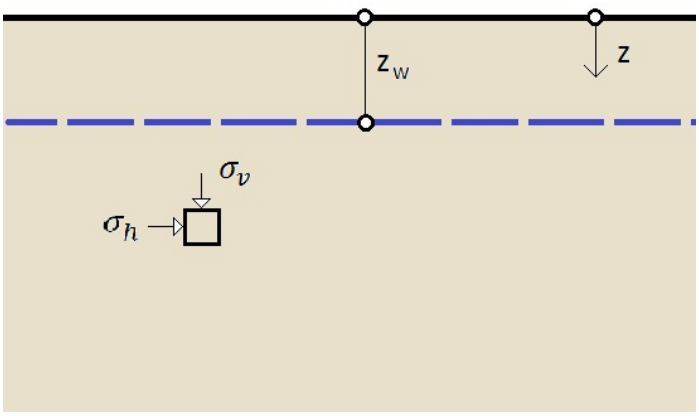

Figure 2 Definitions in soil mechanics

$$u = (z - z_w)\gamma_w \tag{3.3}$$

To obtain the horizontal stresses the coefficient of earth pressure is used:

$$K = \frac{\sigma'_h}{\sigma'_v} \tag{3.4}$$

There are three different coefficients depending on what state the soil is in; K_0, K_a and K_p which are the at rest, fully mobilized active- and passive pressures respectively.

3.1 Rankine theory

Rankine theory describes the soil failure as a so called zone failure (Sällfors, 2001). This means that the entire soil body is in failure, see Figure 3. For the active failure this gives failure surfaces with the angle 45+ ϕ /2 to the horizontal plane. And for the passive failure the angle is instead 45- ϕ /2.

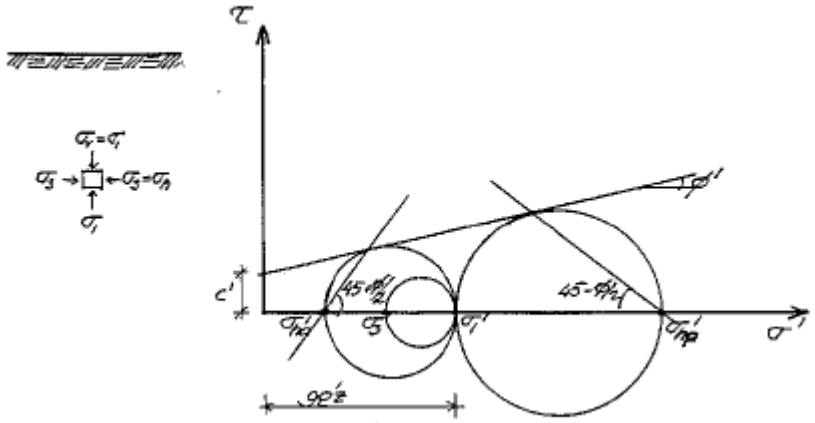

Figure 3 Mohr's circles at failure

For a smooth wall (i.e. no wall friction) the active and passive pressures are expressed differently depending on the type of soil. For a cohesive material the horizontal pressure, when there is no ground slope and q is a uniform semi-infinite surcharge, can be calculated according to:

$$\sigma'_a = (\sigma'_{v0} + q)K_a - 2c'\sqrt{K_a} \tag{3.5}$$

$$\sigma'_p = (\sigma'_{v0} + q)K_p + 2c'\sqrt{K_p} \tag{3.6}$$

For a frictional material, soils that are characterized by being independent of cohesion, the last term of the horizontal stress equation above is excluded. This means that the failure envelope starts in the origin instead of at c' on the y-axis. Sometimes also normally consolidated clays can be calculated as a frictional material without the cohesive factor. The equations are thus simply:

$$\sigma'_a = (\sigma'_{v0} + q)K_a \tag{3.7}$$

$$\sigma'_p = (\sigma'_{v0} + q)K_p \tag{3.8}$$

The earth pressure coefficient K_a and K_p do not differ between the different types of soil, unless they have different friction angles. This is because it is the only variable term in the equation for the earth pressure coefficient, since Rankine does not

consider the roughness of the wall, the inclination of the wall or the ground slope for the equations below:

$$K_a = tan^2\left(\frac{\pi}{4} - \frac{\phi'}{2}\right) \tag{3.9}$$

$$K_p = \frac{1}{K_a} = tan^2\left(\frac{\pi}{4} + \frac{\phi'}{2}\right) \tag{3.10}$$

If the earth pressure equation for cohesive material is studied more closely it can be seen that the active pressure would have a negative value down to the depth where $(\sigma'_{v0} + q)K_a > 2c'\sqrt{K_a}$. This would mean that there is an tensile stress applied to the wall down to the depth z. Because of this it is advisable to be careful when choosing a value for c' (often set to 0).

Since cohesive materials are very dense, water can be standing in cracks near the structure, which is why water pressure is assumed from the top of the wall. The depth to where tensile cracks can occur can be calculated by:

$$z = \frac{1}{\gamma'}\left(\frac{2c'}{\sqrt{K_a}} - q\right) \tag{3.11}$$

If the geometry contains sloping backfill, Rankine assumed the wall friction angle to be the same as the ground slope angle. The stress resultant on the side of an element acts parallel to the ground, so the actual horizontal stress has to be derived as a component of the resultant. If the ground is horizontal, Rankine assumes that there is no wall friction. However, the wall friction is of utmost importance since it effects the direction of the lateral thrust as well as the magnitude, see Figure 4. With these assumptions the coefficient of active pressure can be written as:

$$K_a = \frac{X_a}{\sigma_v} = \frac{X_a}{\gamma' z} \tag{3.12}$$

$$X_a = \sqrt{(\sigma_h^2 + \tau_a^2)} \tag{3.13}$$

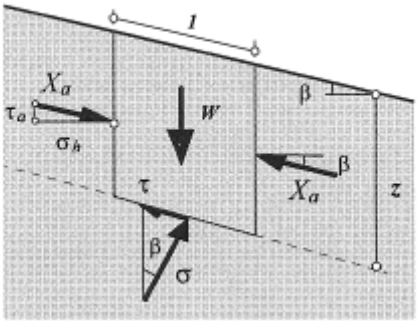

Figure 4 Sloping backfill and direction of thrust (azizi)

By using the Mohr's circle representation the quantities from these equations can be found:

$$K_a = \cos\beta \frac{\cos\beta - \sqrt{\cos^2\beta - \cos^2\phi'}}{\cos\beta + \sqrt{\cos^2\beta - \cos^2\phi'}} \tag{3.14}$$

$$K_p = \cos\beta \frac{\cos\beta + \sqrt{\cos^2\beta - \cos^2\phi'}}{\cos\beta - \sqrt{\cos^2\beta - \cos^2\phi'}} \tag{3.15}$$

The resultant thrusts acting parallel to the slope of the backfill on the vertical wall is thus:

$$P_a = \frac{1}{2} \cdot \gamma \cdot H^2 \cdot K_a \tag{3.16}$$

$$P_p = \frac{1}{2} \cdot \gamma \cdot H^2 \cdot K_p \tag{3.17}$$

3.2 Coulomb failure theory

The Mohr-Coulomb failure theory illustrates the limiting values for active and passive pressure for a certain soil condition. The method requires the stresses σ_1 and σ_3 (σ_v and σ_h) on an element to describe the Mohr circle, see equation 3.19. Common triaxial tests to shear failure may be used to decide these parameters, since in a test the major and minor stresses are known. Also the cohesion, the internal friction angle and effective normal stresses are required in order to describe the failure envelope, the Coulomb equation, see equation 3.18. Inserted in the Mohr circle together with the slip surface angle, α_f, multiplied by two, the shear strength can be decided, see figure

1.

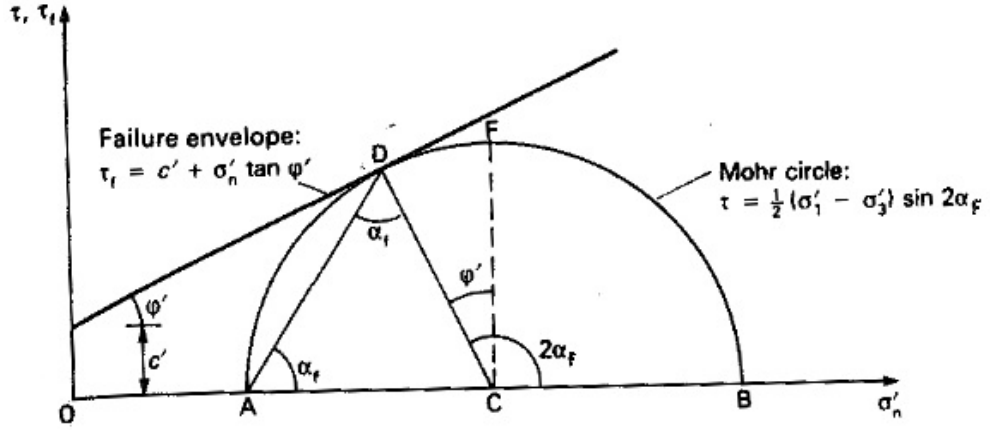

Figure 5 The Mohr-Coulomb failure diagram.

$$\tau_f = c' + \sigma_n' \cdot tan(\varphi') \tag{3.18}$$

$$\tau_f = \frac{1}{2} \cdot (\sigma_1' - \sigma_3') \cdot sin(2 \cdot \alpha_f) \tag{3.19}$$

The Coulomb theory is defined as an elastic – perfectly plastic model. Until the stress path has tangented the failure envelope, no plastic deformation follow; only elastic. Specific for the Coulomb failure theory, is that the hardening constant is not used. Hence no expansion of the yield surface occurs (Kullingsjö, 2007). If the soil is described as an elastic material, the deformation will depend only on the total change in load (surcharges, excavations). A scenario that is false since soils are elasto-plastic, which is why the stress paths are important. In other words, the order of loading and unloading is important to a soil mass which decides for example which modulus to use in calculations (Whitlow, 2001).

A disadvantage of the Coulomb failure theory is that it does not take volume change into account. That means that even if the soil mass is compacted due to loading, it will not apply the increase in the soil strength, as shear stress, by the compaction (Whitlow, 2001).

The method calculates a straight slip surface, where the body that rotates is rigid (Kullingsjö, 2007). The assumed slip surface for the passive side is distinctly different compared to the actual case, an error that results in an overestimation of the passive side's resistance, see Figure 6.

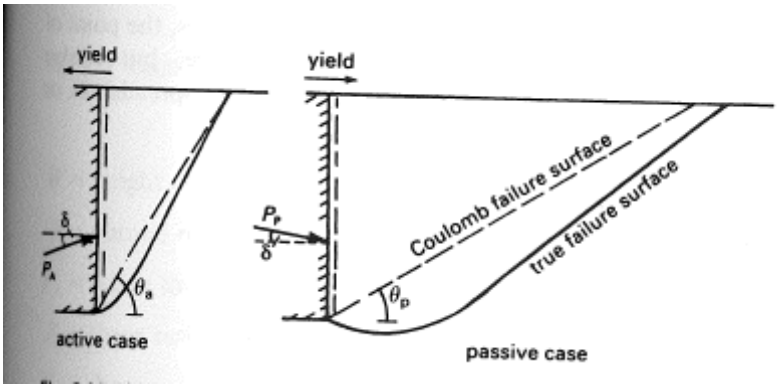

Figure 6 Coloumb slip surface

The assumed straight slip surface on the active side has a negligible error. To adjust the underestimation of slip surface in the first case several methods has arisen; the most common is Caquot and Kerisel.

Comparing Mohr-Coulomb with the Rankine theory, one difference is the boundary conditions. An upper bound solution is used, which means that the passive pressure is overestimated and at the same time that the active pressure is underestimated for the Mohr-Coulomb theory (Azizi, 2000). The distribution from vertical to horizontal stress is calculated by:

$$\sigma_h' = \gamma' \cdot z \cdot K \tag{3.20}$$

Where:

$$K_a = \frac{sin^2 \cdot (\alpha + \varphi')}{sin^2(\alpha) \cdot sin(\alpha - \delta) \cdot \left[1 + \sqrt{\frac{sin(\varphi' + \delta) \cdot sin(\varphi' - \beta)}{sin(\alpha - \delta) \cdot sin(\alpha + \beta)}}\right]^2} \tag{3.21}$$

$$K_p = \frac{sin^2 \cdot (\alpha - \varphi')}{sin^2(\alpha) \cdot sin(\alpha + \delta) \cdot \left[1 - \sqrt{\frac{sin(\varphi' + \delta) \cdot sin(\varphi' + \beta)}{sin(\alpha + \delta) \cdot sin(\alpha + \beta)}}\right]^2} \tag{3.22}$$

Where α is the inclination of the wall in relation to the vertical, β the ground slope, φ' is the internal friction angle and δ the inclination of the friction resultant between wall and soil.

The wall friction angle, δ, is commonly set to $\frac{2}{3}\varphi'$ for active pressure and $\frac{1}{2}\varphi'$ for passive pressure or maximum 20 degrees if it exceeds it (Whitlow, 2001).

3.3 Boussinesq theory

Unlike Coulomb and Rankine theory, Boussinesq assumes a non-linear failure surface, as compared in Figure 7. This is closer to the actual failure surface and makes the model less conservative.

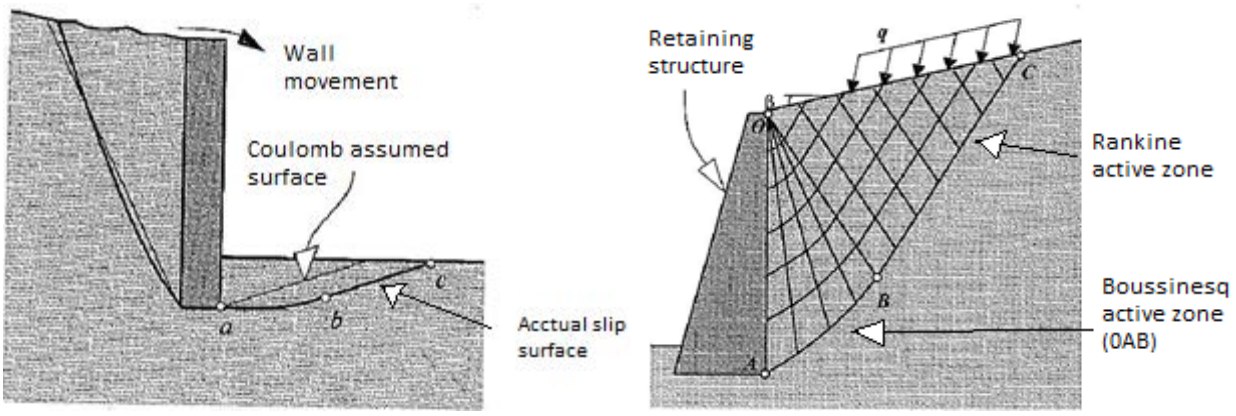

Figure 7 Boussinesq non-linear slip surface

Boussinesq theory considers three independent contributors to the lateral earth pressure (Azizi, 2000):

- The self-weight of a cohesionless soil
- The pressure induced by a surcharge on a weightless cohesionless soil
- The pressure from a cohesive, weightless soil

The self-weight of the slip surface is determined to be able to calculate the earth pressure coefficient for that specific wedge. However, numerical solutions have been made by Caquot and Kersiel in 1948, meaning that the calculation of K_a and K_p is excluded and can be found in tables (Azizi, 2000).

To calculate the additional lateral thrust from a uniform surcharge with infinite extent the surcharge load is multiplied by K'_a or K'_p, see equation 3.23 and 3.24. As with the values of K_a and K_p the coefficiens for calculation of the pressure from a uniform semi-infinite surcharge has been evaluated numerically and assembled in tables.

$$\sigma_a = K'_a \, q \tag{3.23}$$

$$\sigma_p = K'_p \, q \tag{3.24}$$

Boussinesq considered cohesive soils to act like frictional soils. To simulate the cohesion, a normal stress is applied through the expression:

$$c' \cdot \cot \phi' \tag{3.25}$$

In the general case with a retaining wall that has an angled back and with a sloping backfill the active pressure due to cohesion normal to the wall is (Azizi, 2000):

$$\sigma_{an} = -c' \cdot cot\phi'(1 - K'_a \cdot \cos \delta) \tag{3.26}$$

Where K'_a is given from the same table as for the pressure due to a uniform surcharge. This gives the shear stress along the wall:

$$\tau = c' \cdot cot\phi' \cdot K'_a \cdot sin\,\delta \tag{3.27}$$

The addition to the passive pressure from a surcharge is derived in the same way as the active and the equation for it is:

$$\sigma_{pn} = c' \cdot cot\phi'\left(K'_p \cdot cos\,\delta - 1\right) \tag{3.28}$$

Strip loads can be used to simulate stresses from railroads, which has a small width but are elongated, see Figure 8. There are two assumptions made, the soil is elastic and the wall is stiff (Azizi, 2000). The stiffness of the wall is done by reflecting the load on an equivalent distance from the wall, hence the doubling of the equation, see equation below (Whitlow, 2001). The angle $\propto$ and β are expressed in radians.

$$\sigma'_h = 2 \cdot \frac{q}{\pi}(\beta - sin(\beta) \cdot cos(\beta + 2\alpha)) \tag{3.29}$$

There is also an equation for the vertical stresses due to a strip load:

$$\Delta\sigma_z = \frac{q}{\pi}[\beta + sin\,\beta\, cos(\beta + 2\alpha)] \tag{3.30}$$

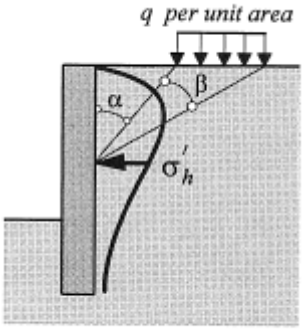

Figure 8 Load distribution from a strip load

3.4 Culmann's graphical method

Karl Culmann created in 1866 a graphical method to obtain the active pressure on a retaining wall as well as the critical (linear) slip surface (Varghese, 2005). However, it does not determine the location of the thrust. Culmann based it upon the Coulomb theory and is applicable for a retaining wall of any angle, sloping backfill and different layers with varying unit weights. Since it is derived from the coulomb theory, the failure plane is a rigid body.

Procedure to find the active thrust, see Figure 9:

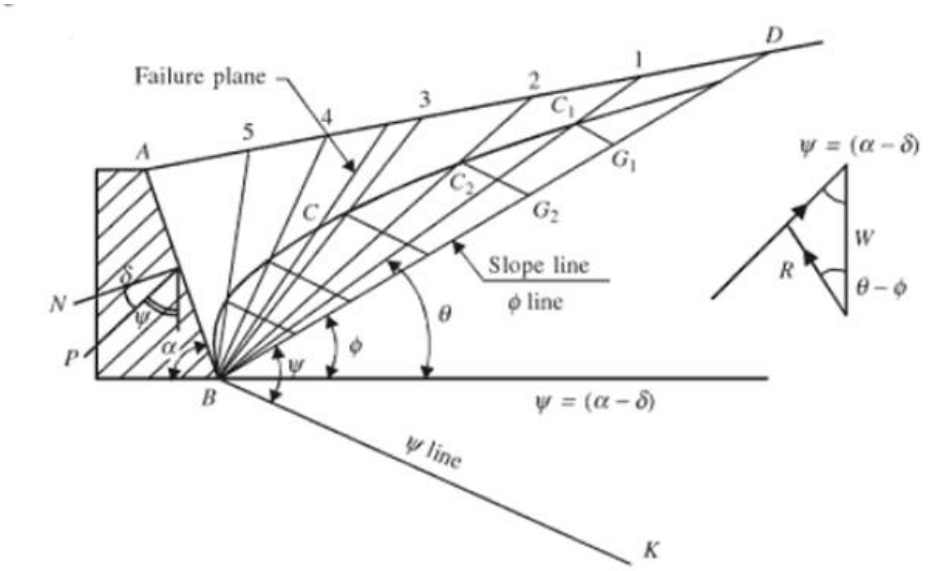

Figure 9 Illustration of Culmann's graphical method

i. Draw the ϕ-line with the angle ϕ (internal friction angle) to the horizontal.
ii. Draw the ψ-line with the angle ψ to the φ-line. Where $\psi = (\alpha - \delta), \delta = wall\ friction\ angle,\ \alpha = wall\ inclination$
iii. Take a trial wedge, say AB1, and calculate its weight (proportional to its area) and plot the weight along the ϕ-line to obtain point G_1. An appropriate scale for the weight could be to use the full extent of the ϕ-line to represent the largest trial wedge.
iv. Draw a line from G_1 parallel to the ψ-line to where it intersects the line B1, returning the point C_1. The length of the line G_1C_1 represents the earth pressure from that failure wedge
v. Assume different wedges to be able to draw more lines that intersect the failure line of the respective wedges. By drawing a smooth curve, the so called Culmann line, between these points C_1 to C_n the active earth pressure can be obtained. This is found where the maximum distance between the ϕ-line and Culmann line when drawing lines parallel to the ψ-line. By making a parallel line of the internal friction angle and tangent the Culmann line, the maximum thrust can be found.

To find the passive thrust, a similar procedure is done. The Culmann line becomes overturned and the minimum distance between the internal friction angle line and the Culmann line decides the passive thrust.

3.5 Earth pressure coefficient

The stress due to the soils self-weight is calculated down to the upper edge of the footing of the cantilever, since only the stresses on vertical construction are of interest. The internal friction angle has the effect that in case of a low value, a lot of the vertical stress is distributed as horizontal stress since the active earth pressure coefficient increases. If the angle of the ground slope is increased the active earth pressure coefficient increases as well, see Table 3 and Figure 10.

The load is decided by TK GEO to 44 kPa. Due to the stiffness of the sleeper it is assumed that the load is applied at its bottom.

Table 3 shows how the active earth pressure coefficient changes when each individual variable increases.

	Internal friction angle, φ	Ground slope, β	Wall roughness, δ	Inclination of wall, α
K_a	↓	↑	↓	↓

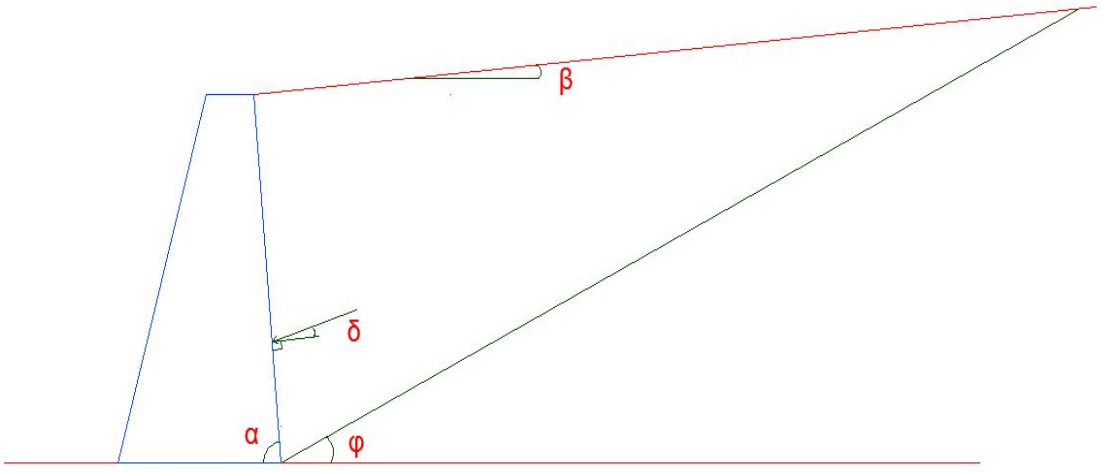

Figure 10 Definition of angles

4 Conceptual model

The geometry of the cantilever and the soil layers are from the Södertälje project, where the railway bottleneck is being improved. The retaining wall is in the vicinity of a railroad bridge, which determines the boundary of the superstructure. The superstructure consists of two fractions, the single graded ballast and the unbound blasted material (0-150 mm). The superstructure is constructed upon gravelly sand. The material properties can be seen in Table 4 below. The ground water level is below the superstructure, hence it is drained conditions.

Table 4 Soil properties

	Ballast	Blasted material	Sand
E [MPa]	50	50	25
φ [°]	42	42	35
C' [kPa]	0	0	0
γ [kN/m^3]	20	18	18

Even though the width of the rail is 1450 mm, it is beneath the sleeper the load distribution begins due to its stiffness. The width of the sleeper is 2500 mm and the height 155 mm, see Figure 11.

In the construction of the retaining wall there will be a fill material outside the construction to prevent the wall from failure of the ground from slide. Since the objective is not to evaluate these hazards, a simplification has been made to not use front fill as resistance. Since, the project aims to evaluate the active earth pressure and the passive earth pressure will only lead to lower deformations in the PLAXIS model. The cantilever wall has been modeled as plate elements in PLAXIS and the properties for these plates can be found in Table 5.

Table 5 Cantilever wall properties

	Cantilever wall
E [GPa]	50
EA [kN/m]	$1.25 \cdot 10^7$
EI [kN m^2/m]	$2.6 \cdot 10^5$
d [m]	0.5
W [kN/m/m]	0

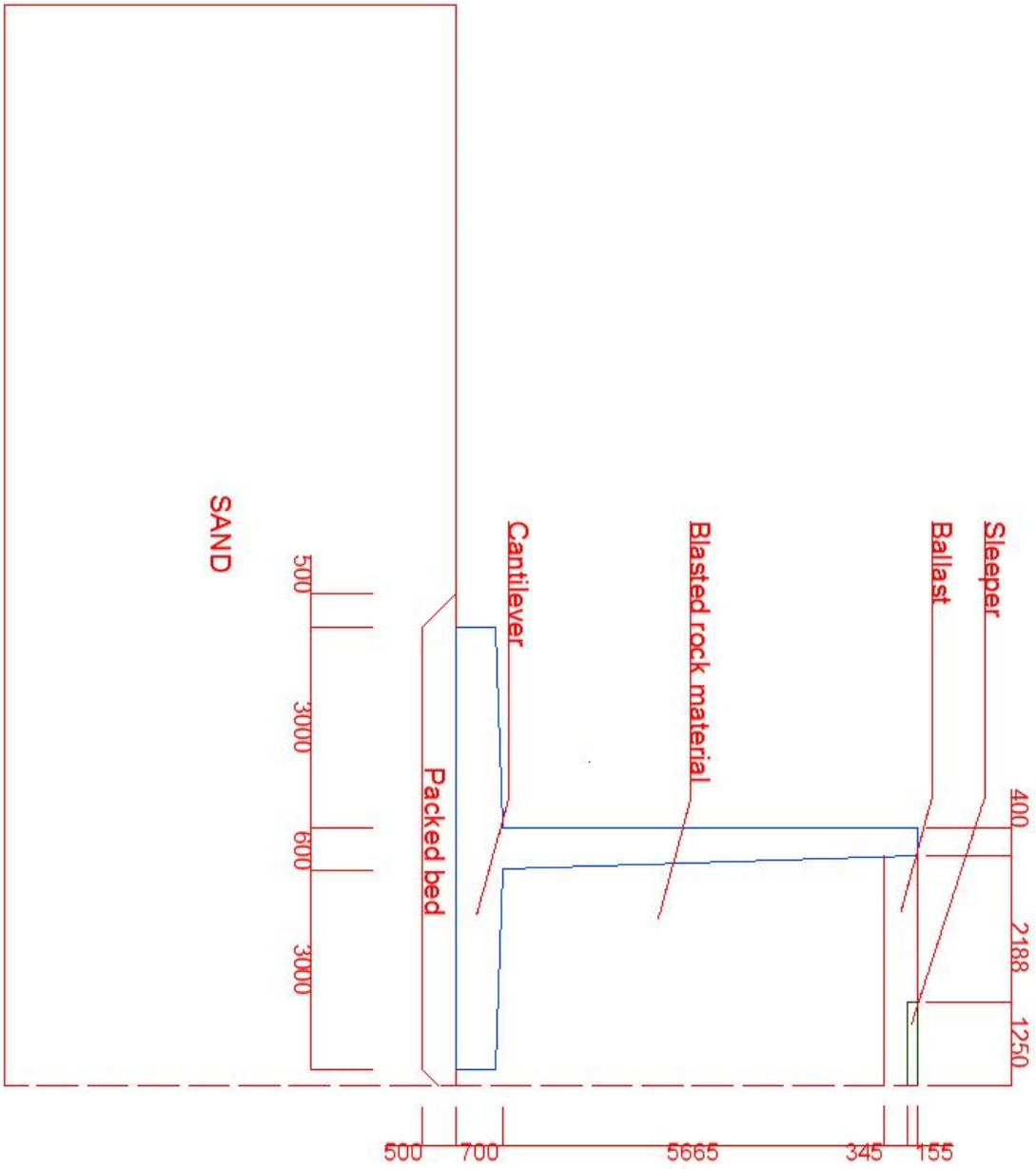

Figure 11 Conceptual model

5 PLAXIS

The finite element program PLAXIS offer ten different soil models:

- Linear elastic model
- Mohr-Coulomb failure criteria model
- Hardening soil model
- Hardening soil model with small-strain stiffness
- Soft soil model
- Soft soil creep model
- Jointed rock model
- Modified Cam-Clay model
- NGI-ADP model
- Hoek-Brown model

For this projects specific task, only the Mohr-Coulomb model is relevant. The linear elastic model is excluded since it does not simulate any plastic deformations, and is therefore more suitable when analyzing stiff structures in the soil, such as gravity walls and cantilevers. Linear elastic models can be used for a first estimation.

5.1 Linear elastic model

The linear elastic model is the basis of all the material models. The model is isotropic and described according to Hooke's law.

$$E = \frac{\sigma}{\epsilon} \tag{5.1}$$

E, described as M in PLAXIS, is the material stiffness matrix and depends on the Poisson ratio (coefficient of contraction), see equation:

$$\upsilon = -\frac{\epsilon_{transversal}}{\epsilon_{longitudinal}} \tag{5.2}$$

Since the model is linear elastic, there is neither plasticity nor failure. It does simulate structural behavior of constructions well, but to a soil the model is inaccurate. The strength of the model is the short calculation time and it can give a first estimation.

5.2 Mohr-Coulomb failure criteria model

The model depends on five variable parameters:

1. Young's modulus: The secant modulus, E_{50}, is used when modeling with loadings on the soil. It is chosen as the gradient of the line drawn from the origin and the point of 50% of the failure stress. In a case of unloading, as for excavations and tunneling, the unload-reload modulus, E_{ur}, is used instead. Notice, that for drained conditions Young's modulus for compression is lower than for shear . Alternative modulus that can be used in the Mohr-Coulomb model is the shear modulus, as mentioned above, and the Oedometer modulus. Hooke's law gives a relation between the three alternative modulus, see below:

$$G = \frac{E}{2(1+v)} \tag{5.3}$$

$$E_{oed} = \frac{(1-v)\cdot E}{(1-2\cdot v)(1+v)} \tag{5.4}$$

Depending on which modulus that is put into PLAXIS it will automatically calculate the other by these relationships, why different modulus cannot be used at the same time.

2. Poisson's ratio: For a one-dimensional loading(compression) the Poisson's ratio can be evaluated by the relationship:

$$K_0 = \frac{\sigma_h}{\sigma_v} \tag{5.5}$$

Where:

$$\frac{\sigma_h}{\sigma_v} = \frac{v}{(1-v)} \tag{5.6}$$

PLAXIS suggests that common Poisson ratios should be in the range 0,3-0,4. This relationship does not allow values > 1, which can be the case for highly over consolidated clays. For unloading, v is appropriate to be between 0,15-0,25.

3. Cohesion: A disadvantage is that when using effective strength parameters, c' and φ', is that the real stress path is not followed in the Mohr-Coulomb model, which more advanced models are better at. An advantage is that the shear strength is modified with the consolidation automatically. When frictional material is analyzed, cohesion has to be set $\neq 0$ to avoid complications. PLAXIS suggest $c > 0.2\ kPa$, an alternative called tension cut-off can be used to limit the tension forces that will occur (Brinkgreve, Engin, & Swolfs, PLAXIS 3D Reference Manual 2011, 2011).
4. Friction angle: The friction angle is important in the calculation of the undrained material parameters in the alternative drainage type "undrained A" and also for drained material properties. If cohesion is set to the shear strength and the friction angle equal to zero, the drainage type to use is "undrained B" or "undrained C" for analyzing the material properties. According to PLAXIS Mohr-Coulomb results in a more realistic approximation of the soil strength compared to the Drucker-Prager method.
5. Dilatancy angle: Input values shall be in degrees. For a sand, the dilatancy depend largely on the friction angle and the density. A common approximation of the dilatancy is:

$$\psi = \varphi - 30° \tag{5.7}$$

If the friction angle is smaller than thirty degrees the value of dilatancy is set to zero, which also is the value that clays are set as unless they are highly over consolidated. When drainage type undrained B or C is chosen the angle has to be set to zero and for undrained A great consideration has to be taken for positive values on dilatancy, which can result in unlimited strength due to suction.

In the advanced options there are alternatives for increasing stiffness and cohesion per unit depth.

As clarified in the chapter the Mohr-Coulomb theory, the theory has some disadvantages. The modulus is not stress dependent, not stress path dependent nor consider anisotropy of the soil and therefore not in the modulus. This results in why the model is perfectly plastic, since there is no change of the yield surface due to increased modulus (Brinkgreve, Engin, & Swolfs, PLAXIS 3D Reference Manual 2011, 2011). The strain is divided into two parts, the elastic strain and the plastic strain. The yield conditions are expressed by six equations, formulated by principal stresses, see equation below. The result is a yield surface with a hexagonal conical nature, see Figure 12.

$$f = \frac{1}{2} \cdot \left(\sigma_x' - \sigma_y'\right) + \frac{1}{2} \cdot \left(\sigma_x' + \sigma_y'\right) - c \cdot \cos\varphi \tag{5.8}$$

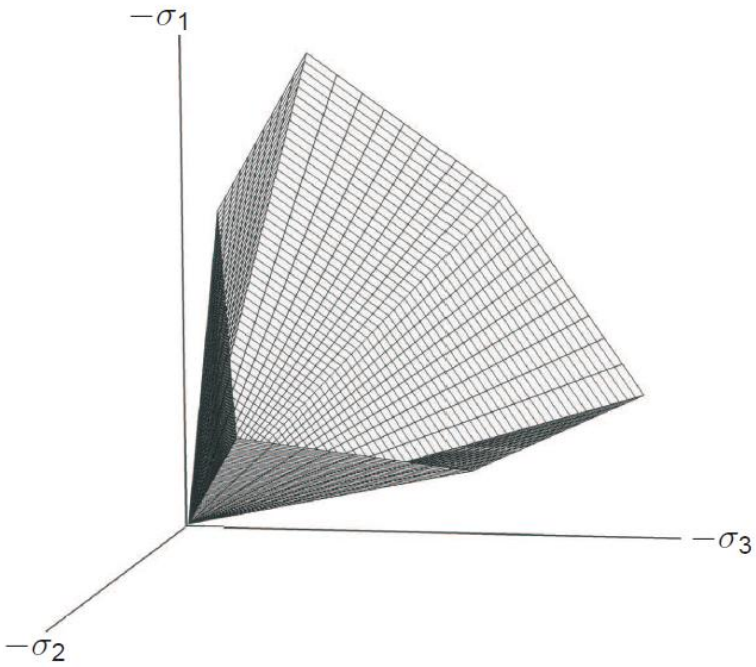

Figure 12 Mohr-Coulomb hexagonal yield surface

5.3 PLAXIS model

A symmetry line is chosen in the middle of the railway section, meaning that half the extension of the load is used in the model. The cantilever wall and backfill has been modeled in PLAXIS as a plane strain model. This means that the geometry of the cross section is assumed to be fairly constant along the z-axis. It is also assumed that there are no strains or displacements in the z-direction. This type of model is applicable for slope stability problems, trenches, road constructions and oblong excavations.

The elements for the finite element model are triangles consisting of either 6 or 15 nodes, see Figure 13. For this model the 15-node element has been chosen. The 15-

node element leads to a higher precision in results concerning displacements and stresses.

The downside to using the 15-node element over the 6-node is that it requires more memory capacity and the calculation and the operation speed is severely decreased.

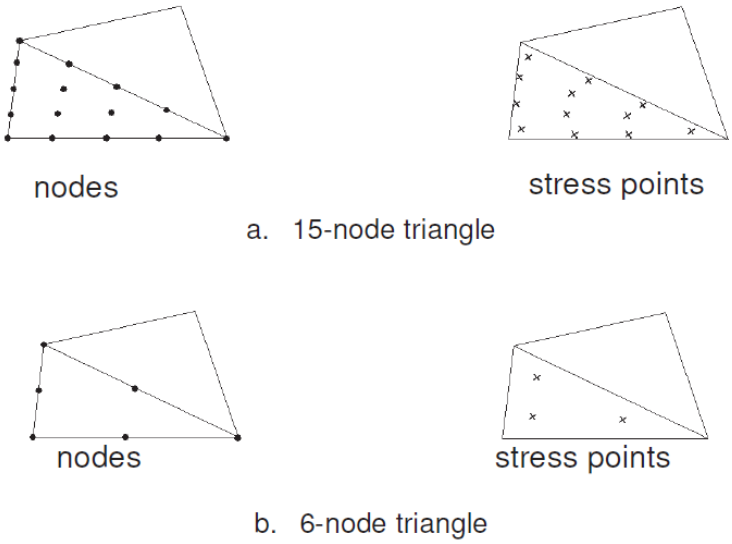

Figure 13 6- and 15-node elements

The loading input "staged construction" is used, it allows to define the different construction steps of the railway. As default in PLAXIS the first phase is an in-situ stress calculation. It is the starting point of the forthcoming construction of the superstructure. Otherwise PLAXIS will interpret the sand as a new material, and displacements due to its self-weight will be included in the calculations. The in-situ values is calculated by either K_0-procedure or by an alternative called gravity loading. To provide the same conditions for the hand calculations and PLAXIS the K_0-procedure is chosen. Hence, the K_0-procedure determines the earth pressure coefficient according to:

$$K_0 = 1 - \sin(\varphi) \tag{5.9}$$

For the gravity loading option, K_0 is instead decided by the Poisson ratio. Due to the relation to the internal friction angle, it is a more appropriate choice when comparing to the hand calculations. For the gravity loading the in-situ situation is decided by the volumetric weight. It is preferred in situations with sloping ground or non-horizontal layering of the soil. When the in-situ situation has been calculated, the calculation type is changed to plastic drained. The superstructure has high permeability, why the plastic drained option is appropriate choice.

After the in-situ calculation, the model could be divided into different phases that represented how it was constructed in reality, see Figure 14.

- In-situ calculation (1)
- Excavation and fill to prepare bed beneath cantilever (2)
- Construction of cantilever (3)
- Superstructure, divided into layers that is built continuously (4-10)
- Load is applied (11)

When the load is in the center of the superstructure it is possible to model the geometry with a symmetry line, meaning that only half of the construction is drawn, see Figure 14.

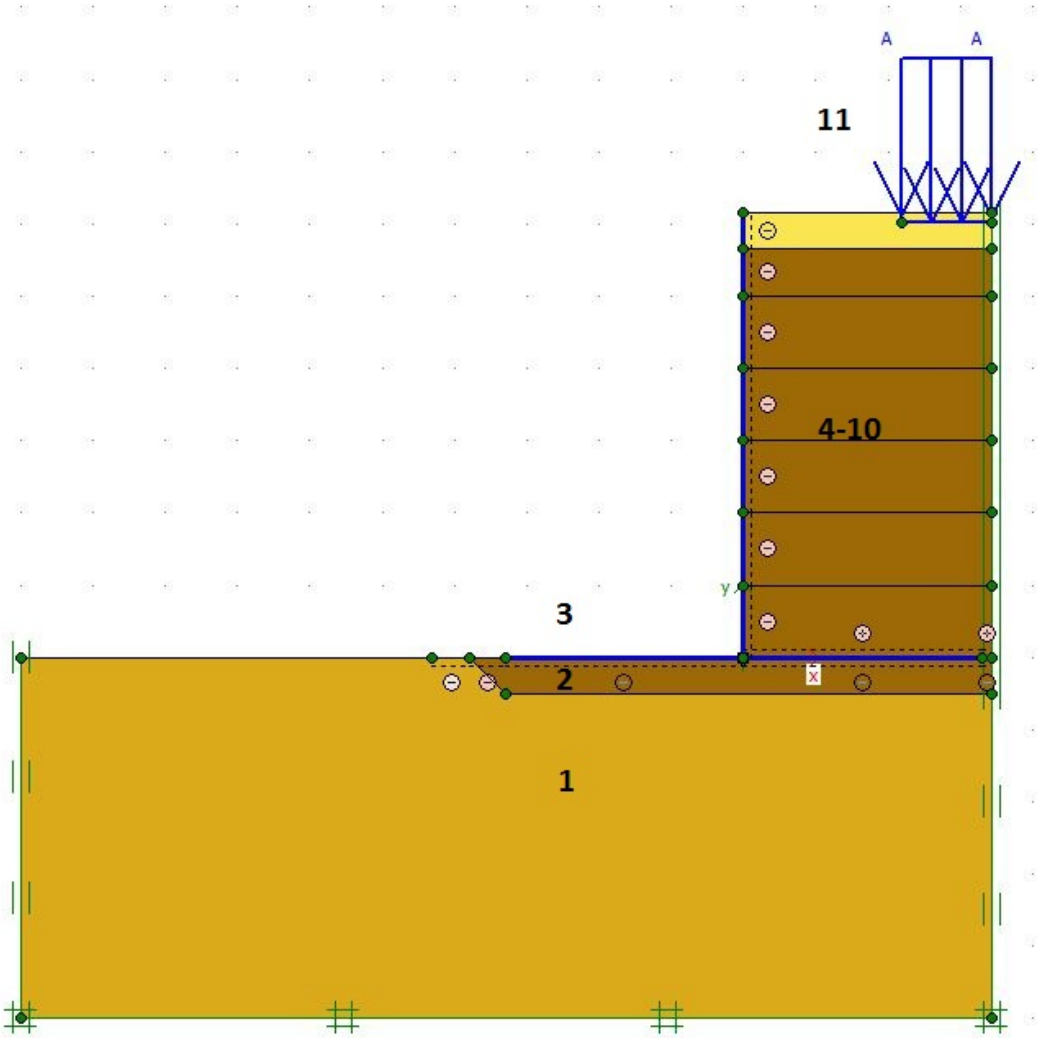

Figure 14 Phases in the PLAXIS model

Depending on phase, the dotted interface of the cantilever can be activated. The properties of the interfaces elements are defined by the surrounding soil. Interfaces can be used to model soil-structure mechanisms. For this finite element model the interface tool has been used to give the wall friction for the cantilever wall. It has been set to 0.48, which means that the friction angle of the wall is equal to 48% to that of the soil, which in this case is 20 degrees. Additional calculations have been done with different values for wall friction. PLAXIS applies the load in stages; therefore the arc length control option should be enabled. Arc-length control is an option that accurately can find at what load the soil body reaches collapse. If this option is not activated PLAXIS may have a problem finding a convergent solution. The program tries to apply the next increment of the load but instead of finding the convergent answer to the amount of displacement it will find that it is unsolvable and will simply remove the load increment and repeat the load step over and over, see Figure 15.

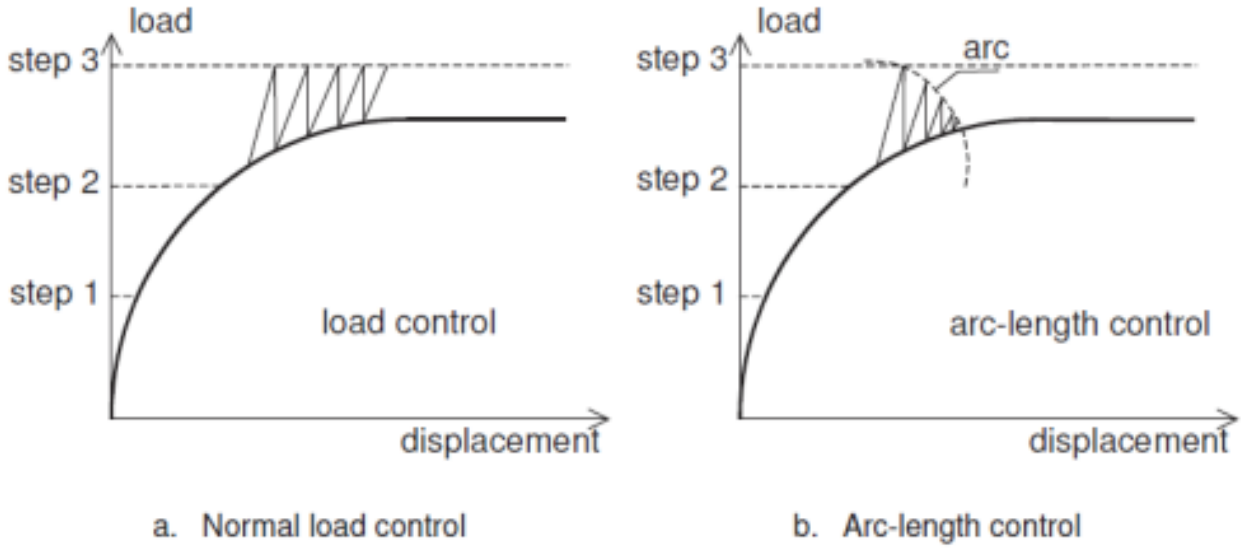

Figure 15 Illustration of normal load control and arc-length control

For a calculation where the load is lower than the failure load there is no difference between the results from a calculation using arc-length control and one that is not using it.

For a safety analysis it is recommended to use arc-length control. The safety factor is usually overestimated when calculating stability without the arc length control.

6 Results

6.1 Mathcad calculation method

In Figure 16 the pressure on the cantilever wall from the soils self-weight, the surcharge and the total pressure is displayed.

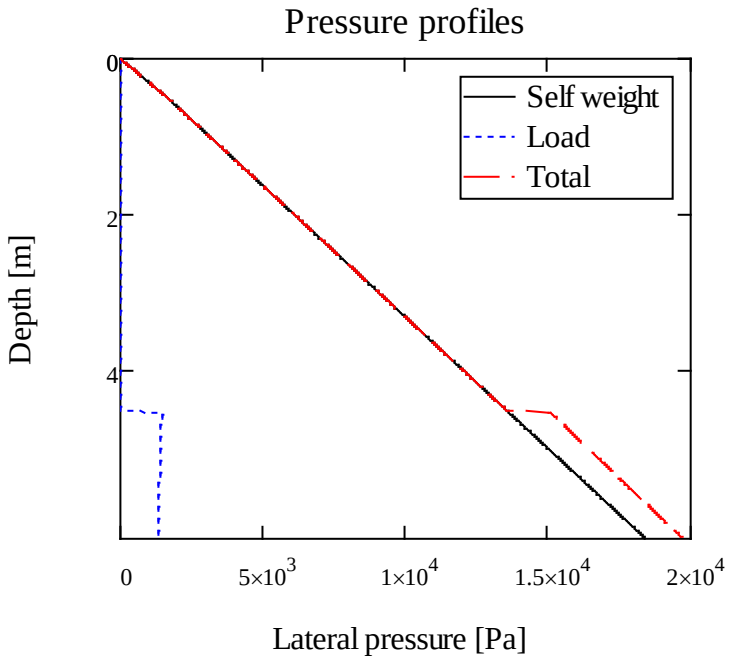

Figure 16 Typical graph showing the pressures on the cantilever wall

To find the exact position of the thrust, three steps have to be performed. Integration of the pressure over the length H_{wall} is done to determine the total thrust. Moment around the top of the wall is calculated. By dividing the moment over the total thrust the center of mass is determined, see equation 6.1, 6.2 and 6.3. To verify the center of mass, a calculation of the moment around the center of mass is performed to confirm that it is equal to zero.

$$P_{tot} = \int_0^{H_{wall}} \sigma_h(z)dz \tag{6.1}$$

$$M_x = \int_0^{H_{wall}} (\sigma_h(z) \cdot z)dz \tag{6.2}$$

$$x_{cm} = \frac{M_x}{P_{tot}} \tag{6.3}$$

6.2 Hand calculations - at rest pressure

For the at rest pressure calculations it is the load distribution methods that differs. This is because the self-weight will be calculated with the same earth pressure coefficient. For a soil with an internal friction angle of 42 degrees the at rest earth pressure coefficient is 0.331.

Table 6 Results from Mathcad calculations, at rest pressure

Calculation method	Total thrust [kN/m]	Center of mass from the top of the wall [m]	Center of mass - 2*H/3 [m]	Maximum bending moment [kNm]
2:1-Method	123,3	4,18	0,07	244.8
Modified 2:1	135,3	4,08	-0,03	282.1
Boussinesq	167,9	3,73	-0,38	408.8
Modified Boussinesq	131,4	4,11	0,00	270.0
Infinite surcharge	204,9	3,65	-0,46	515.3

Table 6 shows that all the different load distribution methods, except for the 2:1-method, give a resultant that is at or above one third from the bottom of the wall. A negative value in the fourth column indicates a resultant that is higher up the wall than one third measuring from the bottom, see Figure 17.

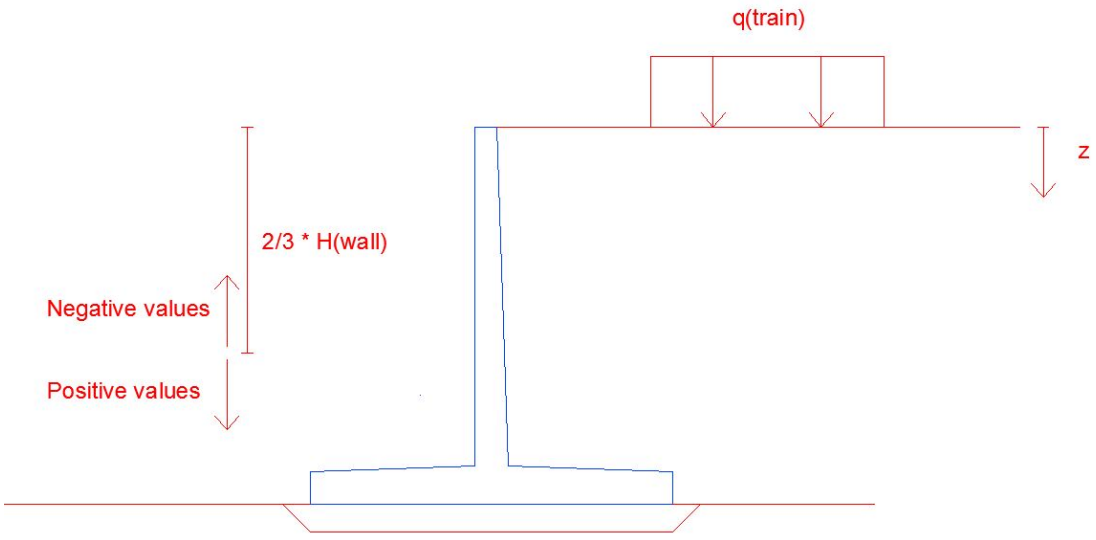

Figure 17 Illustration explaining the table of results

6.3 Hand calculations - active pressure

In the table below the results from four different earth pressure models combined with three different load distribution methods can be found.

Table 7 Results from Mathcad calculations, active pressure

Calculation method	Total thrust [kN/m]	Center of mass from the top of the wall [m]	Center of mass - 2*H/3 [m]	Maximum bending moment [kNm]
Rankine				
2:1-Method	73,9	4,176	0,066	147.0
Modified 2:1	81,1	4,08	-0,030	169
Boussinesq	95,4	3,769	-0,341	228.5
Modified Boussinesq	78,7	4,105	-0,005	162.1
Infinite surcharge	122,8	3,651	-0,459	308.7
Coulomb				
2:1-Method	68,3	4,176	0,066	135.8
Modified 2:1	74,9	4,074	-0,036	156.6
Boussinesq	90,1	3,75	-0,360	217.6
Modified Boussinesq	72,7	4,105	-0,005	149.8
Infinite surcharge	113,4	3,651	-0,459	285.1
Boussinesq				
2:1-Method	59,5	4,141	0,031	120.4
Modified 2:1	62,8	4,08	-0,030	130.9
Boussinesq	83,7	3,724	-0,386	204.3
Modified Boussinesq	65,3	4,105	-0,005	134.5
Infinite surcharge	101,9	3,651	-0,459	256.2
Culmann	83,9	4,271	0,161	158.4

Most of the results in the table above show that the resultant is above one third of the height of the retaining wall, measuring from the bottom of the wall, see Table 7.

If only the self-weight from the soil is considered the only thing that changes the lateral active pressure is the coefficient of active earth pressure. The different K_a values can be seen in Table 8.

Table 8 Earth pressure coefficients

Soil model	K_a
Rankine	0.198
Coulomb	0.195
Boussinesq	0.186

6.4 PLAXIS results

The soil model that has been used for this finite element model in PLAXIS is Mohr-Coulumb. Three different soil clusters have been used: sand, blasted rock material land ballast.

To avoid instant failure of the soil body when the train load is applied the ballast layer, the first 0.5 meters, has been given a cohesion of 0.5 kPa.

6.4.1 Mesh quality

It is important that the elements in the mesh are not “too pointy” to avoid numerical problems. To see if the mesh is acceptable the tool “Quality View” in PLAXIS can be used. In Figure 18 the quality of the mesh is displayed for the conceptual model where most of the elements are of very high quality.

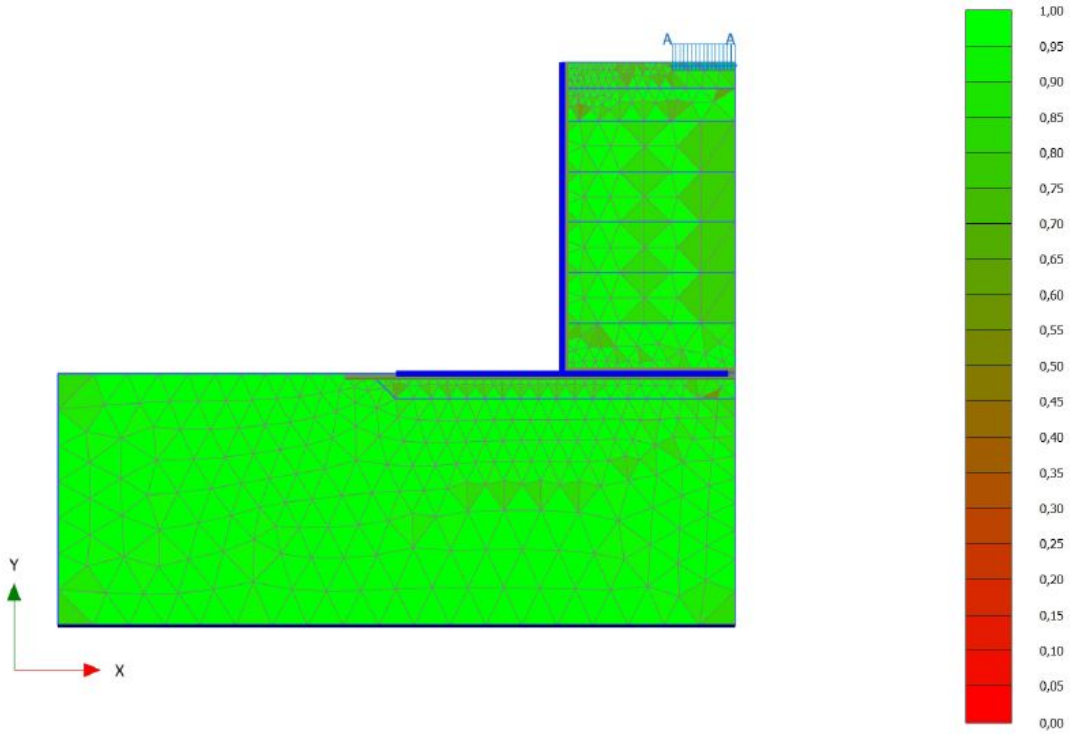

Figure 18 Quality view indicates if the mesh has god numerical possibilities.

6.4.2 Deformations in the soil

The total deformations of the soil and cantilever wall are relatively small. The maximum displacement is about 2.6 centimeters. The largest deformations can be found in the soil under the train load, see Figure 19. This figure is taken from a model where the wall roughness was 20 degrees and the surcharge was in the center.

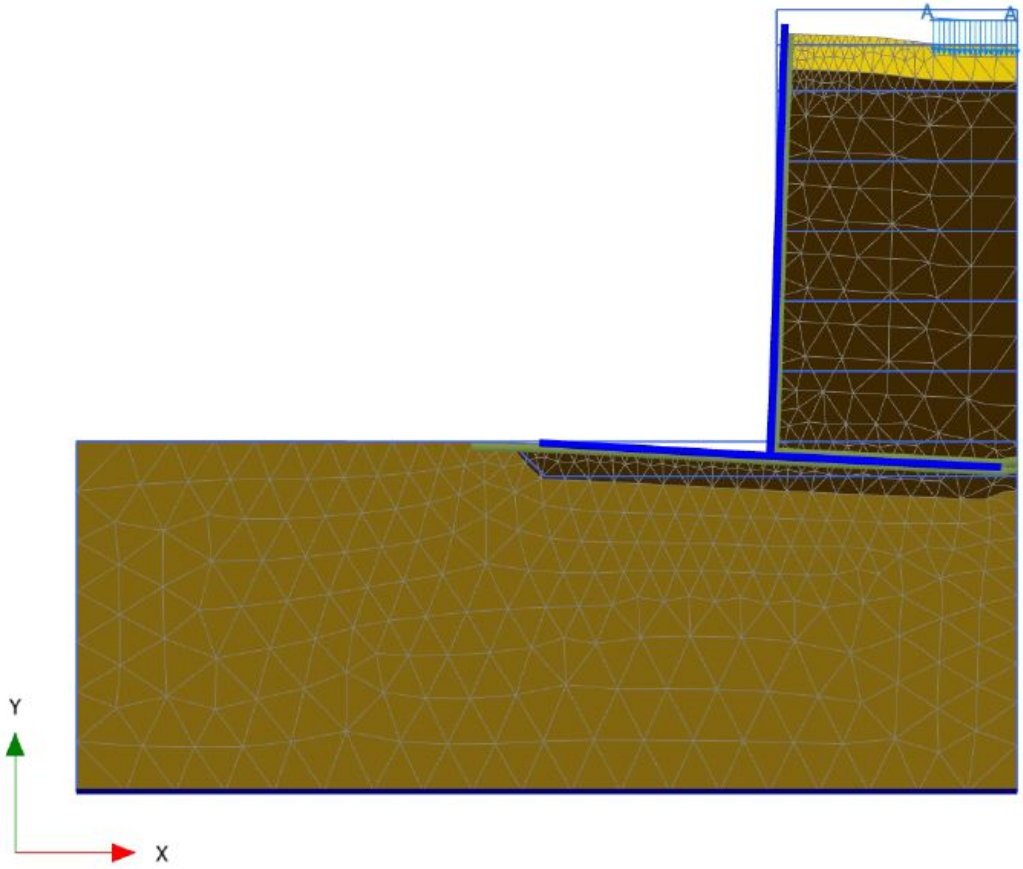

Figure 19 Total displacements view show how much the nodes in the mesh moves

6.4.3 Wall displacement

When viewing the movement of the cantilever wall it can be seen that it is mostly moving downwards and also slightly rotating clockwise. The largest displacement is 1.9 centimeters in the lower right part of the cantilever wall, see Figure 20. In the model this will lead to an active pressure on the lower part of the vertical wall and passive pressure on the upper part. To reach fully active pressure in a dense frictional material the horizontal displacements need to be 0.1% – 0.2% of the wall height. For passive pressure the value is approximately 0.5% of the wall height (Sällfors, 2001).

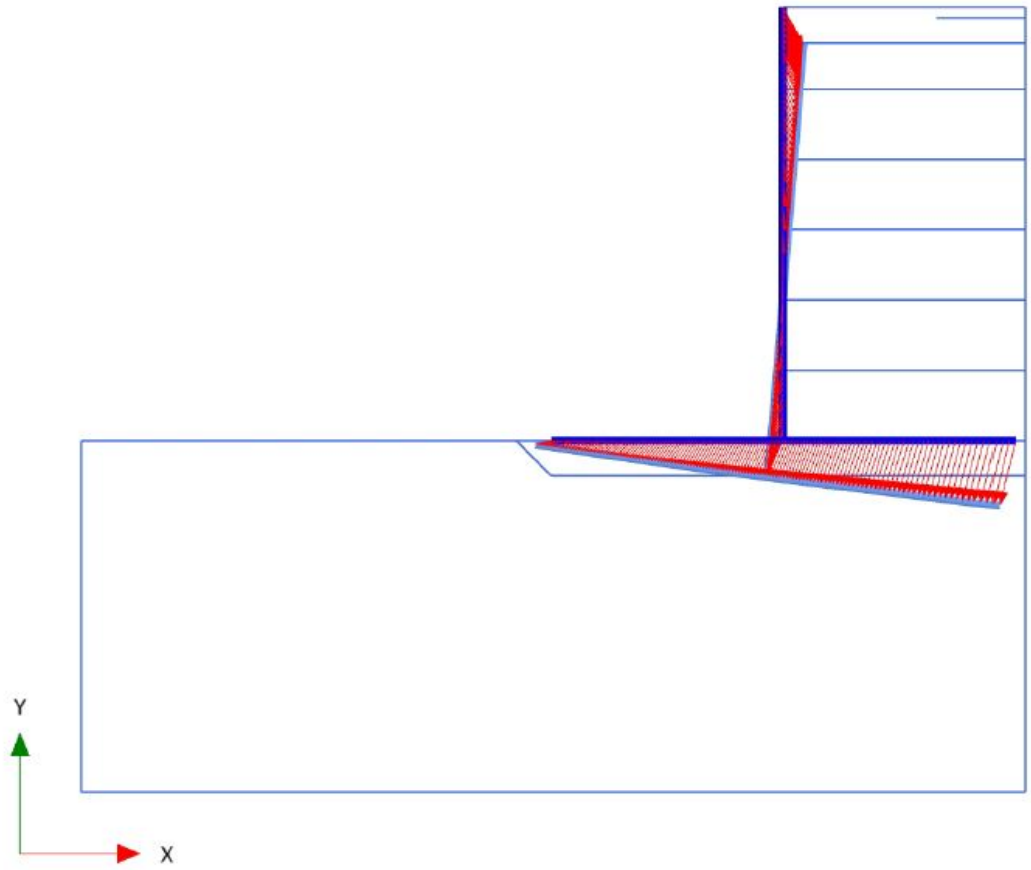

Figure 20 Wall displacements view tell direction and magnitude of displacement of the structure

The lateral earth pressure on the cantilever wall has been calculated with a number of different options. Two different calculations have been made, without wall weight (the weight of the wall mostly affects the axial forces in the wall) with either 100% wall friction or 48% wall friction. With these wall displacements and soil deformation the resultants obtained from PLAXIS are as showed**Error! Reference source not found.**in Table 9. The values are taken from the normal stresses from the interface between the cantilever wall and the soil. This is the most reliable way of finding the lateral pressure acting on the wall (Wong, 2012).

Table 9 Resulting forces from PLAXIS, wall weight excluded

Wall weight excluded	Load and δ=1	No load and δ=1	Load and δ=0.48	No load and δ=0.48
F_x [kN/m]	120.3	95.1	141.5	106.3
F_y [kN/m]	95.1	69.0	50.1	45.4

6.5 Load distribution methods

6.5.1 Infinite load

The simplest way to model the surcharge on top of the soil next to the cantilever wall is by simply assuming that it extends infinitely as in Figure 21. This will give an increase in stress in the entire soil mass by, in this case, 44 kPa. Assuming an infinite load gives a thrust due to the surcharge between 45 and 55 kN/m depending on the earth pressure coefficients in the soil models. If at rest pressure is assumed, the value increases to 90 kN/m.

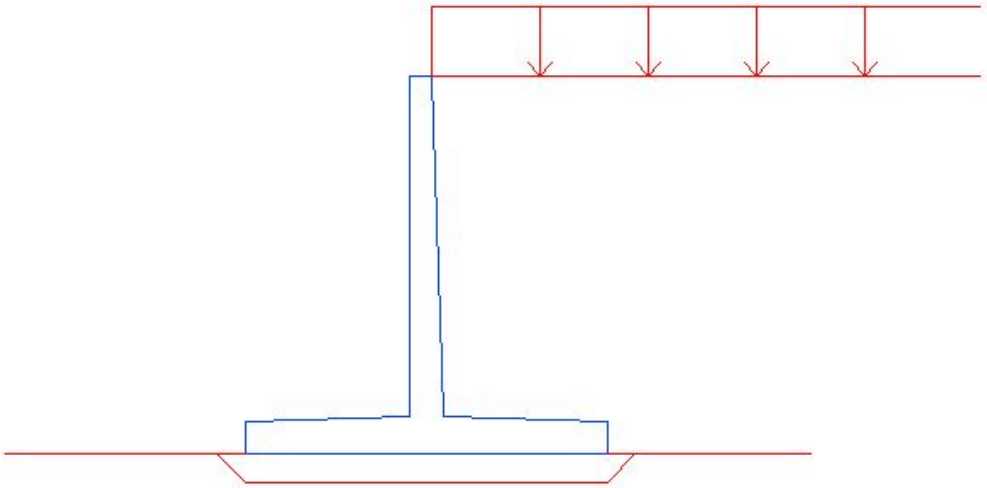

Figure 22 Illustration of infinite surcharge

6.5.2 2:1 method

In the case of using the 2:1 load spread method for surcharges, assumptions to adapt the method has to be made. The 2:1 method is common when calculating settlements, hence a stress level directly beneath the load is assessed in the theory. In case of determining the stresses on a retaining structure, the values in the middle beneath the surcharge are of no interest. The stresses on the descending 2:1 line are wanted. Still, the calculated values have been used unaltered for this situation. In the 2:1 method, the stresses at depth is calculated as if the surcharge is distributed evenly, see Figure 23 and equation 6.4:

$$b(z) = b(surcharge) + 2(\frac{z}{2}) \tag{6.4}$$

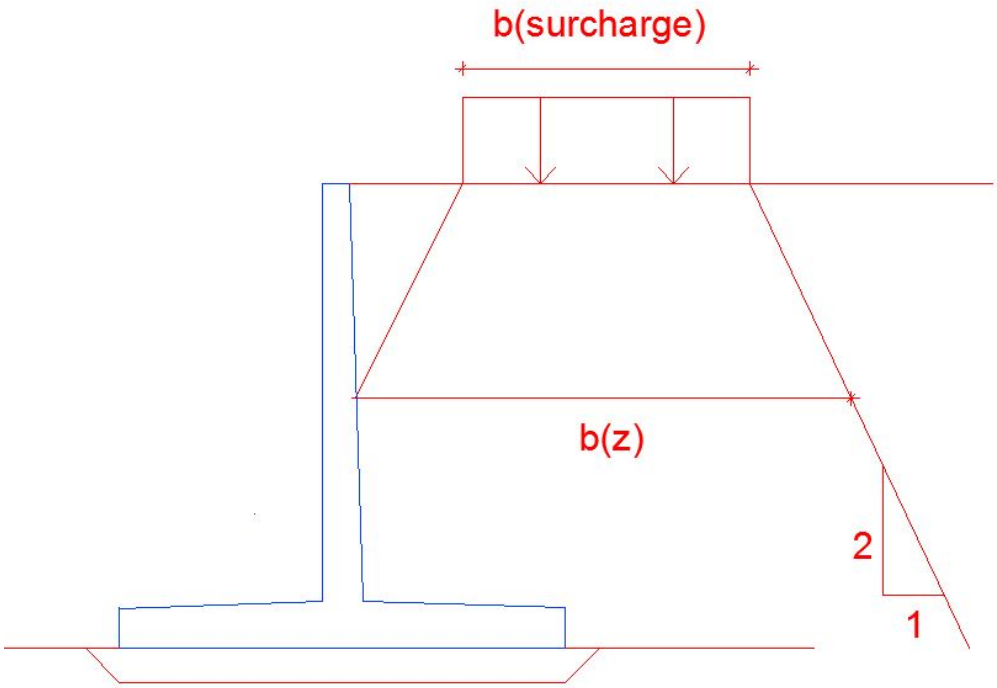

Figure 23 Illustration of the 2:1-method

The method assumes that there is an unopposed distribution with depth, since there is a retaining wall on one side that is not the case. Therefore a hypothesis has been made that the extension of the surcharge is only developing in the direction where there is no wall, resulting in that the stresses is decreasing in a slower pace with depth.

For this project, it means that the horizontal stresses influence the retaining structure first at the depth of twice the distance between retaining structure and the surcharge. That is not very likely situation since distribution in the soil skeleton act as in Figure 1. To mimic a more realistic distribution, an adjustment was made in Mathcad to assume a linear increase of the horizontal stress from zero at the ground level to the stress level achieved from the original 2:1 method at the depth it starts to affect the retaining wall, see Figure 24.

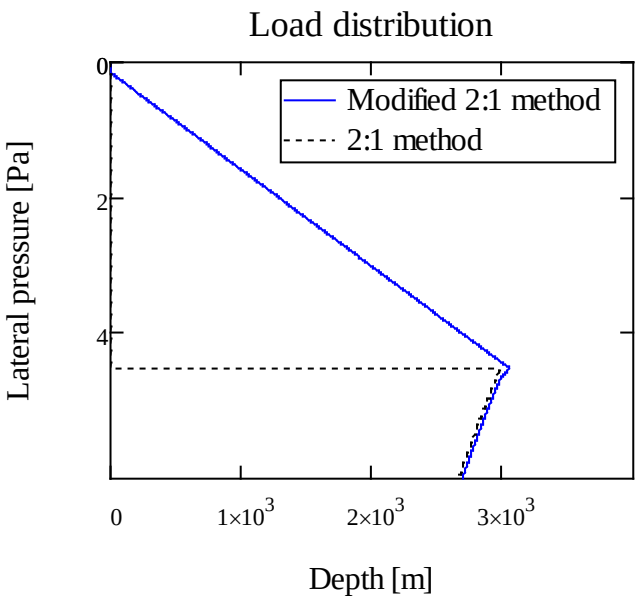

Figure 24 Assumed linear increase of lateral stress until depth from where 2:1 method affects the wall.

6.5.3 Boussinesq

To calculate the lateral earth pressure, values for K_a were taken from tables. There is no closed form solution which is why tables with values for the coefficients have been assembled where the coefficients have been evaluated numerically. The values for this specific case can be found in Table 8. The horizontal stress from the soils self-weight with these earth pressure coefficients can be seen in Figure 25.

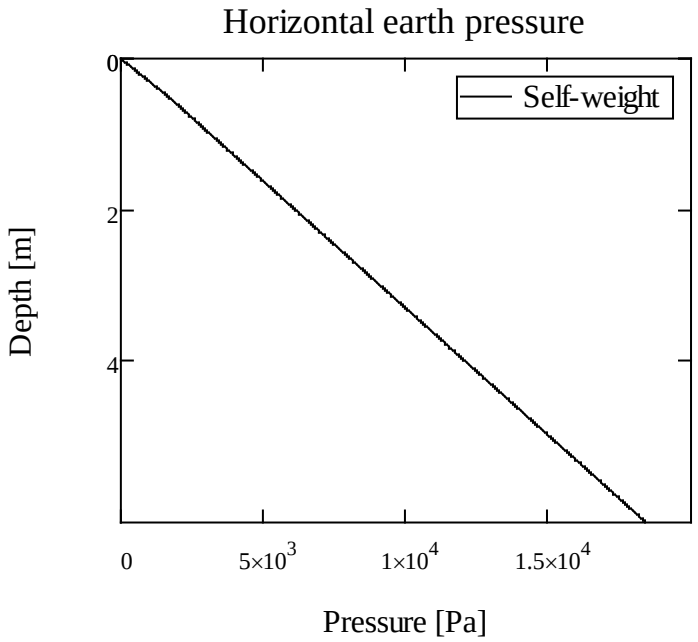

Figure 25 Horizontal earth pressure from self-weight

Boussinesq has derived an equation that yields the stress with depth, called Boussinesqs elastic solution. The additional pressure on the cantilever wall is distributed as seen in Figure 26 and equation 3.29:

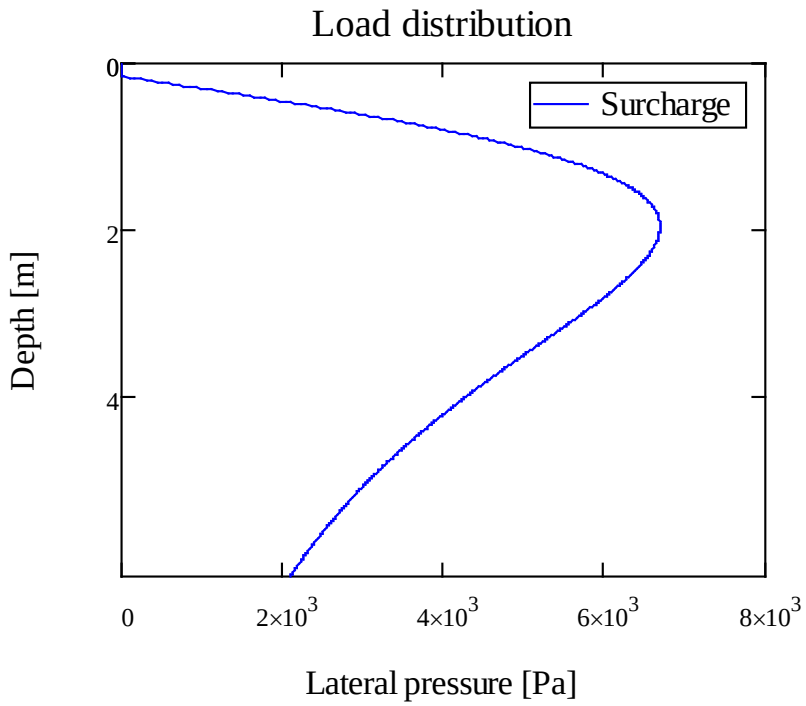

Figure 26 Boussinesq's elastic solution for a strip load

Using this method to calculate the additional pressure from a surcharge increases, in this case, the total thrust by 26 kN/m.

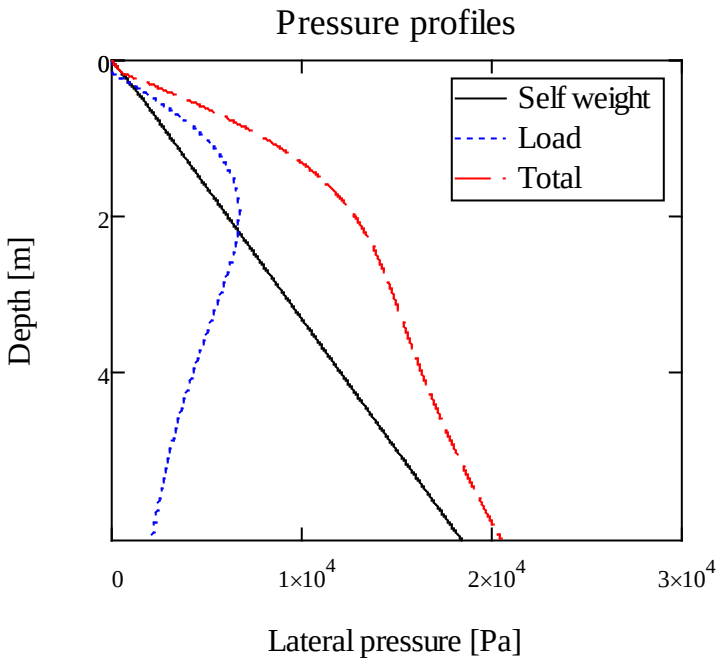

Figure 27 Earth pressure from self-weight, surcharge and the total pressure

Figure 27 displays how the earth pressure on the cantilever wall is distributed when Boussinesq's elastic solution is applied.

6.6 Modified Boussinesq load distribution

In addition to the method earlier described of converting a strip load into lateral pressure, the vertical pressure increase was calculated using Boussinesq theory specific for vertical pressure. This additional vertical pressure was then multiplied by the earth pressure coefficient of the different soil models to get the horizontal pressure, see equation 3.30. This resulted in a curve with an entirely different character compared to the previous Boussinesq-method, see Figure 28. For this load the concentration point is about two thirds down compared to the previous Boussinesq method where the concentration point was approximately one third down.

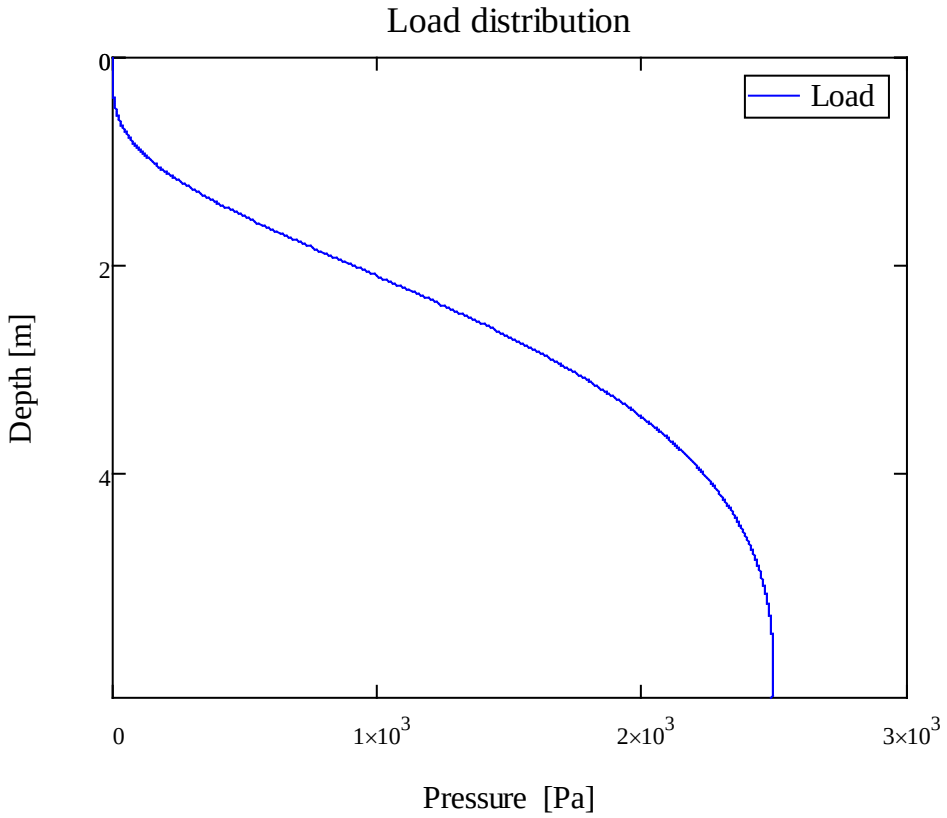

Figure 28 Load distribution from Boussinesq's solution for vertical pressure

This method of calculating gives approximately 8-10 kPa additional horizontal thrust from the strip load.

6.7 Culmann graphical method

The starting point from where the Φ-line and ψ-line are drawn is the point where the vertical and horizontal parts of the cantilever wall are joined. To be able to calculate the thrust with Mathcad an assumption concerning the wall-friction and the wall angle had to be made. The wall is in the real case inclined by 1.8 degrees but in this model it is assumed to be vertical, see Figure 29. The wall-friction has been set to 0 which significantly simplifies the calculation of the maximum thrust.

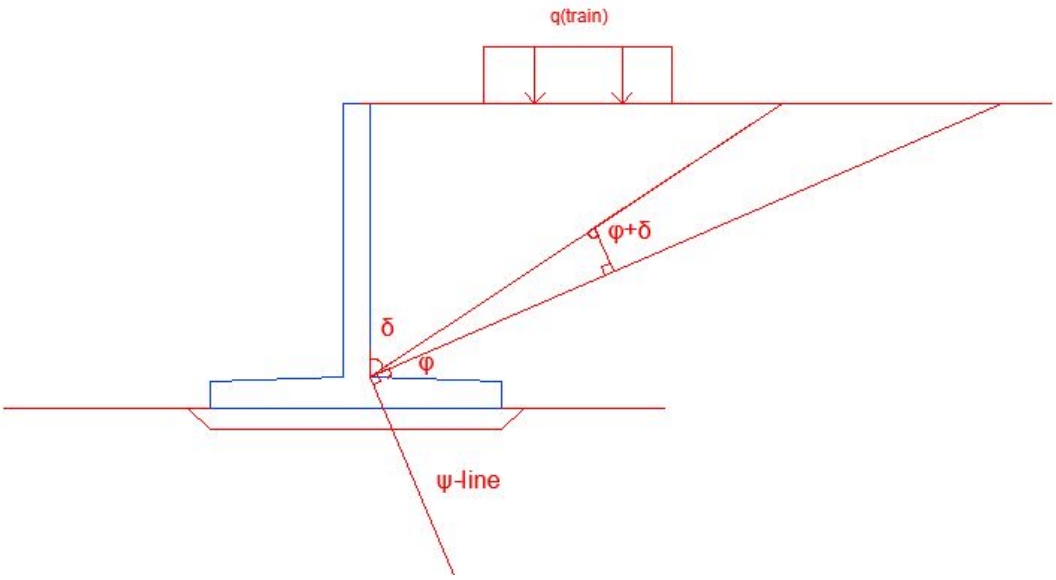

Figure 29 Definitions of angles in Culmann's graphical method

Instead of calculating a number of different trial wedges to be able to draw the Culmann line a function could be written that was dependent on the angle between the failure plane of the trial wedge and the vertical wall. To be able to take the train load into account the function had to have three different equations; the first part did not include the load, the second would increase the load gradually and the last part would include the entire load. This produced the Culmann-line in one step and from this function the maximum value was retrieved and hence also the maximum thrust and the most critical failure plane.

In Figure 30 the variation in thrust depending on the angle of the failure plane can be seen. The highest thrust is found when the plane angle is 0.456 radians which is approximately 29 degrees. For this failure wedge the horizontal thrust would be 84 kN/m.

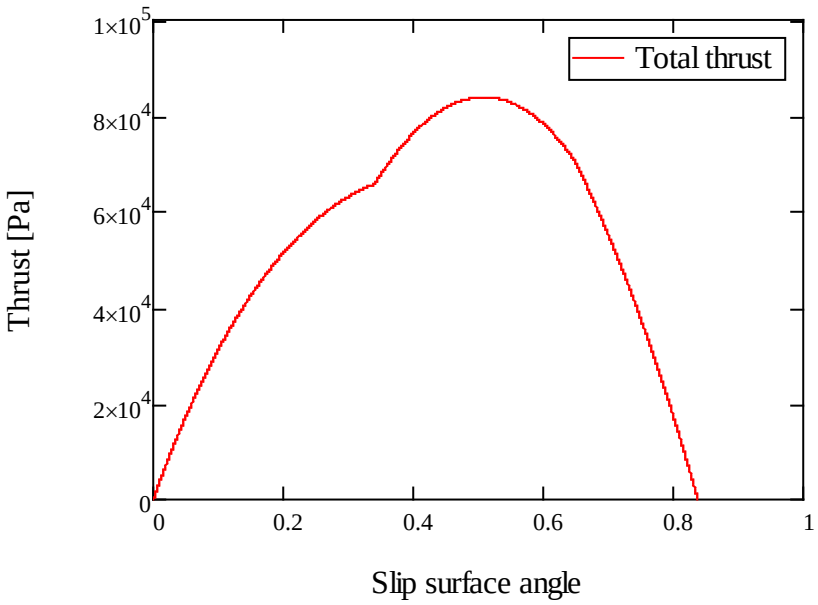

Figure 30 Angle of slip surface and corresponding thrust

When removing the surcharge from the calculations and only considering the weight of the soil the maximum thrust is 67.8 kN/m and consequently the thrust from the surcharge is 16.1 kN/m for the most critical slip surface.

To be able to find where the resultant is positioned average pressures were calculated along the wall by calculating the pressure over a smaller portion of the wall. The new calculation would give another resultant and the difference between the first and second resultant divided by the vertical length between them gives the average pressure, see Figure 31. For example, P_{tot}-P1 divided by Δz gives the average pressure over the lowest part of the wall.

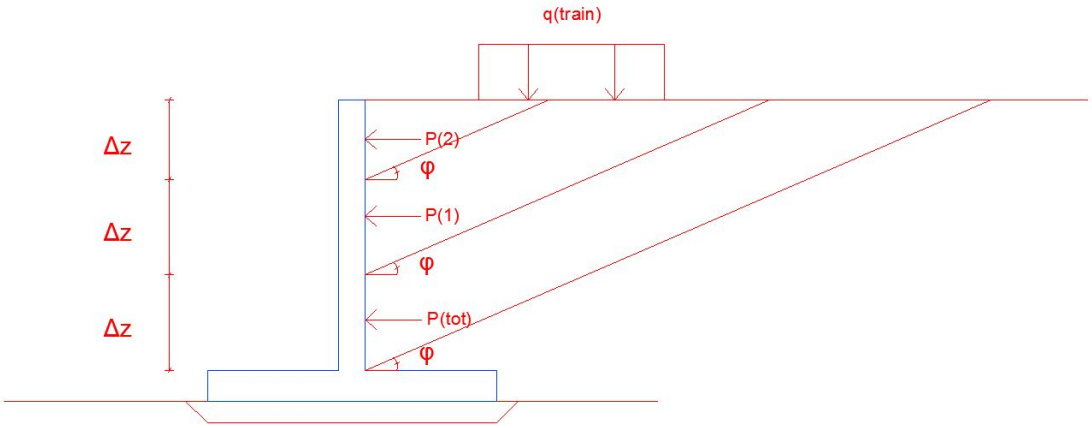

Figure 31 Segments of failure surface and their thrusts to determine resultant position.

This was performed for 12 segments, resulting in a line that later was divided into two trend lines. Since the curve representing the lateral pressure looks to be close to linear at first and then changes into a polynomial a single equation could not represent it very well, see Figure 32.

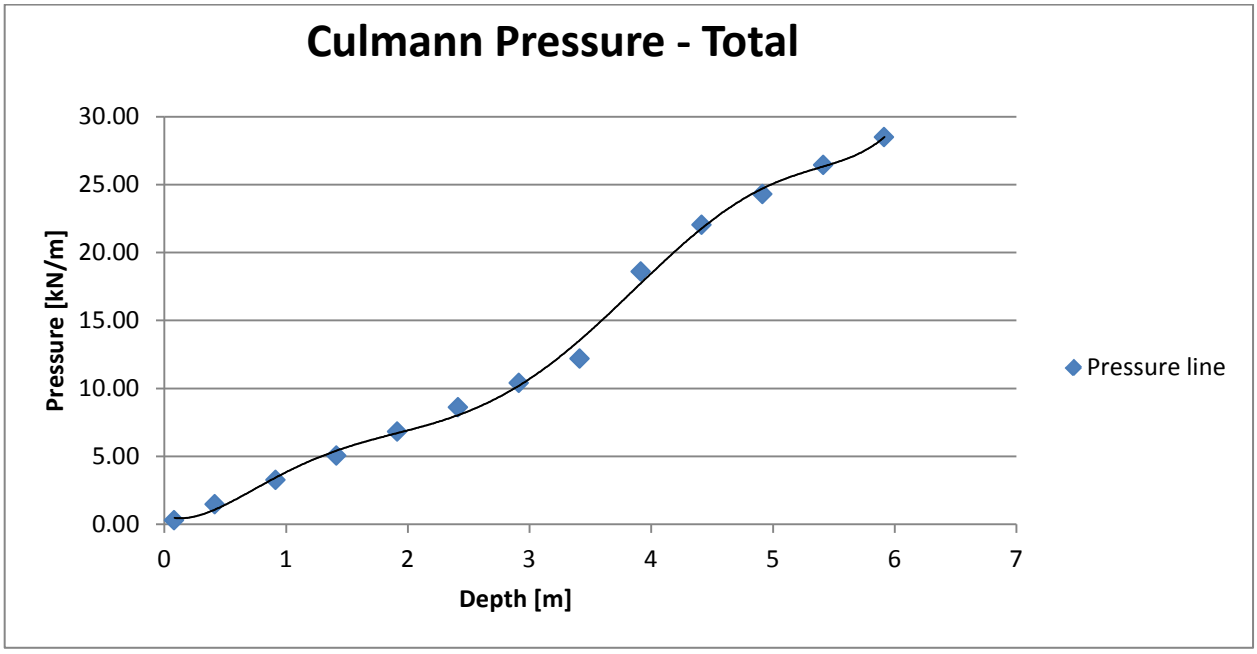

Figure 32 Part-thrusts by segments for the critical failure surface

Instead an equation for each part was made, see Figure 33 and Figure 34. A suitable trend line for the first segment could be found using an equation of the 2nd degree and for the second segment a 4th degree equation was used.

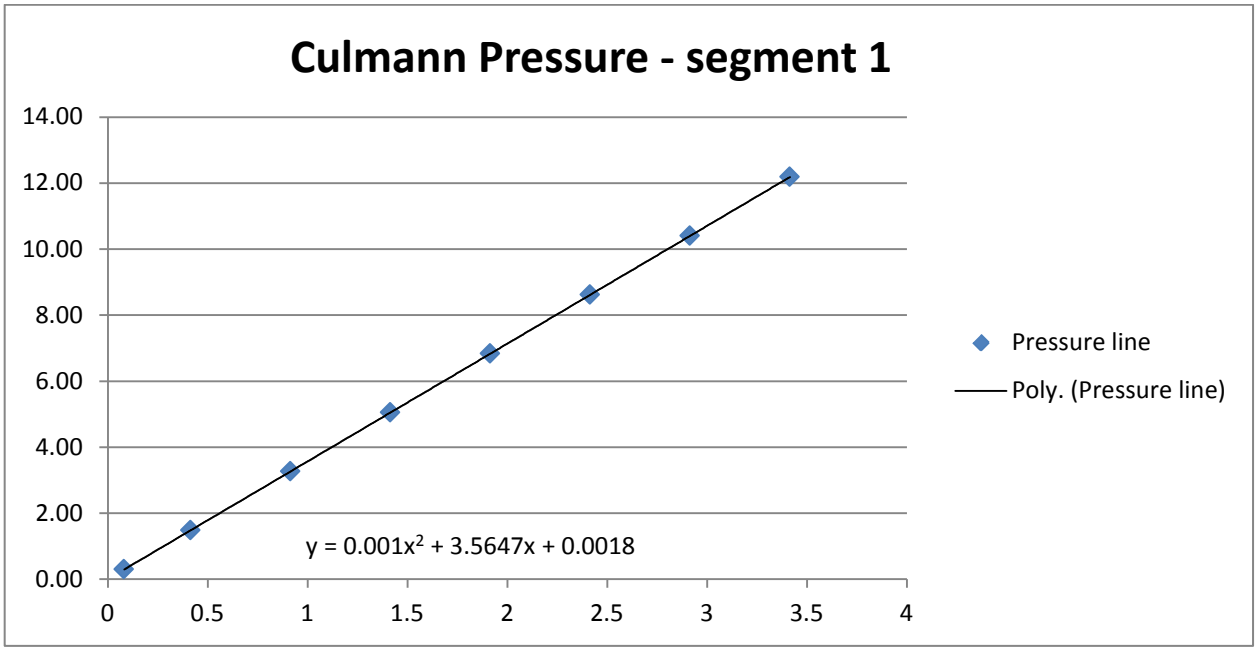

Figure 33 Trend line for segment 1

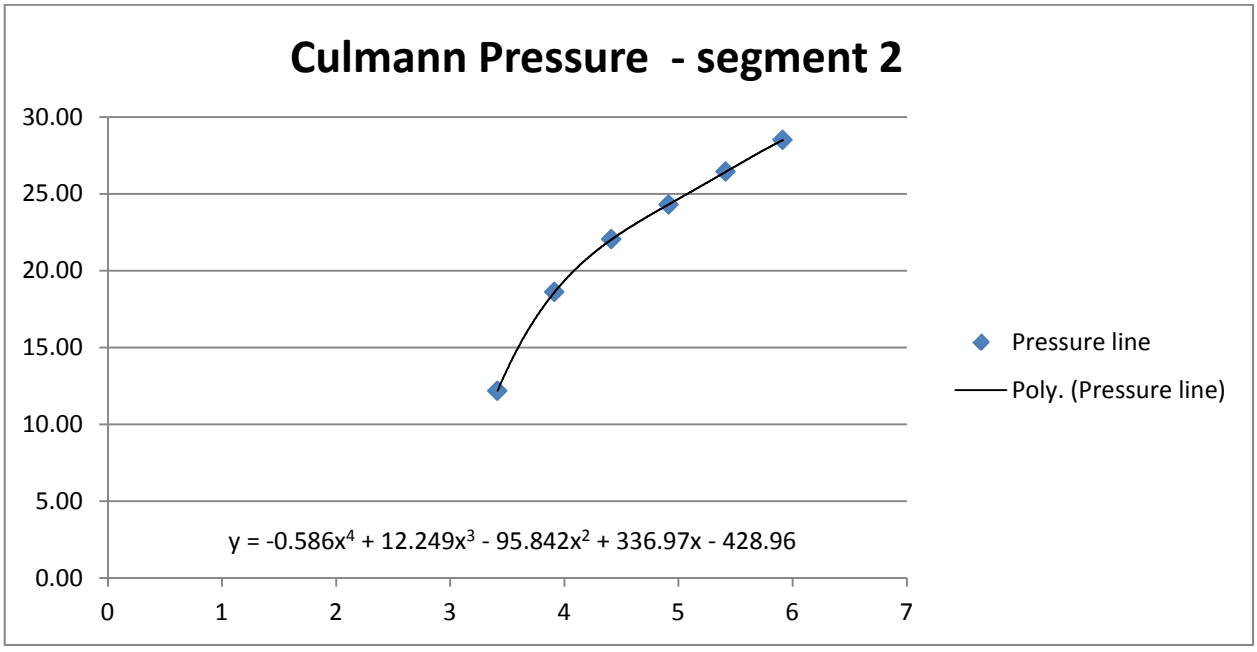

Figure 34 Trend line for segment 2

These two trend lines could then be expressed as one equation that changes when the x-value reaches approximately 3.4 meters. This combined equation could then be integrated over the length of the wall to give the total thrust and to find the position at which it is applied.

The position of the resultant is calculated to 1.89 meters above the bottom of the retaining wall which is about 16 centimeters below the H/3-method.

6.7.1 Effect of surcharge

In other hand calculation methods it is easy to plot the impact from a surcharge. Since Culmann includes the surcharge as weight of the soil, there is no easy approach to plot the distribution. Two different equations were made in Mathcad, one that shows how the maximum thrust changes depending on how large part of the surcharge that is included in the wedges. In the second the surcharge is excluded; by subtracting, the difference is likely to illustrate how the Culmann method handles a strip load, see Figure 35. The dotted line represents the thrust from both the self-weight of the soil and the surcharge. The continuous line is the thrust from the soils self-weight only and the dashed line is the difference is therefore the impact on the total thrust from the surcharge. Noticeable in this case is that the most critical failure plane does not include the entire strip load.

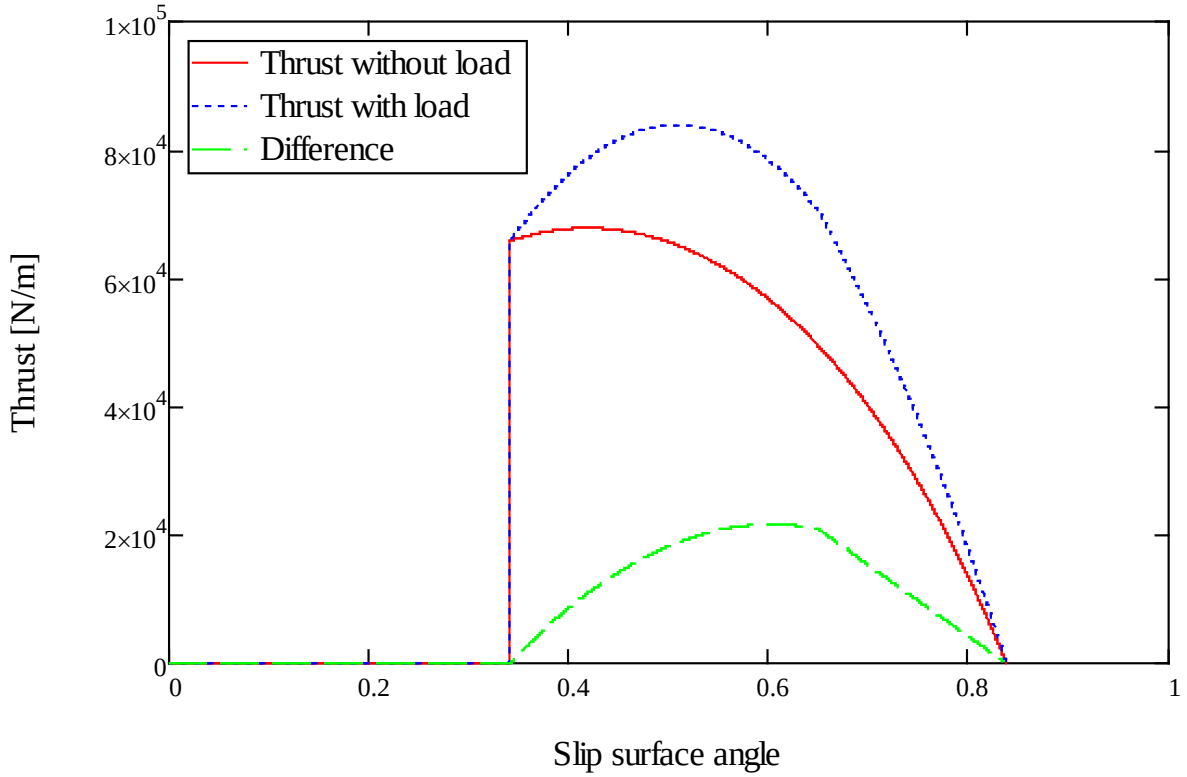

Figure 35 Graph showing the impact on the total pressure from a surcharge

6.8 Impact of surcharge load location

To be able to analyze the importance of the position of the load a number of calculations have been executed. The load has been positioned at the edge of the cantilever wall and then been moved in steps to the original position. The surcharge is 44 kPa. The calculations were made using Rankine theory for active pressure. From these calculations the position of the resulting thrust can be found, see Figure 36 (Note the scale on the Y-axis, the change of scale was made to see the results more clearly).

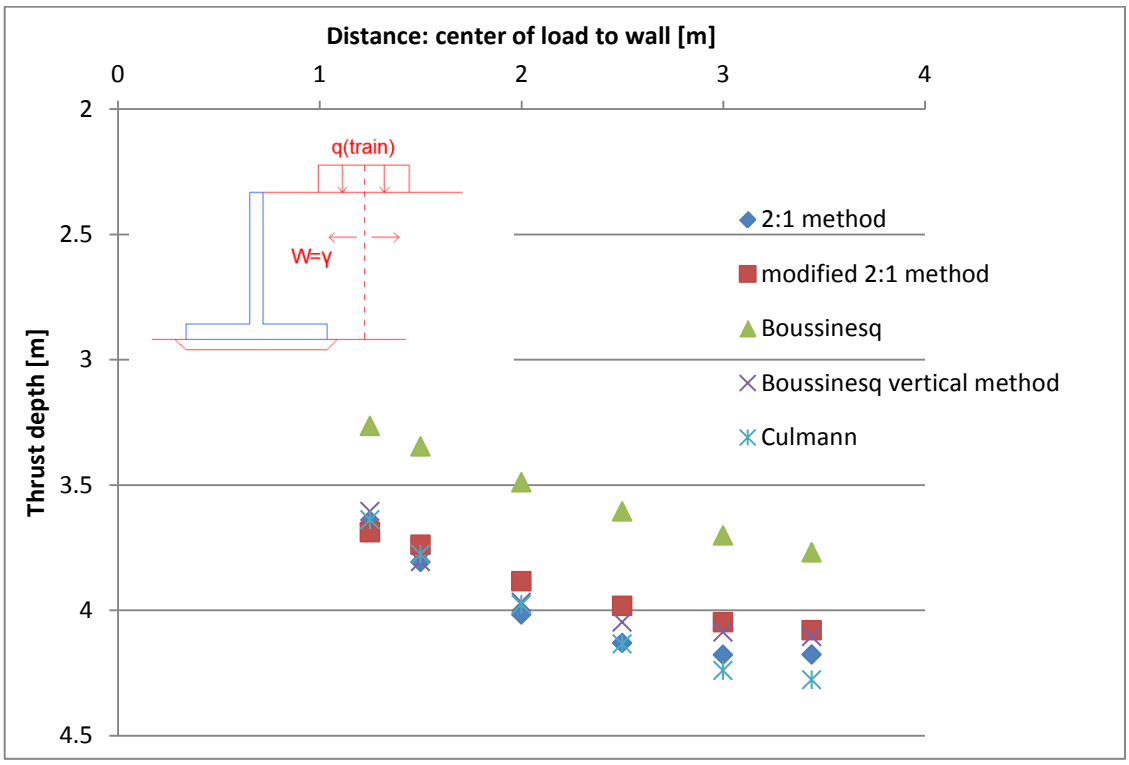

Figure 36 Graph showing the position of the thrust depending on the surcharge placement.

The position of the thrust varies between 3.3 meters depth and 4.3 meters. Calculations were also made that excluded the thrust from the soil weight to see the change of the thrust from the load more distinctly, see Figure 37 (Note that the Y-axis now is scaled from the surface down to the maximum depth).

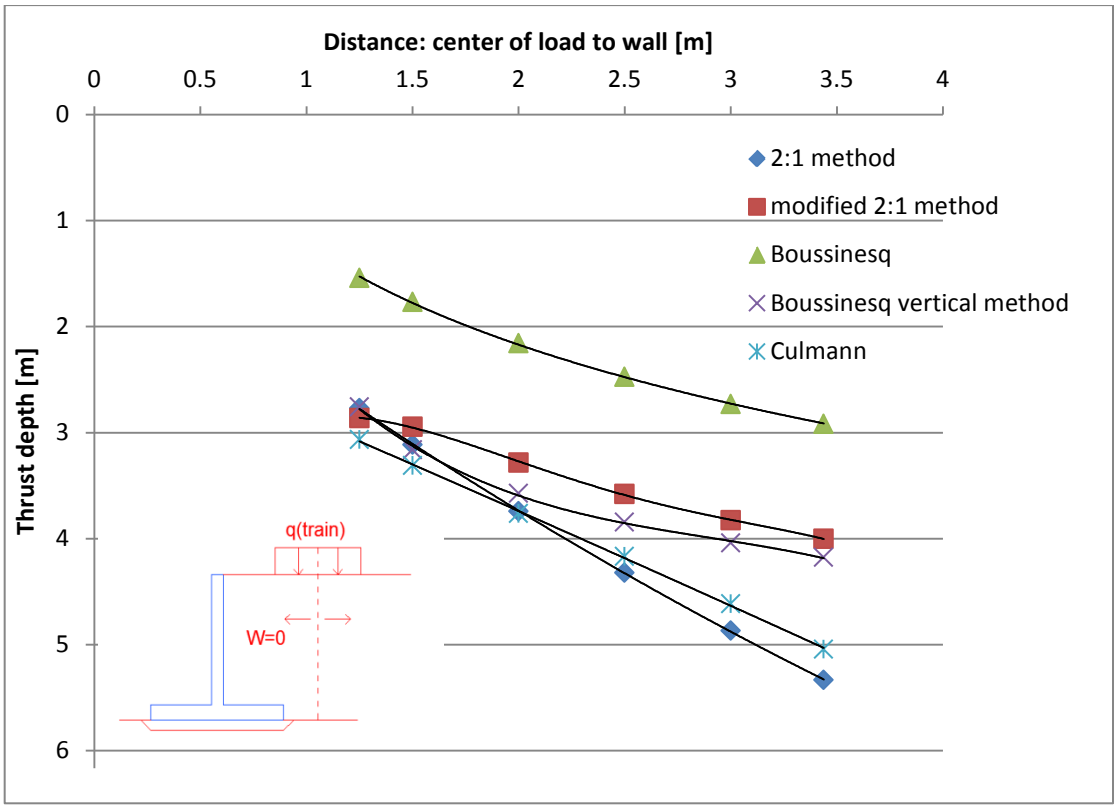

Figure 37 Graph showing the position of the thrust from the surcharge (soil weight excluded) depending on the position of the surcharge.

When the soil is modeled without weight and the thrust is only from the surcharge the depth of the thrust varies between 1.5 meters and 5.3 meters depending on distance from the wall and load distribution method.

To get further understanding on how the positioning of the surcharge affects the load distribution and thrust on the cantilever wall the change in thrust magnitude has been observed. The surcharge is of the same magnitude and the positioning is the same as for the two previous graphs, see Figure 38.

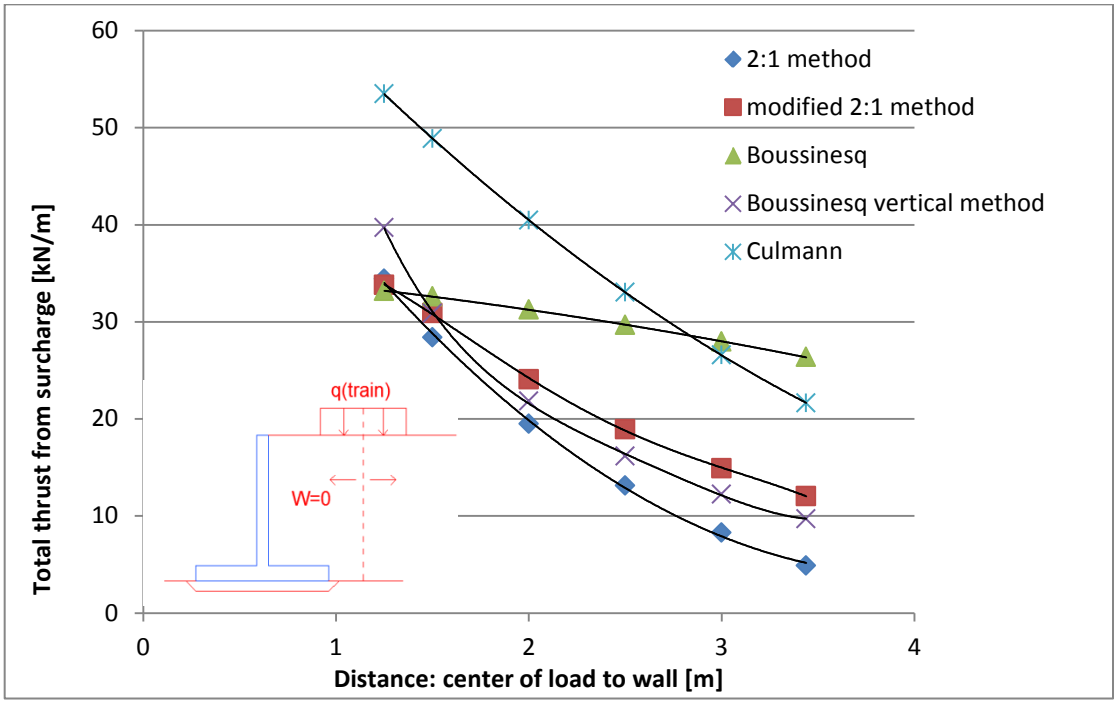

Figure 38 Graph displaying how the magnitude of the thrust from the surcharge varies.

Figure 39 shows the same thing as Figure 38 but in this graph the soil weight is included and this is why the curves do not differ as much.

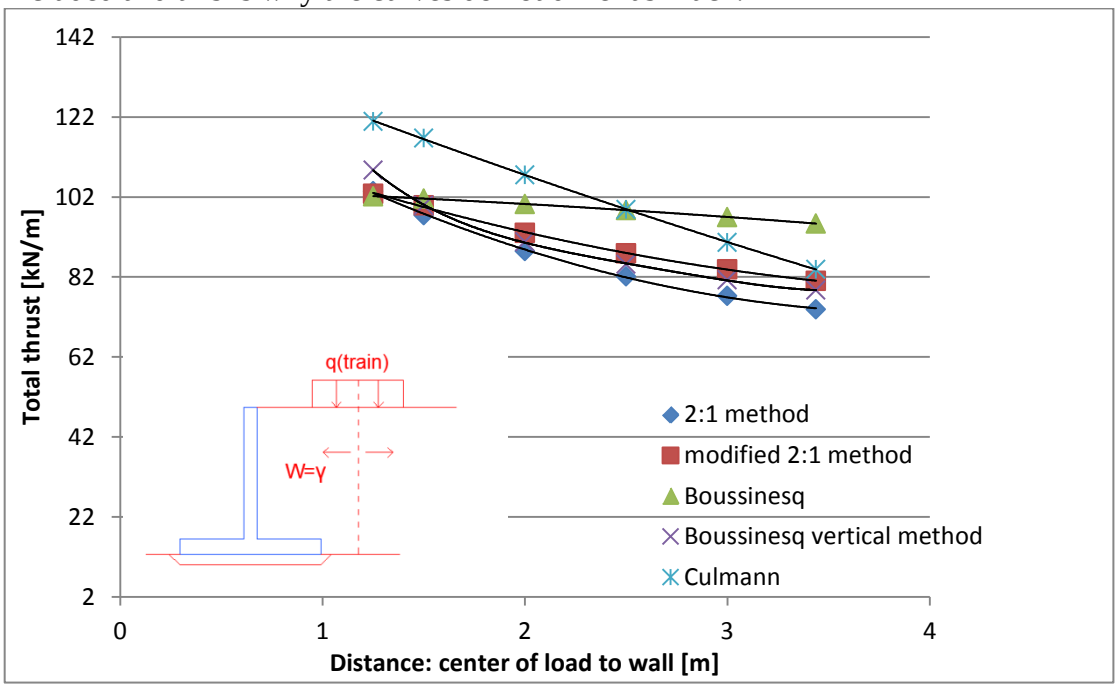

Figure 39 Graph displaying the magnitude of the total thrust depending on surcharge position

An important factor to consider when designing a cantilever wall is the bending moment in the structure. The bending moment depends both on the magnitude of the thrust but also its position. Figure 40**.** displays how the moment varies depending on the position of the surcharge and what load distribution method that is used. For this graph the soil weight is excluded.

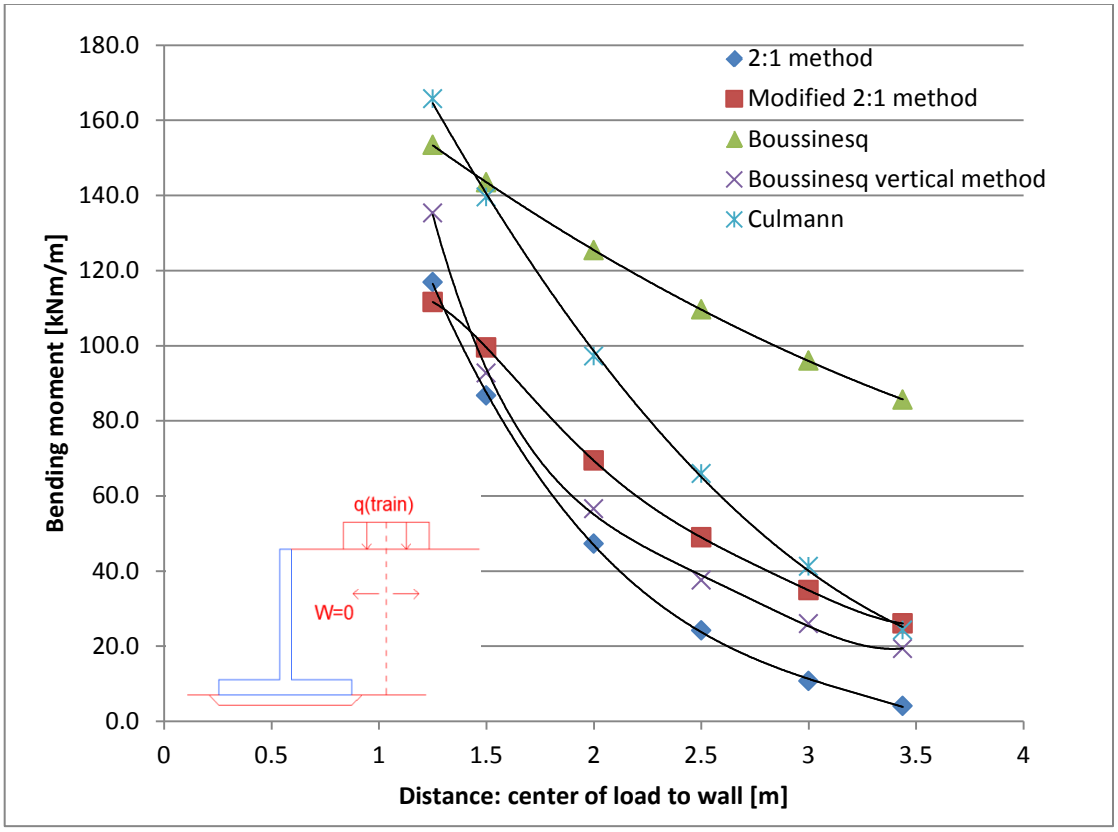

Figure 40 Graph shows the moment depending on thrust position

If the calculations of the bending moment, depending on where the surcharge is placed, are executed when at rest pressure is assumed the results can be compared to results from PLAXIS. The calculations done in PLAXIS have had the same surcharge locations as for the hand calculation methods, see Figure 41. For this graph soil weight is included.

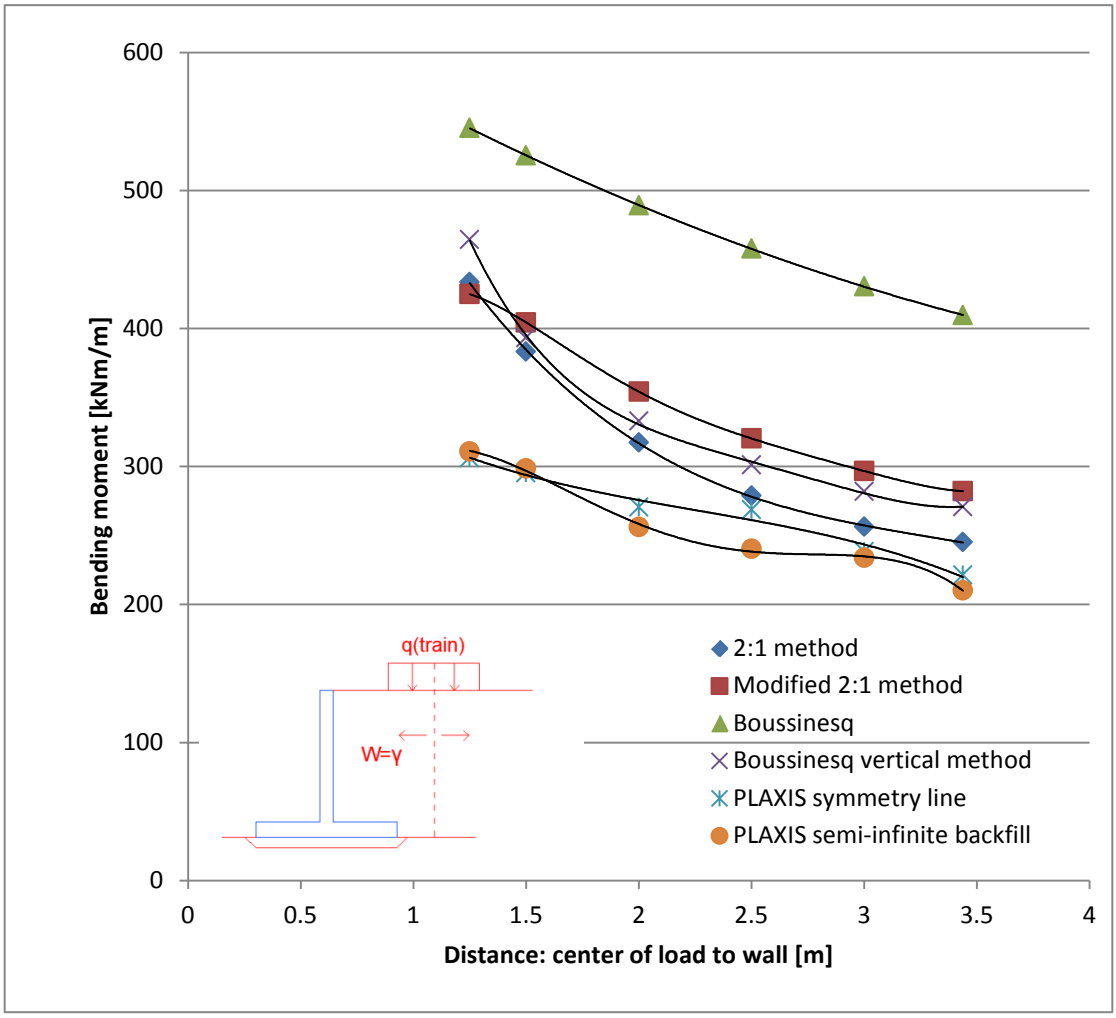

Figure 41 Graph displaying the maximum bending moment depending on surcharge location

7 Discussion

There are some limitations as to which calculations that are comparable. The common hand calculation methods Rankine and Coulomb theory can be implemented both for active- and passive earth pressure. Boussinesqs theory can also be used for both mobilized active and passive pressures, though there are inconsistencies. The Boussinesq elastic equation for horizontal pressure is assuming a rigid wall, resulting in difficulty to interpret for active pressure. To be able to compare Boussinesq theory to active pressure an assumption to exclude the term from the Boussinesq equation that Fehti Azizi refers to in Applied Analyses in geotechnics when describing a rigid wall when calculating for active pressure in this thesis. For at rest pressure the equation is unaffected. The vertical Boussinesq theory is an unused method that is carefully change to mimic the average appearance of the earth pressure profiles, rigidity has been unaffected and the earth pressure coefficient has been included.

The Culmann graphical method is derived from Coulomb method and it is assumed that the body is in failure. Meaning that it is a method that can be compared to mobilized earth pressure but not to the at rest pressure.

The horizontal displacement of the construction is governing in PLAXIS to determine which values that are at mobilized- or at rest pressure. The guidelines for how large displacements are needed to reach active- or passive failure according to Sällfors are compared to the vertical displacement in PLAXIS to determine each case (Sällfors, 2001).

7.1 Cohesion in frictional material

In PLAXIS the soil reaches failure instantly at ground level since it does not contain any strength according to the program. Cohesive soils do not have this problem due to the cohesion, see equation below for Rankine method:

$$\sigma_{horizontal} = \sigma_{vertical} \cdot K_a - 2 \cdot c \cdot \sqrt{K_a} \tag{7.1}$$

Meaning there is strength at the top of the layer. Since PLAXIS result in failure, cohesion is added to the ballast layer even though it is a frictional material (Brinkgreve, Engin, & Swolfs, PLAXIS 3D Material Models Manual 2011, 2011)). The reason such an assumption can be done is as that there is not only one failure envelope describing the stresses at failure. By the Mohr circle made by σ_a and σ_p arbitrary failure envelopes can be made, for example by adding cohesion, moving the envelope in the y-axis and change the internal friction angle so that the envelope intersects the Mohr circle, see Figure 42. In other words, as long as the boundary conditions to failure are the same, the envelope can be modified. Also, the linear Coulomb failure envelope is an assumption (Ahlén, 2012). It is not a linear function but is more logarithmic, increasing greatly at low stresses to later move towards an asymptote at higher stresses, see Figure 43

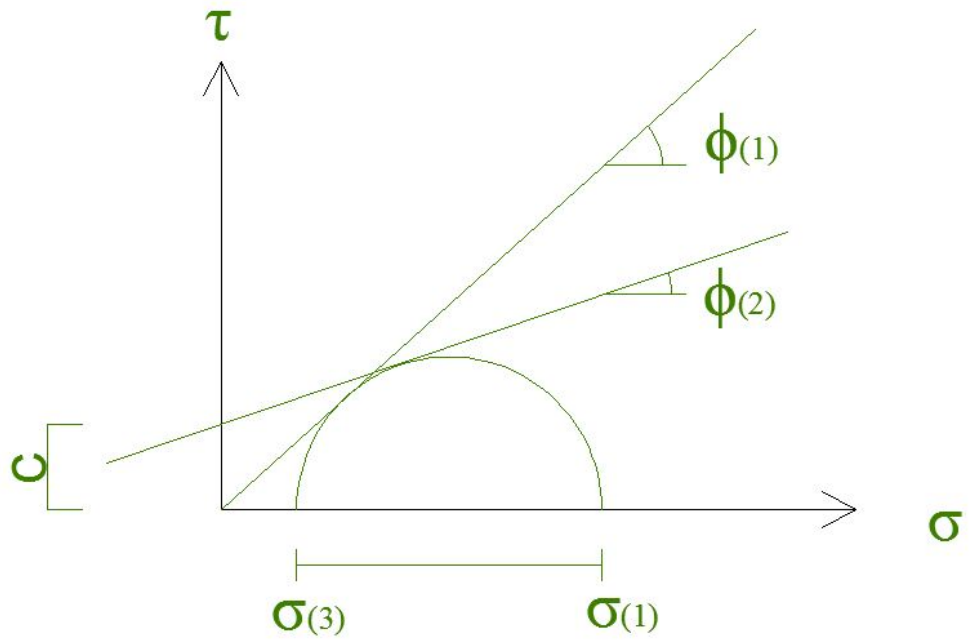

Figure 42 Illustration of how specific Mohr circle can have different resulting failure envelopes

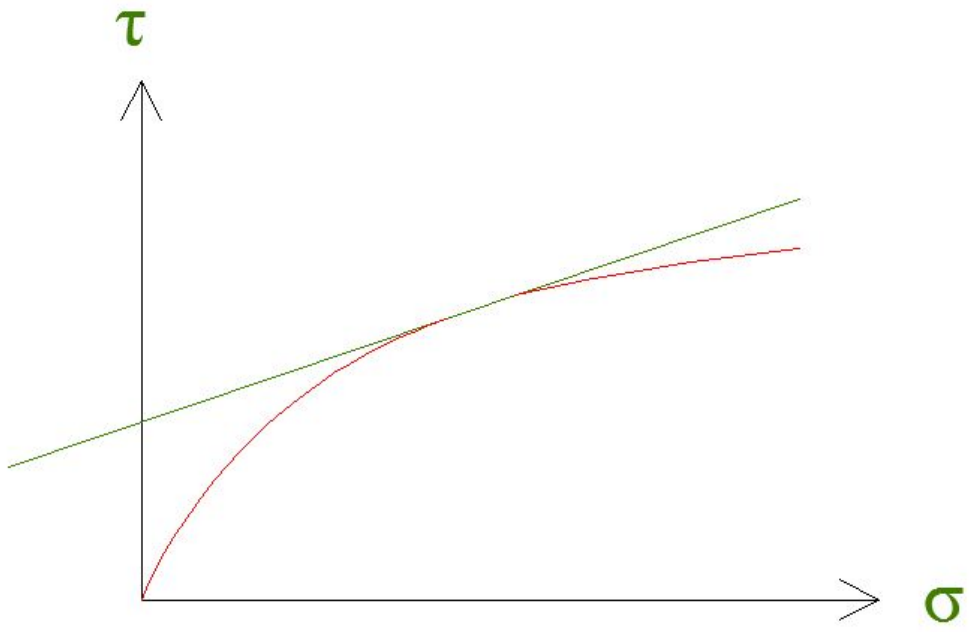

Figure 43 Assumed straight failure envelope and realistic failure envelope

To evaluate the impact by cohesion in a frictional material, an extra Mathcad calculation was performed where Rankine theory and 2:1 load distribution was used. An added cohesion of 3 kPa to the ballast layer contributed according to equation 7.1. The result is presented in Figure 44, Figure 45 and Table 10.

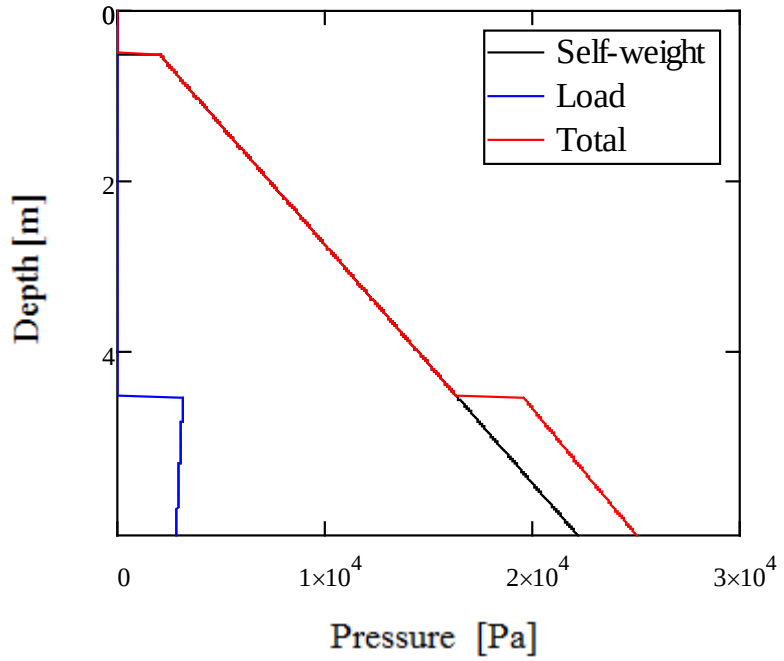

Figure 44 Calculations with cohesion included

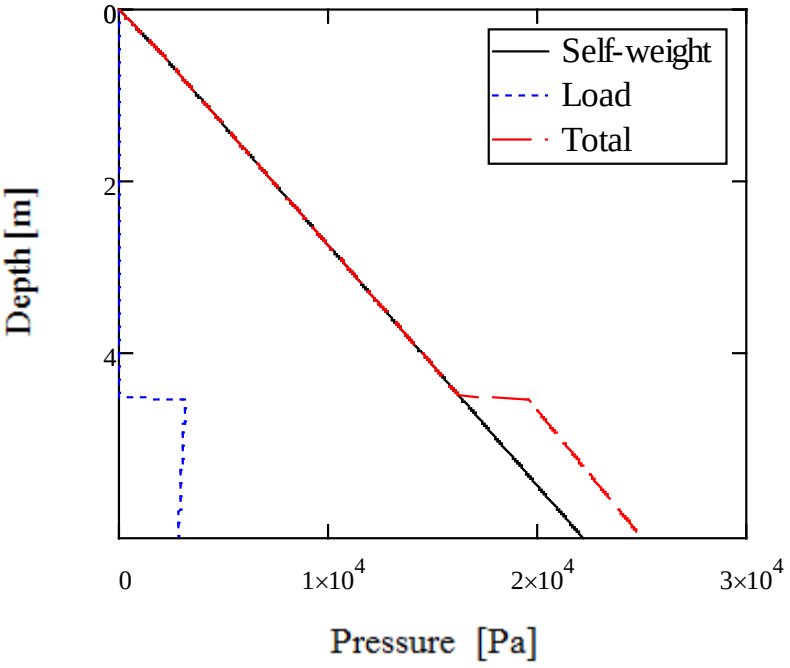

Figure 45 Calculations without cohesion

Table 10 Comparison of results cohesion included and excluded

	Rankine	Rankine - cohesion
P_{tot} [kN/m]	73,9	73,4
M_x [kNm/m]	147	144
X_{cm} [m]	4,176	4,203

A conclusion is that, by adding 3 kPa and lowering the internal friction angle to 20 degrees in the ballast layer, the resulting change is negligible.

Another way to avoid failure at ground surface is to assign the ballast layer elastic model instead of the Mohr-Coulomb model. In an elastic model, the soil cannot reach failure or plasticity (Olsson, 2012). Since this project aims to discuss the earth pressure against a retaining wall, cases such as bearing capacity failure in the ballast layer can be rejected which is why an elastic model is still within the projects limitations.

7.2 Wall roughness

Wall roughness affects the resultant by changing its direction and also its magnitude. In Rankine theory the wall roughness equals the slope of the backfill, meaning that the resultant will have the same angle as the backfill. In the case of the Södertälje project the backfill is horizontal and therefore no wall roughness is taken into account. This gives an overestimation of the magnitude of the horizontal component of the earth pressure and an underestimation on the axial forces of the wall since the angle of the resultant is changed. This could lead to failure of the plate and a more expensive vertical part of the wall than necessary.

Both Boussinesq theory and Coulomb theory takes wall roughness into account independent of the slope of the backfill.

7.3 Multi criteria analysis

To determine which soil models to use for calculations of the soil stresses a multi criteria analysis is performed. Scoring is made depending on how the method satisfies different aspects of the calculation of soil stresses (Gamper, Thöni, & Weck-Hannemann, 2006).

The scoring in the multi criteria analysis is:

- -1: Not acceptable solution.
- 0: Acceptable solution.
- +1: Satisfactory solution.

	Rankine	**Coulomb**	**Boussinesq**	**Culmann**
Wall roughness	0	1	1	1
Ground slope	1	1	1	1
Wall inclination	0	1	1	1
Slip surface (active side)	0	0	1	0
Slip surface (passive side)	1	-1	1	-1
Finding failure surface angle	0	0	0	1
Hand calculation	1	1	1	0
Computer	1	1	1	-1
Total	**4**	**4**	**7**	**2**

Explanations to the different criteria:

- Does the method include parameters wall roughness, ground slope and wall inclination?
- Slip surface (active side): is the assumed slip surface close to the reality?
- Slip surface (passive side): is the assumed slip surface close to the reality?
- Finding failure surface angle: does the method assume a failure angle or does it determine it?
- Hand calculation/Computer: Is the method easy to put into practice?

Boussinesq is given the best score for the slip surface criteria. That is because it uses a non-linear surface, much closer to reality than a linear. The Coulomb- and Culmann graphical method is set a non-acceptable score for the passive slip surface. Since Coulomb results in higher passive pressure and thrust which leads to an underestimation of the need of retaining structure's strength. The same will relate to Culmann since it is based on Coulomb theory.

Culmann's graphical method is the only method that determines the most critical failure surface, hence it is given a higher score than the others. For the other methods the angle depends on the internal friction angle according to (Azizi, 2000):

$$\alpha(active) = \frac{\pi}{4} - \frac{\varphi}{2} \tag{7.2}$$

$$\alpha(passive) = \frac{\pi}{4} + \frac{\varphi}{2} \tag{7.3}$$

All the methods, except Culmann's, are simple to use for both hand calculations and for e.g. Mathcad. Culmann's on the other hand can be awkward to use at first and for the use in computer programs several simplifications were made. Hence it is declined the highest score compared to the other methods.

7.4 Culmann's graphical method

The active earth pressure was calculated using the software Mathcad instead of doing it by hand. By doing so some trigonometric difficulties arose which lead to a more time consuming programming. The advantage of this is that by using trigonometry the human error from drawing lines and measuring with a ruler is removed. Another advantage is that the location of the thrust can be found more effectively than if it was done by hand.

An advantage to using Culmann's graphical method is that it includes surcharges in a very simple way. A strip load for example is simply added as weight to the soil (if the surcharge is part of the current trial wedge). For the other hand calculation methods a strip load has to be added by using some kind of load distribution method.

A disadvantage of the Culmann method is that it is not possible calculate the at rest pressures. The trial wedges are in a state of failure so only the active, or passive, pressures are obtained. This means that additional calculations need to be made, using a different soil model.

Culmann's graphical method assumes planar slip surfaces just like Rankine and Coulomb. This is a decent representation of an active failure but the Boussinesq non-linear slip surface is closer to reality.

Culmann's graphical method can be considered as an easy hand calculation method. However, to obtain the location of the thrust the calculations are far too time consuming to do without a computer. The strength and the benefit of the method are therefore reduced when calculated by hand.

As mentioned earlier the angle of the failure plane is not predetermined in the Culmann method but rather calculated from it. With this the surcharge may be excluded, partially included or fully included into the thrust. When the calculations were made with, for example, Rankine theory the thrust from the surcharge does not affect the angle of the failure plane but is simply added by using one of the load distribution methods. According to equation 7.2 the angle of the failure plane is 24 degrees. With this failure wedge only around 0.6 meters of the surcharge is included and by adding the entire load to the total thrust an overestimation of the active earth pressure is likely to occur.

7.5 Load distribution methods

Chapter 7.4 discusses the yielding of the wall and the corresponding earth pressure coefficient to be used. Since the yielding at the top and bottom is the same, the at rest pressure coefficient come close to being the average between the two boundaries. When comparing results for the different calculations, we also find that the at rest pressure coefficient gives the most reasonable results compared to PLAXIS.

Since at rest pressure is the most suitable state to investigate compared to PLAXIS there is no need to separate the soil pressure models since they use the same K_0-value.

7.5.1 Infinite load

The assumption of an infinite load from a train is of course a great overestimation of the effects from the train load. The reason to why it is included in this thesis is solely for the purpose of comparison. When analyzing the different results it is obvious that choosing a load distribution will lower the pressure severely and will lead to a more suitable and cheaper retaining construction.

7.5.2 2:1-Method

The 2:1-method gave the lowest thrust of all the distributions that were tested. This is probably due to the fact that the purpose of the 2:1-method is to find an average pressure underneath the loaded area, and not the distribution of a load horizontally. The two points in Figure 46 are the points where the 2:1-method gives accurate results. These values are assumed to be the same for the entire horizontal line.

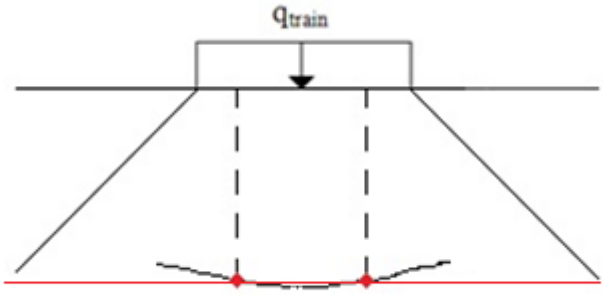

Figure 46 A secant is drawn from the two accurate points

When comparing the results to PLAXIS it is obvious that the method is inappropriate when the load is not close to the retaining structure, the difference in thrust is approximately18.2 kN/m. When the load is in the vicinity of the retaining structure the results are more similar to the PLAXIS results than Boussinesq elastic solution. In this case the method becomes more similar to how load distribution acts.

Noticeable is that the 2:1 method results in a thrust that is approximately as high as any of the other load distribution methods when the load is in contact to the wall, a case commonly used for calculating the forces during a derailing. In this case the 2:1-method gives a resultant that is 38 kN/m higher than PLAXIS.

7.5.3 Boussinesq's elastic solution

When viewing the different results from both the hand calculations and the FE-models there is one load distribution method that stands out greatly. Boussinesq's elastic solution for calculating the increase in horizontal pressure from a strip load gives results that are markedly larger than the other methods. This may partially be explained by the fact that the values for the increased pressure are doubled to take the rigidity of the wall into consideration, but even if this doubling is excluded the values greatly exceeds the results from other methods.

The fact that the increase in horizontal pressure is doubled due to rigidity of the retaining wall is also inconsistent to the fact that the calculations for the earth pressure from self-weight has been done using the coefficient of active earth pressure. For this reason we have chosen to exclude the doubling of the equation in the case with mobilized active earth pressure.

The total thrust with Boussinesq's elastic solution is 167,9 kN compared to PLAXIS 141.5 kN. In other words, Boussinesq results in the highest total thrust of all calculation methods when the load is located in the middle of the superstructure and K_0 is used. The stress profile is very different between Boussinesq and PLAXIS, both of them also differ noticeably compared to the other methods. Boussinesq increases drastically in the first meters to later increase almost linearly, PLAXIS on the other hand has very low values the first meters to thereafter increase drastically at depth. The shape of the Boussinesq profile leads to a center of mass that varies very little in depth regardless of the position of the surcharge. This is due to the fact that most of the pressure is concentrated at the first meters for Boussinesq's elastic solution.

7.5.4 Boussinesq's equation for vertical stress

The Boussinesq equation for vertical stress gives a load distribution that has its point of concentration approximately 0.35 meters lower than Boussinesq's elastic solution and the shape of the distribution is more aligned with the other distributions.

Figure 36, Figure 37 and Figure 38 indicate that the method is less conservative than the Boussinesq elastic solution. Also, the Boussinesq's equation for vertical stress leads to similar results as for the two different 2:1 methods. For this specific conceptual model the choice between Boussinesq's equation for vertical stress or modified 2:1 method would be small.

In Figure 47 the pressure profiles for the mobilized active earth pressure from the strip load. It can be seen that Boussinesqs elastic solution is several times larger than the equation for vertical pressure. For this reason we have tampered with the equation to find a more reasonable profile. The best results were found when the equation was doubled.

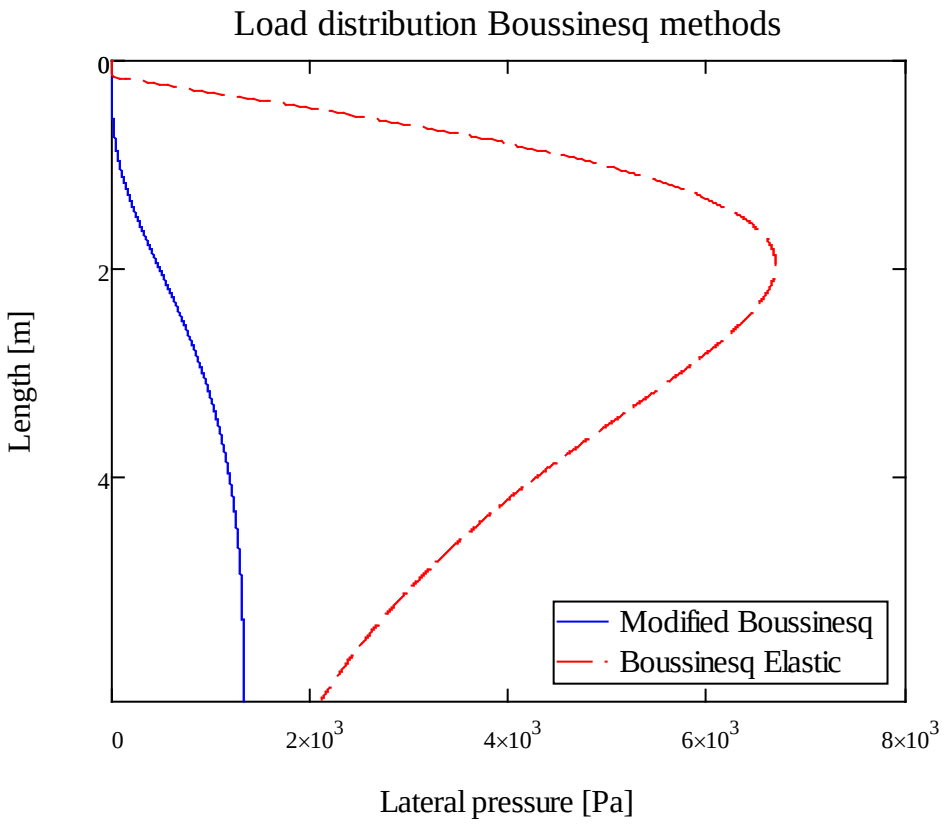

Figure 47 Pressure profiles for the different Boussinesq methods

7.5.5 Bending moment

Table 7 shows the resulting bending moments from different load distribution methods. The moment depends on the magnitude of the thrust and the lever arm (distance between the joint of the cantilever, seen as a fixed-end, and the center of mass of the earth pressure profile). As in the case of Boussinesq, it provides relatively similar thrust as PLAXIS; but the lever arm is very long compared to the other calculation methods in the comparison. See Figure 48 and Figure 49 for an overview of the results in this project.

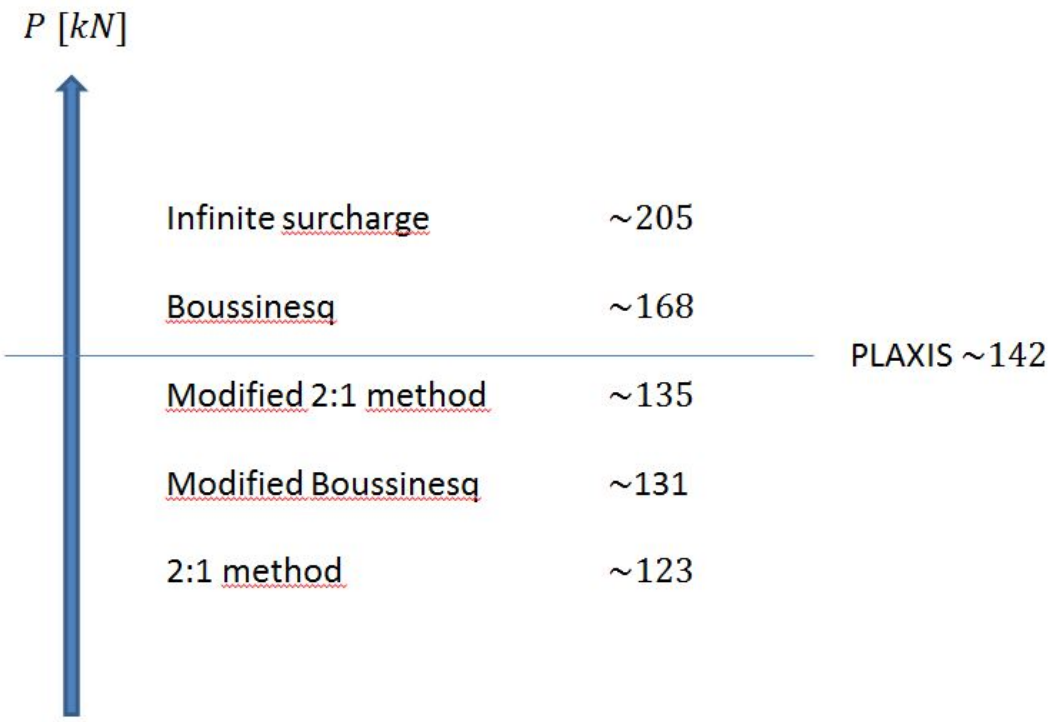

Figure 48 Overview of resulting thrust

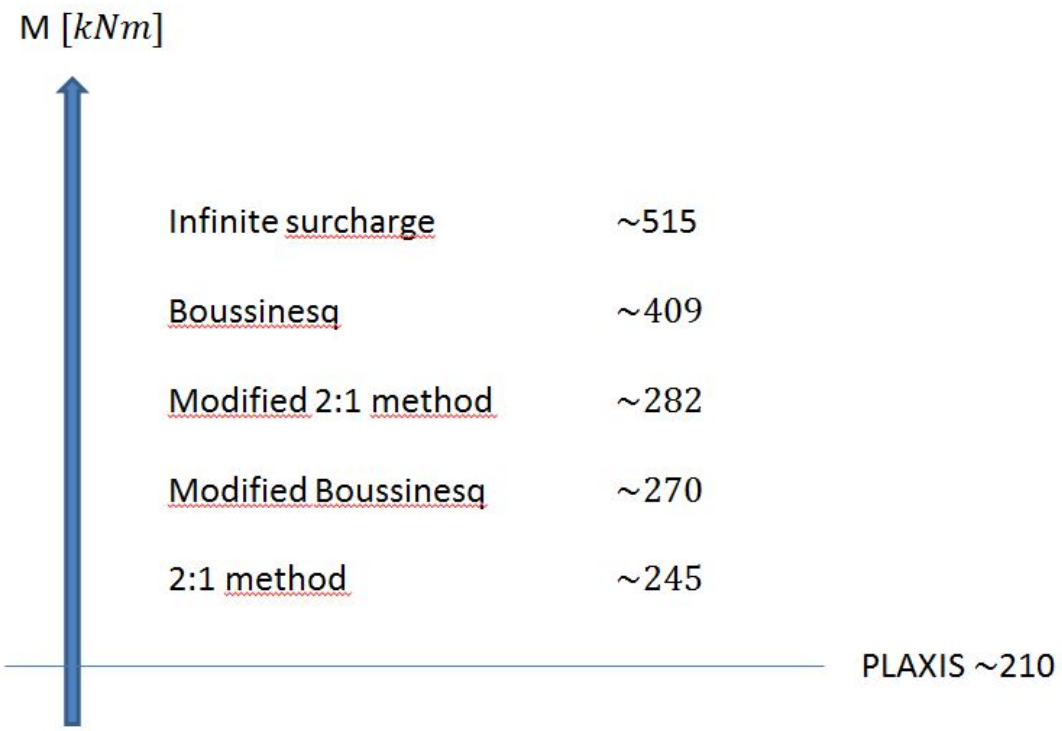

Figure 49 Overview of resulting bending moment

This is a challenge in the choice of an earth pressure calculation method and load distribution method since the choice decides if the construction will be calculated conservatively and therefore at a higher cost than required.

To illustrate the impact of the lever arm the length is set to $\frac{1}{3} \cdot H_{wall}$ instead of the center of mass of the pressure profile. In Table 11 the bending moment is found and also the difference between the magnitude of the moment compared to the result in Table 6. As seen, the change is minor except for the Boussinesq elastic solution, which decreases by 16%.

Table 11 Bending moment when the lever arm is chosen as 1/3 of the wall height

Load distribution method	Bending moment [kNm]	ΔM [kNm]
2:1 method	253	+8
Modified 2:1 method	278	-4
Boussinesq elastic solution	345	-64.5
Boussinesq vertical method	270	-0.5

For surcharges with lower magnitude than that of a single track railway a lever arm decided by the $\frac{1}{3}$ −method could be satisfactory. For larger surcharges the affect from the load distribution method will have a very large impact on the pressure profile

which may make the $\frac{1}{3}-$method inapplicable. Another factor that may make the $\frac{1}{3}-$method inappropriate is if the material properties in the soil profile vary a lot.

7.6 PLAXIS

For many of the models arc length control has been disabled. This is because an error, "Load advancement procedure failure", occurs. This may change the results slightly but according to the PLAXIS support this should not make a significant difference (Xing-Cheng, 2012).

To achieve fully mobilized active pressure the displacements need to be approximately 0.1% the total height of the retaining structure. For passive pressure the displacements need to be 0.5%, see Figure 50. As seen in Figure 20 the cantilever wall is rotating clockwise. When measuring the wall movements at the top and bottom of the wall we find that the displacements at the top are approximately 0.07% which is about a tenth of what is needed to reach fully mobilized passive pressure. At the bottom of the wall the displacements reach 0.104% of the total wall height which is just enough to reach active pressure (Sällfors, 2001). This means that there will only be fully mobilized active earth pressure, where K_a should be used, at the very bottom of the wall. Up to the point of rotation the earth pressure coefficient would have a value between K_a and K_0, and above the center of rotation the coefficient would be between K_0 and K_p.

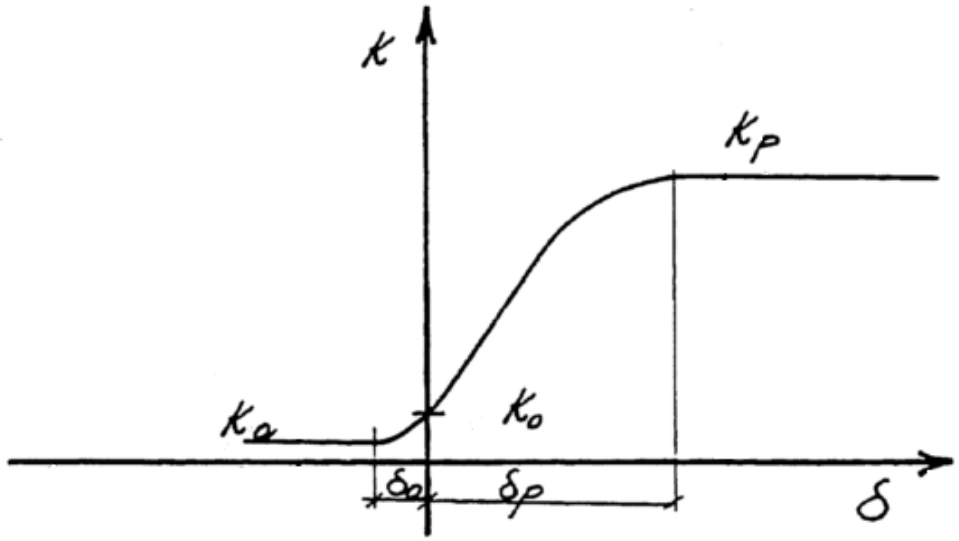

Figure 50 Graph displaying how the earth pressure coeffiecent differs with displacement of the wall

This means that the soil in the hand calculations is in a different state compared to the PLAXIS model. In the hand calculations the entire soil mass is either in a state of active pressure or at rest pressure whereas the soil in the PLAXIS model is in at rest, active and passive pressure depending on depth. Perhaps the wall movements can be predicted and adjustments can be made to the hand calculations accordingly.

7.7 Impact of surcharge location

What can be seen from Figure 36 is that all thrusts descended approximately 0.5 meters when the load was moved from the closest to the farthest location. When this

is compared with the values from Figure 37 we can see that the thrusts of all the distributions except for the 2:1-method and the Culmann method are lowered by approximately the same length (ca. 1 meter). The reason to why the total thrusts are changing at more or less the same rate is that the 2:1-method and the Culmann method decrease rapidly in magnitude as can be seen in Figure 38. Of course the thrust from the soil weight mitigates any such affects. In Figure 38 we can also see that all the distributions except for Boussinesqs horizontal earth pressure are markedly lowered when the load is moved farther away from the cantilever wall.

A factor that should be kept in mind when comparing these different graphs, especially Figure 38 is that the with the Culmann method the most critical failure plane is found and not predetermined, unlike the other hand calculation methods. This means that the surcharge does not necessarily have the same magnitude if one calculation is made where the soil weight is excluded and one where it is included since the angle of the failure plane may change. This is why the magnitude of the surcharge in the Culmann method looks to be very large in the graphs where the soil weight is excluded.

When analyzing the different calculation results concerning the magnitude of the thrust PLAXIS is one of the highest. From the graphs in Figure 40 and Figure 41 it can be observed that PLAXIS gives the lowest bending moment for all surcharge locations. This is because the location the position of the resultant is markedly lower in PLAXIS compared to most of the hand calculation methods.

When the position of the surcharge is moved the thrust does not change by much, only the position of the resultant. A hypothesis was that this may be because the hand calculations assumed a semi-infinite backfill unlike the PLAXIS model. To test this, a PLAXIS model was made where the backfill extended 30 meters. The results from these calculations were very similar which disproves this hypothesis.

7.8 PLAXIS and hand calculations

With hand calculations executed with the assumption of at rest pressure and putting the results of the different load distribution methods into a graph we can compare these to the results from PLAXIS, see Figure 51.

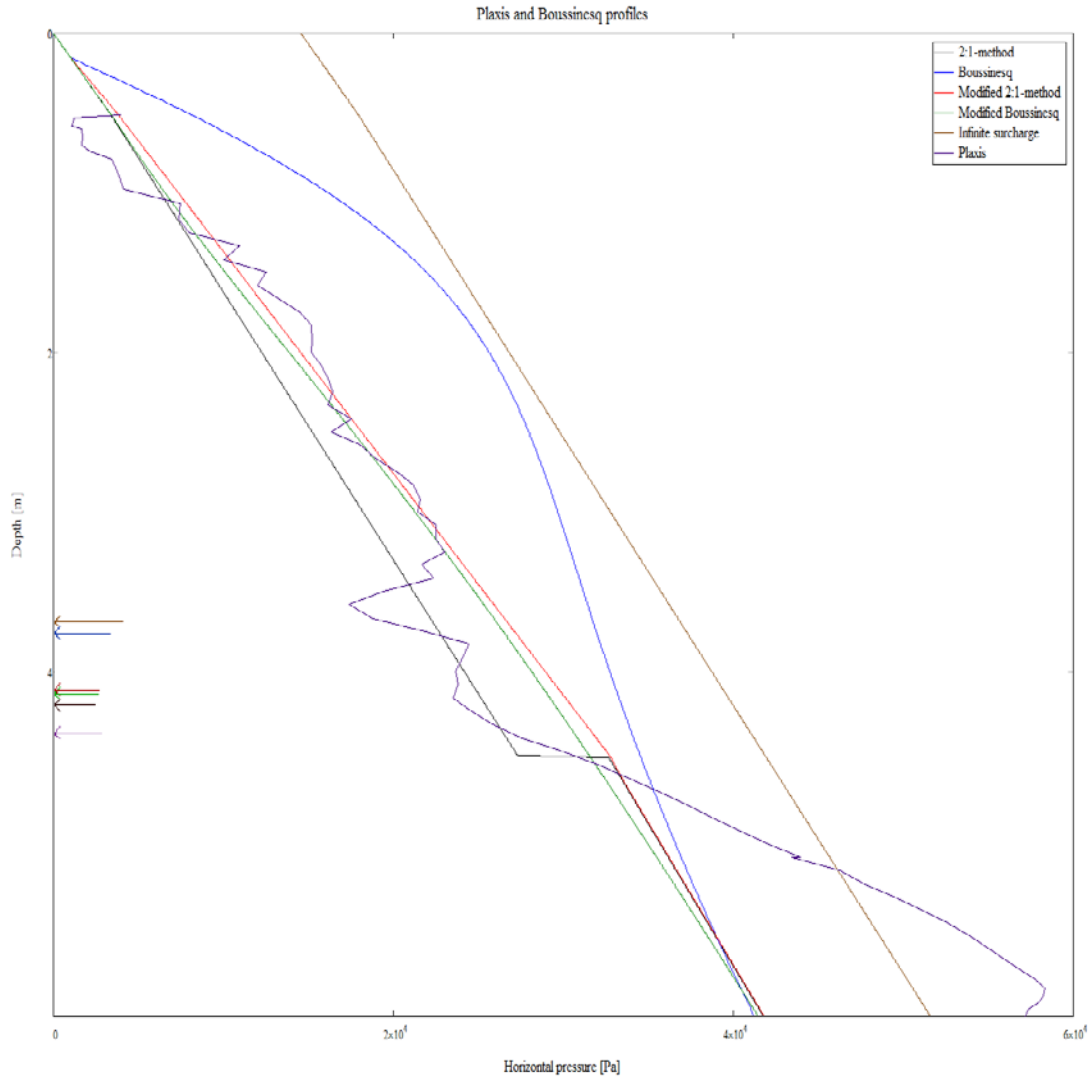

Figure 51 Graph displaying pressure profiles from PLAXIS and hand calculations where at rest pressure is assumed

From this graph it can be seen that the pressure profile from PLAXIS aligns very well with three of the hand calculation profiles but then increases rapidly the last 1.5 meters. The colored arrows, to the left in the graph, show where the resultants act on the cantilever wall as well as their relative magnitude towards each other.

7.9 PLAXIS and ADINA

After calculating a number of models it is clear that the mesh generation has a significant impact on the results. The total thrust may vary by several percent and the location of the resultant. Mesh problems can lead to unrealistic deformations.

When working with these FE-softwares, PLAXIS is noticeably more user friendly in its design. PLAXIS also has more options, probably due to the fact that it is specialized in geotechnical engineering, unlike ADINA which has several fields of application. Both softwares have the ability to change the model with time. PLAXIS uses its so called "staged construction" which is very intuitive and easy to use. ADINA on the other hand uses a function called "birth" or "death" of cells and is not as simple as the staged construction. When using "staged construction" the user has to be very careful not to miss something that is supposed to activated or deactivated such as interfaces that are used to model wall/soil interaction. PLAXIS may be able to calculate the problem without the interface but the results will be less accurate.

What is positive about ADINA is that the user has full control over the model. The user is able to influence the mesh more directly compared to PLAXIS.

Unfortunately we did not manage to make the model in ADINA work properly and therefore we cannot compare any results between the two programs.

7.10 Eurocode

Eurocode has moved the partial factor γ_d from the material properties to the unfavorable loads. This means that when a retaining structure is being built the magnitude of the surcharge has a larger impact on the design than it had before and the material property now has a smaller impact.

The η-value considers a number of different aspects when designing a geo-construction. One thing that it does not take into account is the ratio between the surcharge load and the soils self-weight. The higher the ratio between the surcharge/self-weight the higher the importance of choice of load distribution method is.

8 Conclusions

8.1 Soil model

Since Boussinesq's theory for soil pressure takes wall friction, wall inclination, and backfill slope into account and has a non-linear slip surface we believe that it gives the best representation of how soil behaves. Unfortunately the results cannot be compared to PLAXIS since it is difficult to simulate active pressure.

8.2 Load distribution method

Close to the retaining structure the difference in thrust is negligible between the load distribution methods. Meaning that close to the wall, the choice of method does not matter. Further away, the choice of method becomes more important since they vary a lot. However, the location of the thrust may differ greatly and therefore the bending moment will as well.

From Figure 51 it can be seen that the modified 2:1-method is the one that is closest to the PLAXIS results and is in this conceptual model the recommended method.

8.3 Position of the load

The position of the surcharge on the backfill has a major impact on where the resultant will be located. The closer the surcharge is to the retaining structure, the higher the position of the resultant will be. For the modified 2:1-method and Boussinesqs elastic solution the resultant from the surcharge is constantly above 1/3 of the wall (measuring from the bottom) for the surcharge placements tested. These two methods however do not seem to be applicable at large distances as they do not decrease in magnitude very much (especially the elastic solution).

8.4 Eurocode and η-values

A conclusion concerning Eurocode is that it does not recommend any particular calculation method. The only guide lines concerning the method of calculation is that a number of factors that need to be considered which can be found in chapter 2.1.2.

A η –value could be added to consider the ratio between surcharge and self-weight. The higher the ratio the lower the η -value

The different earth pressure models do not take the same aspects into account when deciding earth pressure coefficients. This leads to some of them being more conservative than others. Rankine is seen as the most conservative since it does not take wall inclination and wall friction into account in the same way as Coulomb and Boussinesq. Eurocode could add guidelines as to which soil model that should be used depending on the circumstances.

8.5 FE-Software

Since ADINA never was able to run the model of the cantilever wall a conclusion on the results is impossible but it can be concluded that PLAXIS is easier to work with and is broader in its applications in geotechnical engineering.

9 Bibliography

Ahlén, C. (2012, 03 23). Cohesion. (M. Petersson, & M. Pettersson, Interviewers)

Azizi, F. (2000). *Applied Analyses In Geotechnics.* London: E & FN Spon.

Brinkgreve, R., Engin, E., & Swolfs, W. (2011). PLAXIS 3D Material Models Manual 2011. Delft: PLAXIS company.

Brinkgreve, R., Engin, E., & Swolfs, W. (2011). PLAXIS 3D Reference Manual 2011. Delft: PLAXIS company.

Gamper, C. D., Thöni, M., & Weck-Hannemann, H. (2006). *A conceptual approach to the use of Cost Benefit and Multi Criteria Analysis in natural hazard management.*

Geoteknik, I. F. (2010). *Tillämpningsdokument Grunder.* Stockholm: IEG.

Kullingsjö, A. (2007). *Effects Of Deep Excavations In Soft Clay On The Immediate Surroundings.* Göteborg: Chalmers University Of Technology.

Olsson, M. (2012, 04 05). Failure in material models. (M. Petersson, & M. Pettersson, Interviewers)

Standardization, E. C. (2004). *SS-EN 1997.* Stockholm: Swedish Standards Institute.

Sällfors, G. (2001). *Geoteknik: jordmateriallära, jordmekanik.* Göteborg: Chalmers University of technology.

Varghese, P. (2005). *Foundation Engineering.* New Delhi: Prentice-Hall of India.

Whitlow, R. (2001). *Basic Soil Mechanics.* Dorschester: Pearson Education Ltd.

Wong, J. (2012, 05 15). Horizontal pressure. *Stress related question*.

Xing-Cheng, L. (2012, 05 17). Arc-length control. *Stress related question*.

Appendix A **Mathcad calculations - Rankine**

$\gamma_{ballast} := 20 \cdot \frac{kN}{m^3}$

$\gamma_{fill} := 18 \cdot \frac{kN}{m^3}$

$\phi := 42 \cdot deg$ See table 5.2-4 TK GEO 11

Geometry

$H_{total} := 6.865 \cdot m$

$H_{slab} := 0.700 \cdot m$

$H_{wall} := H_{total} - H_{slab} = 6.165\,m$

$\alpha_{wall} := 1.85 \cdot deg$ Wall inclination to vertical

$W_{slab} := 6.600 \cdot m$

$W_{wall.bottom} := 0.600 \cdot m$

$W_{wall.top} := 0.400 \cdot m$

$L_{C.track1} := 3.438 \cdot m$ Center of track

$D_{ballast} := 0.510 \cdot m$ Layer thickness

$W_{sleeper} := 2.5 \cdot m$ Assumed width for sleeper

$q_{train} := 44 \cdot kPa$ Assumed load, see Eurocode

$D_{sleeper} := 0.155 \cdot m$

Vertical stresses

$$\sigma_v(z) := \begin{cases} \left(\gamma_{ballast} \cdot z\right) & \text{if } 0 \cdot m \le z \le D_{ballast} \\ \left[\gamma_{ballast} \cdot D_{ballast} + \gamma_{fill} \cdot \left(z - D_{ballast}\right)\right] & \text{otherwise} \end{cases}$$

$z_{plot} := 0m, 0.01m .. H_{wall}$

$\sigma_v(0) = 0\,Pa$

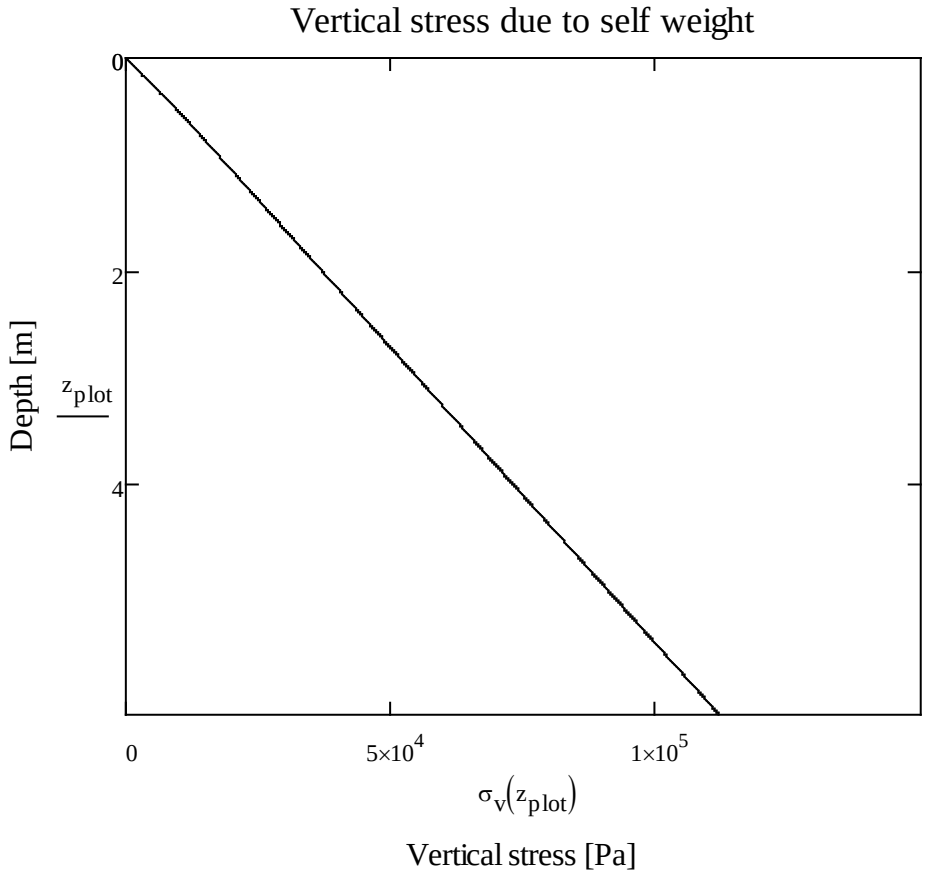

Load distribution - 2:1 method

$$z_{track1} := D_{sleeper} + 2\left(L_{C.track1} - \frac{W_{sleeper}}{2}\right) = 4.531\,m$$

Load distribution 2:1 method beneath track 1

$$q_{track1}(z) := \begin{cases} 0 & \text{if } 0 \le z < D_{sleeper} \\ q_{train} \cdot \dfrac{W_{sleeper}}{\left(W_{sleeper} + z - D_{sleeper}\right)} & \text{if } D_{sleeper} \le z \le z_{track1} \\ \left[q_{train} \cdot \dfrac{W_{sleeper}}{W_{sleeper} + \left[z_{track1} - D_{sleeper} \cdots \right.} \right. & \text{otherwise} \\ \left. \left. + \dfrac{\left[\left(z - D_{sleeper}\right) - \left(z_{track1} - D_{sleeper}\right)\right]}{2} \right] \right] \end{cases}$$

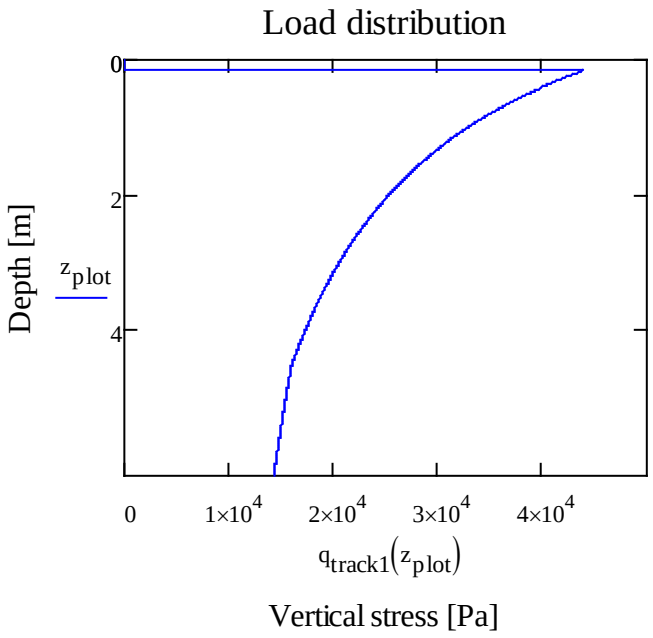

Rankine Theory

Earth pressure coefficients

$$K_a := \tan\left(\frac{\pi}{4} - \frac{\phi}{2}\right)^2$$

$K_a = 0.198$

$$K_p := \tan\left(\frac{\pi}{4} + \frac{\phi}{2}\right)^2$$

$K_p = 5.045$

Horizontal stress due to soil self weight

$\sigma_h(z) := \sigma_v(z) \cdot (K_a)$

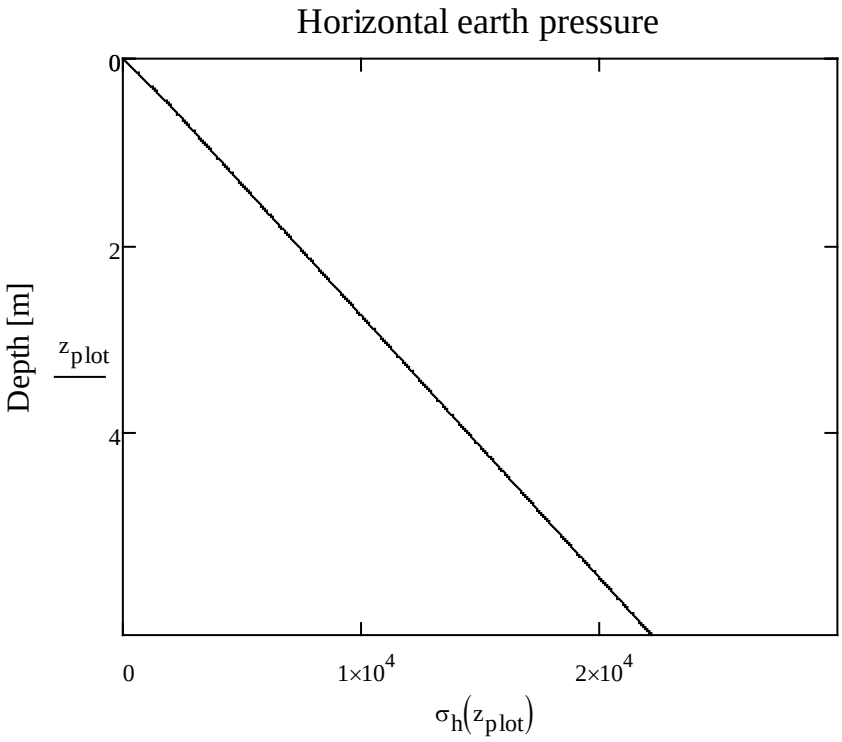

$$q_{track1.h}(z) := \begin{cases} 0 & \text{if } 0 \le z < z_{track1} \\ \left(q_{track1}(z) \cdot K_a\right) & \text{otherwise} \end{cases}$$

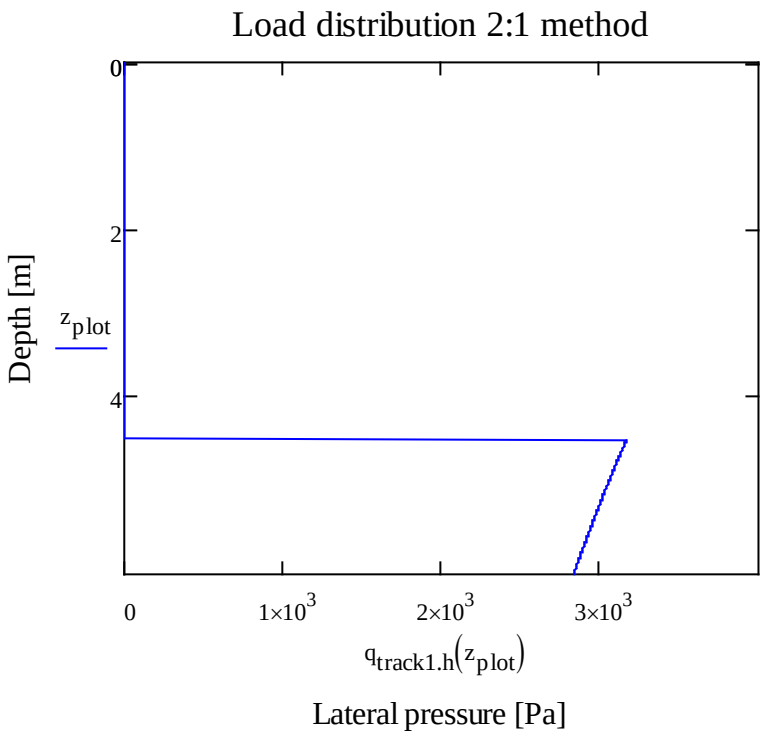

$$\sigma_{h.total}(z) := \begin{cases} \sigma_v(z)\cdot K_a & \text{if } 0 \le z < z_{track1} \\ \sigma_v(z)\cdot K_a + q_{track1.h}(z) & \text{otherwise} \end{cases}$$

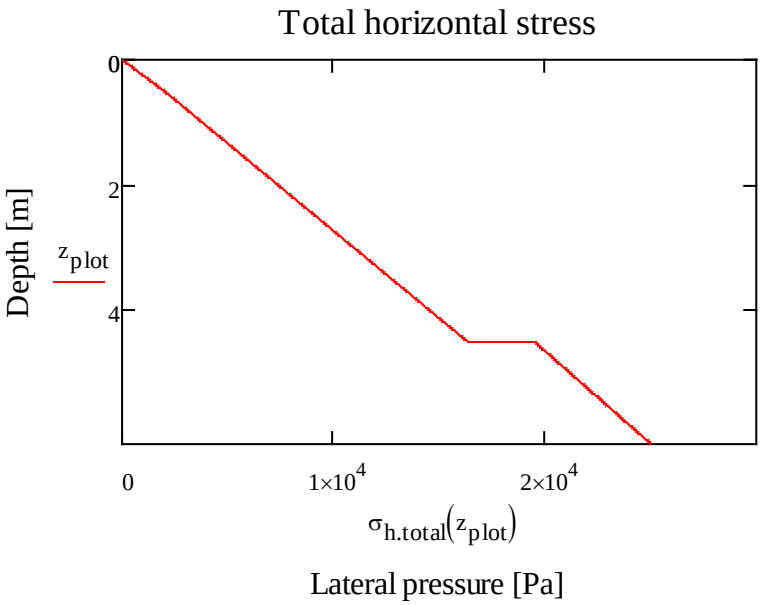

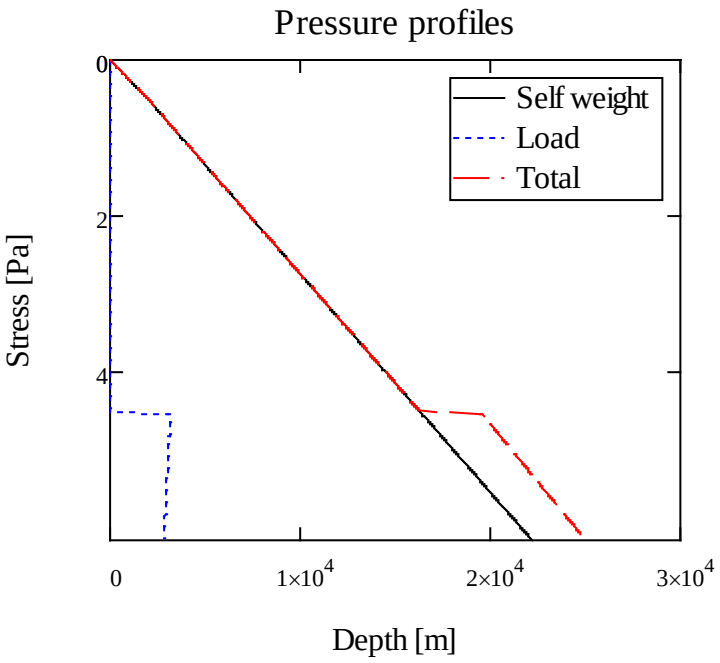

Center of mass with Rankine earth pressure and 2:1-load distribution

Definition x(tp)=M(x=0)/A

$$P_{tot} := \int_0^{H_{wall}} \sigma_{h.total}(z)\ dz = 73.898\,\frac{1}{m}\cdot kN$$ kN/m along the wall

$$A_{integral} := P_{tot}$$

$$M_x := \int_0^{H_{wall}} \left(\sigma_{h.total}(z)\cdot z\right) dz = 3.086 \times 10^5\,N$$ Moment around x=0

$$x_{cm} := \frac{M_x}{A_{integral}} = 4.176\,m$$ Center of mass along x-axis

$$x_{cm} - \left(\frac{H_{wall}}{3}\cdot 2\right) = 0.066\,m$$ Difference between x.cm and the 1/3 from bottom method

$$P_{q.tot} := \int_0^{H_{wall}} q_{track1.h}(z)\ dz = 4.896\,\frac{1}{m}\cdot kN$$ Total thrust from surcharge

Verification

$$P_1 := \int_0^{x_{cm}} \sigma_{h.total}(z)\ dz = 31.911\,\frac{1}{m}\cdot kN$$

$$P_2 := \int_{x_{cm}}^{H_{wall}} \sigma_{h.total}(z)\ dz = 41.987\,\frac{1}{m}\cdot kN$$

$$M_1 := \int_0^{x_{cm}} z\cdot\sigma_{h.total}(z)\ dz$$

$$M_2 := \int_{x_{cm}}^{H_{wall}} z\cdot\sigma_{h.total}(z)\ dz$$

$$M_{verification} := \left(x_{cm} - \frac{M_1}{P_1}\right)\cdot P_1 - \left(\frac{M_2}{P_2} - x_{cm}\right)P_2 = 0.135\,N$$

$$Error := \frac{M_{verification}}{M_x} = 4.375 \times 10^{-7}$$ Negligible

Boussinesq method for surcharge

$$\alpha(z) := \operatorname{atan}\left(\frac{L_{C.track1} - \frac{W_{sleeper}}{2}}{z - D_{sleeper}}\right)$$

$$\beta_{bsq}(z) := \operatorname{atan}\left(\frac{L_{C.track1} + \frac{W_{sleeper}}{2}}{z - D_{sleeper}}\right) - \alpha(z)$$

$$q_{track1.h}(z) := \begin{cases} 0 & \text{if } z < D_{sleeper} \\ \left[\frac{q_{train}}{\pi}\cdot\left(\beta_{bsq}(z) - \sin\left(\beta_{bsq}(z)\right)\cdot\cos\left(\beta_{bsq}(z) + 2\alpha(z)\right)\right)\right] & \text{otherwise} \end{cases}$$

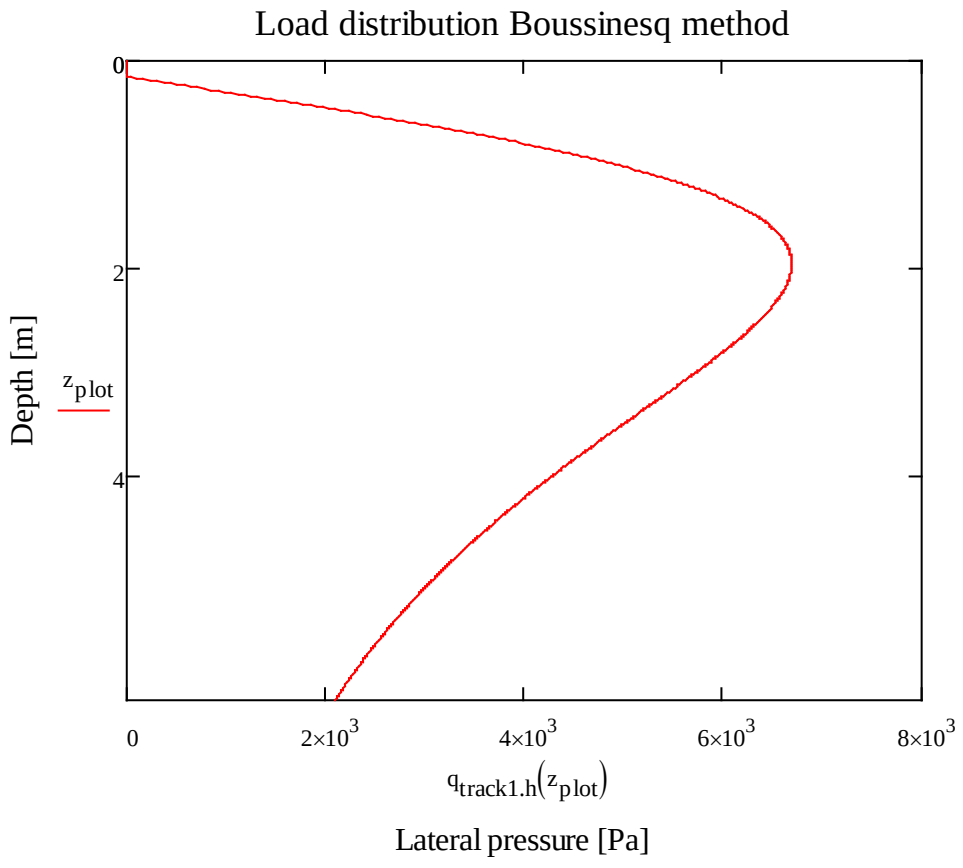

$$\sigma_{h.total}(z) := \begin{cases} \sigma_v(z)\cdot K_a + q_{track1.h}(z) & \text{if } 0\cdot m \le z < D_{ballast} \\ \sigma_v(z)\cdot K_a + q_{track1.h}(z) & \text{otherwise} \end{cases}$$

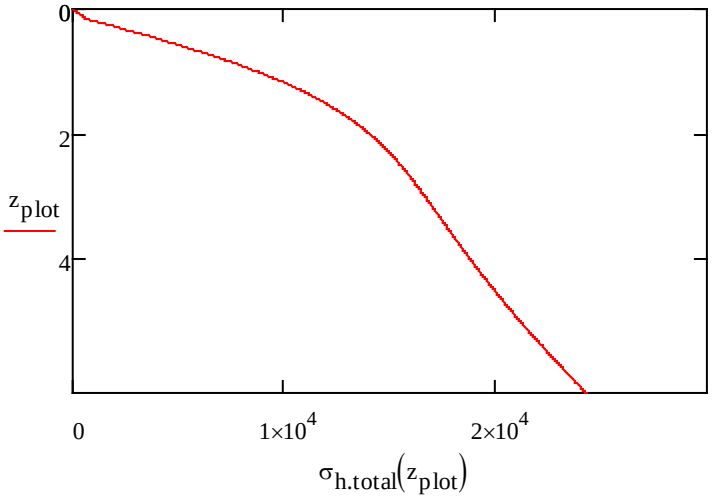

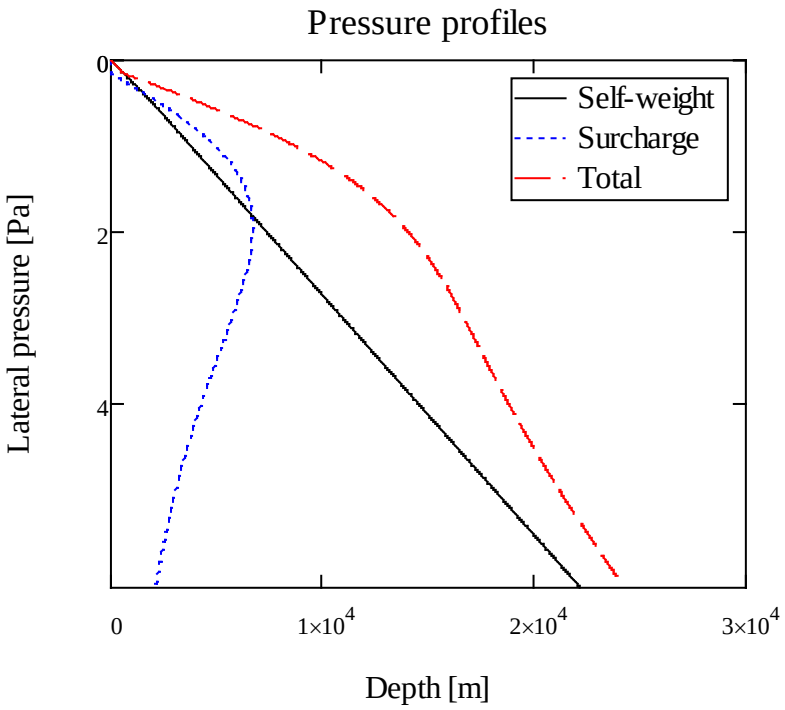

Center of mass with Rankine earth pressure and Boussinesq load distribution

Definition x(tp)=M(x=0)/A

$$P_{tot} := \int_0^{H_{wall}} \sigma_{h.total}(z)\, dz = 95.374 \frac{1}{m}\cdot kN$$ kN/m along the wall

$$A_{integral} := P_{tot}$$

$$M_x := \int_0^{H_{wall}} \left(\sigma_{h.total}(z)\cdot z\right) dz = 3.595 \times 10^5\, N$$ Moment around x=0

$$x_{cm} := \frac{M_x}{A_{integral}} = 3.769\, m$$ Center of mass along x-axis

$$x_{cm} - \left(\frac{H_{wall}}{3}\cdot 2\right) = -0.341\, m$$ Difference between x.cm and the 1/3 from bottom method

$$P_{q.tot} := \int_0^{H_{wall}} q_{track1.h}(z)\, dz = 26.372 \frac{1}{m}\cdot kN$$ Total thrust from surcharge

Verification

$$P_1 := \int_0^{x_{cm}} \sigma_{h.total}(z)\, dz = 44.767 \frac{1}{m}\cdot kN$$

$$P_2 := \int_{x_{cm}}^{H_{wall}} \sigma_{h.total}(z)\, dz = 50.607 \frac{1}{m}\cdot kN$$

$$M_1 := \int_0^{x_{cm}} z\cdot\sigma_{h.total}(z)\, dz$$

$$M_2 := \int_{x_{cm}}^{H_{wall}} z\cdot\sigma_{h.total}(z)\, dz$$

$$M_{verification} := \left(x_{cm} - \frac{M_1}{P_1}\right)\cdot P_1 - \left(\frac{M_2}{P_2} - x_{cm}\right) P_2 = 0.046\, N$$

$$Error := \frac{M_{verification}}{M_x} = 1.284 \times 10^{-7}$$ Negligible

Load distribution - modified 2:1 method

$$q_{track1.h}(z) := \begin{cases} 0 \text{ if } z < D_{sleeper} \\ \left(z - D_{sleeper}\right) \cdot \dfrac{q_{track1}\left(z_{track1} - D_{sleeper}\right) \cdot K_a}{z_{track1} - D_{sleeper}} \text{ if } D_{sleeper} \le z < z_{track1} \\ \left(q_{track1}\left(z - D_{sleeper}\right) \cdot K_a\right) \text{ otherwise} \end{cases}$$

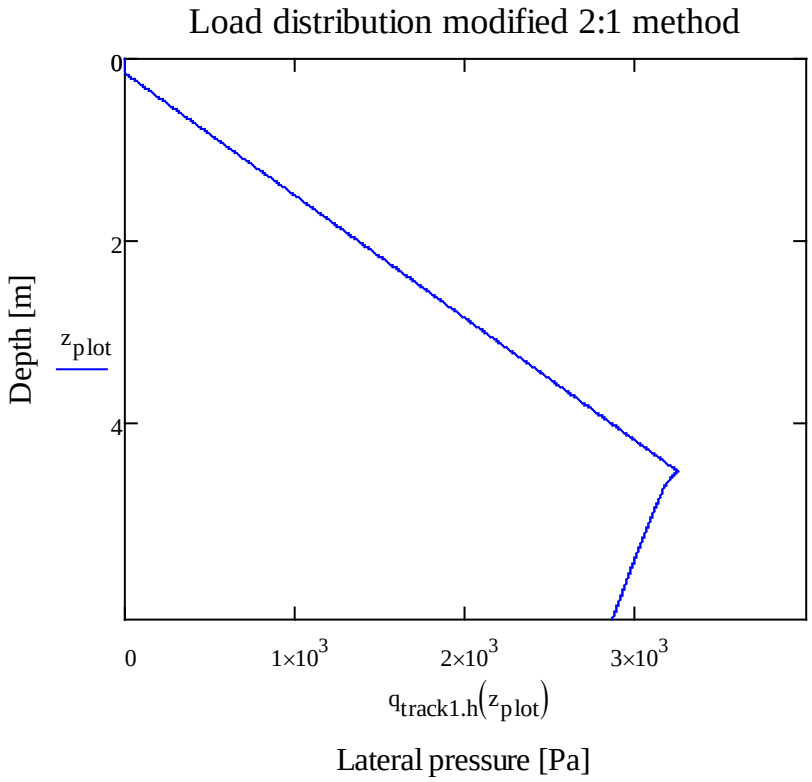

$$\sigma_{h.total}(z) := \sigma_v(z) \cdot K_a + q_{track1.h}(z)$$

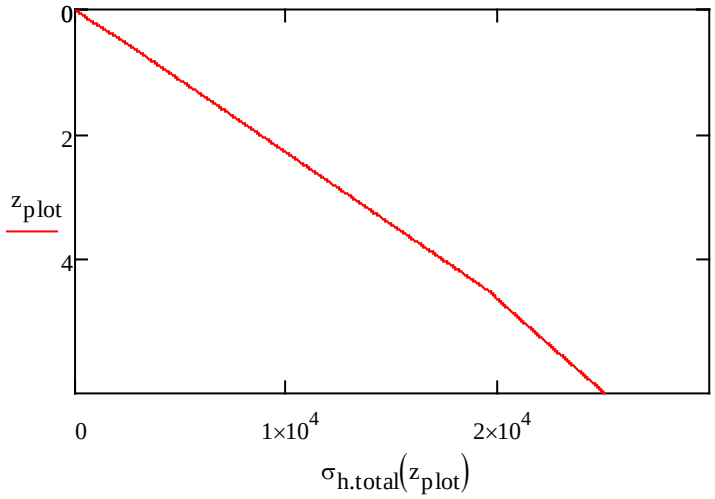

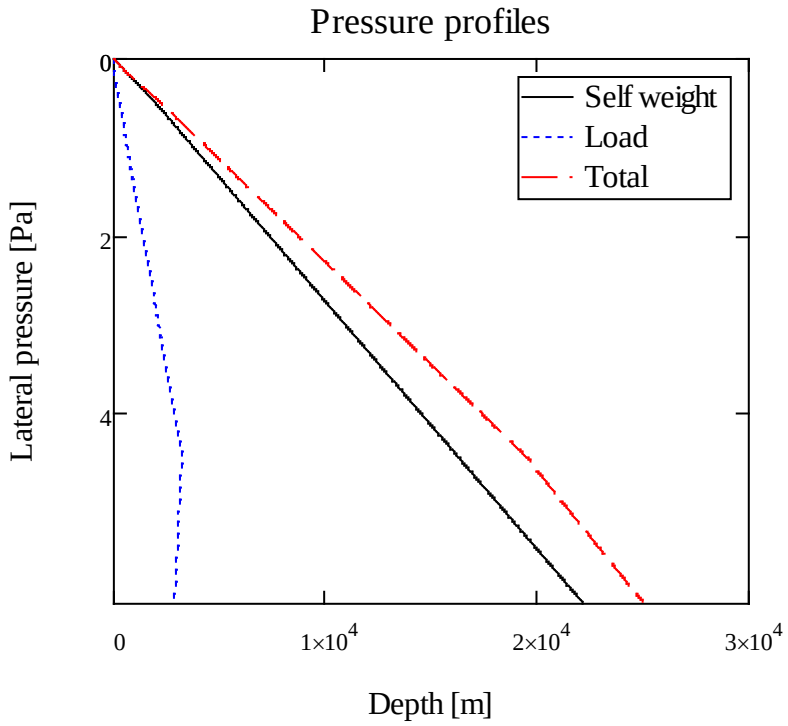

Center of mass Rankine earth pressure and modified 2:1-load distribution

Definition x(tp)=M(x=0)/A

$$P_{tot} := \int_0^{H_{wall}} \sigma_{h.total}(z)\, dz = 81.053 \frac{1}{m}\cdot kN$$ kN/m along the wall

$$A_{integral} := P_{tot}$$

$$M_x := \int_0^{H_{wall}} \left(\sigma_{h.total}(z)\cdot z\right) dz = 3.307 \times 10^5\, N$$ Moment around x=0

$$x_{cm} := \frac{M_x}{A_{integral}} = 4.08\, m$$ Center of mass along x-axis

$$x_{cm} - \left(\frac{H_{wall}}{3}\cdot 2\right) = -0.03\, m$$ Difference between x.cm and the 1/3 from bottom method

$$P_{q.tot} := \int_0^{H_{wall}} q_{track1.h}(z)\, dz = 12.05 \frac{1}{m}\cdot kN$$ Total thrust from surcharge

Verification

$$P_1 := \int_0^{x_{cm}} \sigma_{h.total}(z)\, dz = 36.191 \frac{1}{m}\cdot kN$$

$$P_2 := \int_{x_{cm}}^{H_{wall}} \sigma_{h.total}(z)\, dz = 44.862 \frac{1}{m}\cdot kN$$

$$M_1 := \int_0^{x_{cm}} z\cdot\sigma_{h.total}(z)\, dz$$

$$M_2 := \int_{x_{cm}}^{H_{wall}} z\cdot\sigma_{h.total}(z)\, dz$$

$$M_{verification} := \left(x_{cm} - \frac{M_1}{P_1}\right)\cdot P_1 - \left(\frac{M_2}{P_2} - x_{cm}\right) P_2 = 0.3\, N$$

$$Error := \frac{M_{verification}}{M_x} = 9.071 \times 10^{-7}$$ Negligible

Boussinesq method for surcharge - vertical pressure

$$q_{track1.h}(z) := \begin{cases} 0 & \text{if } z < D_{sleeper} \\ \left[2\frac{q_{train}}{\pi}\cdot\left(\beta_{bsq}(z) + \sin\left(\beta_{bsq}(z)\right)\cdot\cos\left(\beta_{bsq}(z) + 2\alpha(z)\right)\right)\right]\cdot K_a & \text{otherwise} \end{cases}$$

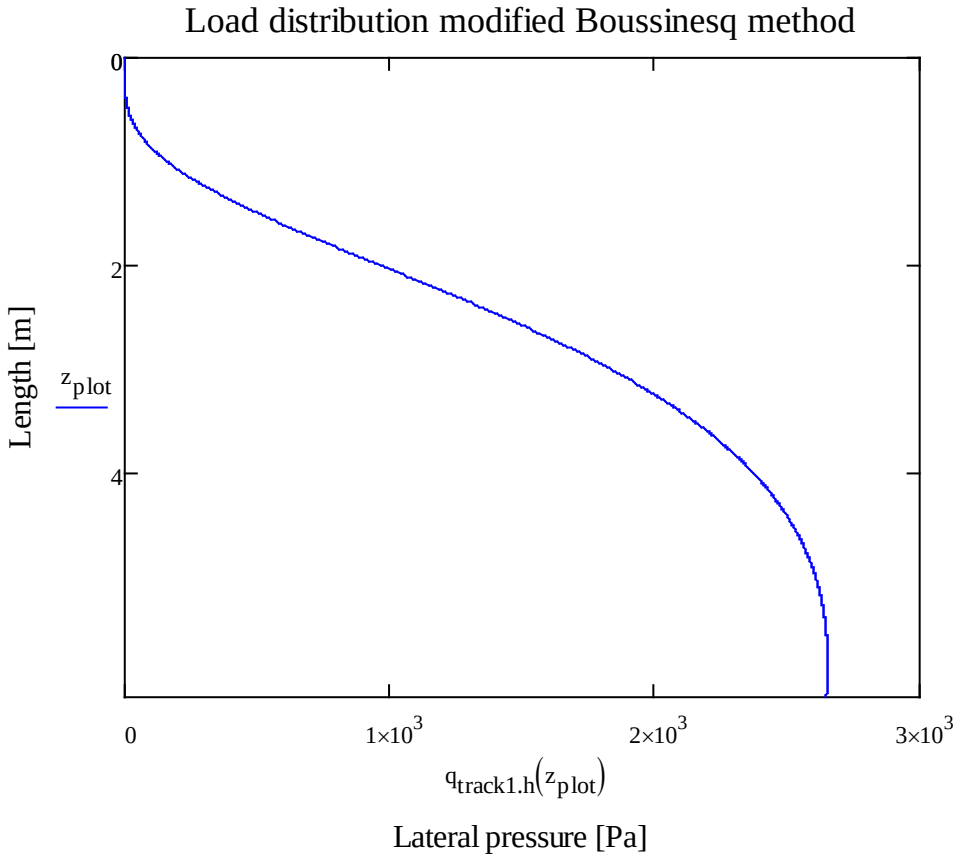

$$\sigma_{h.total}(z) := \begin{cases} \sigma_v(z) \cdot K_a & \text{if } z < D_{sleeper} \\ \sigma_v(z) \cdot K_a + q_{track1.h}(z) & \text{otherwise} \end{cases}$$

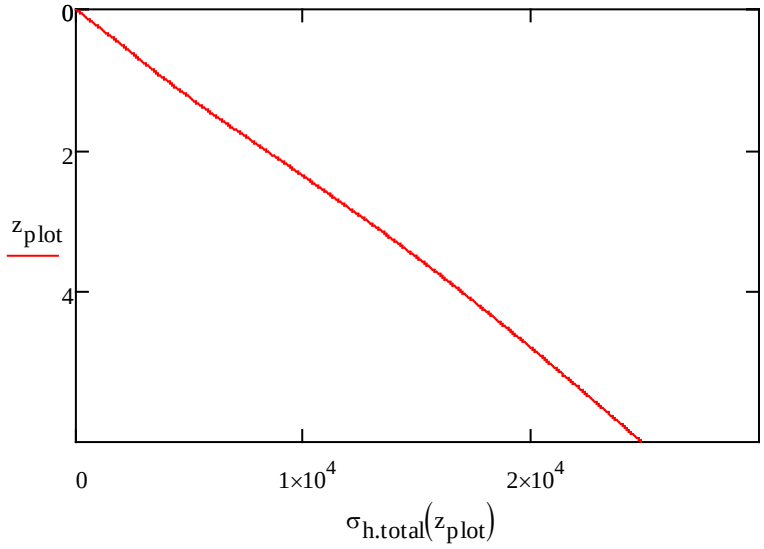

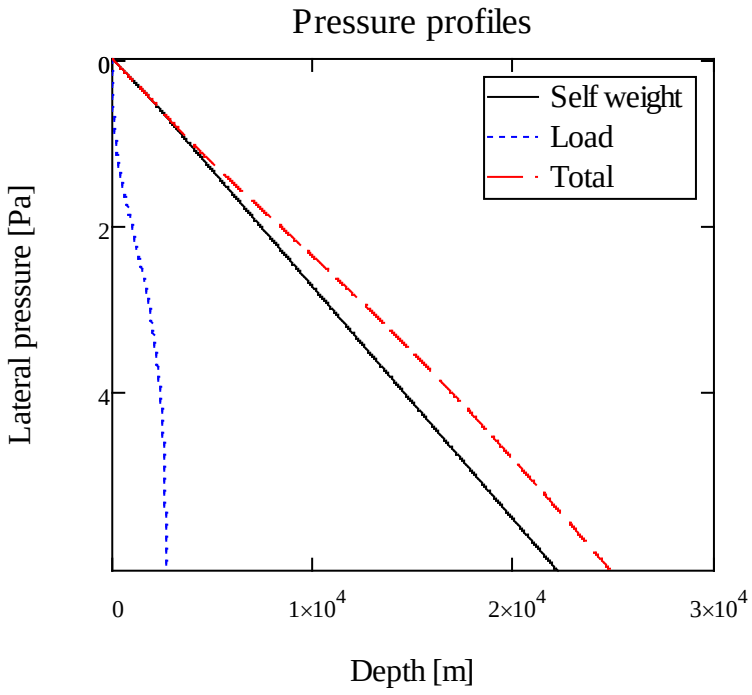

Center of mass Rankine earth pressure and Boussinesq vertical earth pressure

Definition x(tp)=M(x=0)/A

$$P_{tot} := \int_0^{H_{wall}} \sigma_{h.total}(z)\, dz = 78.698 \frac{1}{m}\cdot kN$$ kN/m along the wall

$$A_{integral} := P_{tot}$$

$$M_x := \int_0^{H_{wall}} \left(\sigma_{h.total}(z)\cdot z\right) dz = 3.23 \times 10^5\, N$$ Moment around x=0

$$x_{cm} := \frac{M_x}{A_{integral}} = 4.105\, m$$ Center of mass along x-axis

$$x_{cm} - \left(\frac{H_{wall}}{3}\cdot 2\right) = -5.398 \times 10^{-3}\, m$$ Difference between x.cm and the 1/3 from bottom method

$$P_{q.tot} := \int_0^{H_{wall}} q_{track1.h}(z)\, dz = 9.696 \frac{1}{m}\cdot kN$$ Total thrust from surcharge

Verification

$$P_1 := \int_0^{x_{cm}} \sigma_{h.total}(z)\, dz = 35.195 \frac{1}{m}\cdot kN$$

$$P_2 := \int_{x_{cm}}^{H_{wall}} \sigma_{h.total}(z)\, dz = 43.503 \frac{1}{m}\cdot kN$$

$$M_1 := \int_0^{x_{cm}} z\cdot\sigma_{h.total}(z)\, dz$$

$$M_2 := \int_{x_{cm}}^{H_{wall}} z\cdot\sigma_{h.total}(z)\, dz$$

$$M_{verification} := \left(x_{cm} - \frac{M_1}{P_1}\right)\cdot P_1 - \left(\frac{M_2}{P_2} - x_{cm}\right) P_2 = -0.019\, N$$

$$Error := \frac{M_{verification}}{M_x} = -5.733 \times 10^{-8}$$ Negligible

No load distribution - infinite surcharge

$$q_{train}(z) := \begin{cases} 0 & \text{if } z < 0 \\ (q_{train}) & \text{otherwise} \end{cases}$$

$$\sigma_{h.total}(z) := (\sigma_v(z) + q_{train}(z)) \cdot K_a$$

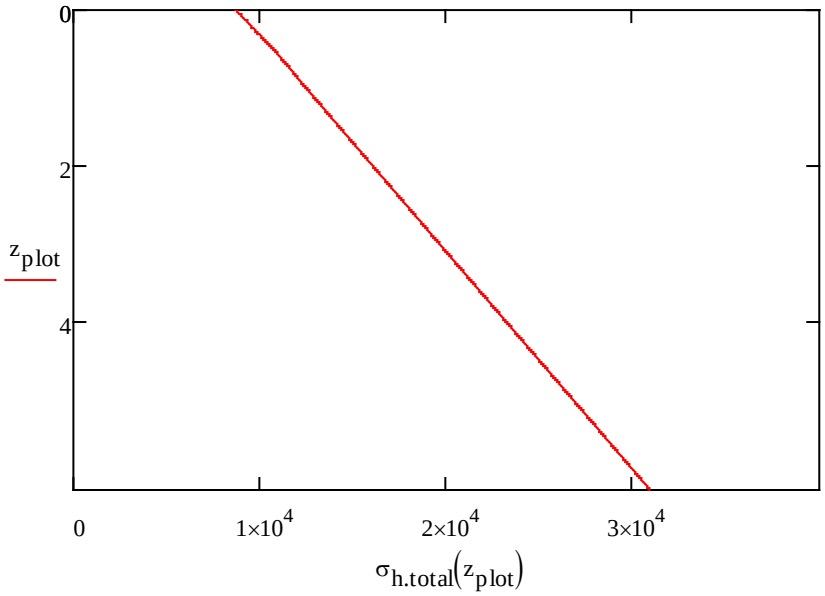

Center of mass Rankine earth pressure and infinite surcharge

Definition x(tp)=M(x=0)/A

$$P_{tot} := \int_0^{H_{wall}} \sigma_{h.total}(z)\, dz = 122.773 \frac{1}{m} \cdot kN$$ kN/m along the wall

$$A_{integral} := P_{tot}$$

$$M_x := \int_0^{H_{wall}} (\sigma_{h.total}(z) \cdot z)\, dz = 4.483 \times 10^5\, N$$ Moment around x=0

$$x_{com} := \frac{M_x}{A_{integral}} = 3.651\, m$$ Center of mass along x-axis

$$x_{cm} - \left(\frac{H_{wall}}{3}\cdot 2\right) = -0.459\,m$$

Difference between x.cm and the 1/3 from bottom method

$$P_{q.tot} := \int_0^{H_{wall}} q_{train}(z)\cdot K_a \, dz = 53.771\,\frac{1}{m}\cdot kN$$

Total thrust from surcharge

Verification

$$P_1 := \int_0^{x_{cm}} \sigma_{h.total}(z) \, dz = 56.317\,\frac{1}{m}\cdot kN$$

$$P_2 := \int_{x_{cm}}^{H_{wall}} \sigma_{h.total}(z) \, dz = 66.457\,\frac{1}{m}\cdot kN$$

$$M_1 := \int_0^{x_{cm}} z\cdot\sigma_{h.total}(z) \, dz$$

$$M_2 := \int_{x_{cm}}^{H_{wall}} z\cdot\sigma_{h.total}(z) \, dz$$

$$M_{verification} := \left(x_{cm} - \frac{M_1}{P_1}\right)\cdot P_1 - \left(\frac{M_2}{P_2} - x_{cm}\right)P_2 = 0.057\,N$$

$$Error := \frac{M_{verification}}{M_x} = 1.279\times 10^{-7}$$

Negligible

Appendix B Mathcad - Coulomb

The calculations for the earth pressure using Coulomb theory follows the same method as the one done for Rankine. This is why most of the calculations have been excluded from this appendix and only the important differences are displayed.

Material properties

$\gamma_{ballast} := 20 \cdot \frac{kN}{m^3}$

$\gamma_{fill} := 18 \cdot \frac{kN}{m^3}$

$\phi := 42 \cdot deg$

$$\delta_a := \begin{cases} \frac{2 \cdot \phi}{3} & \text{if } \frac{2 \cdot \phi}{3} < 20 \cdot deg \\ 20 \cdot deg & \text{otherwise} \end{cases} = 20 \cdot deg$$

Resultant friction angle to horizontal

$$\delta_p := \begin{cases} \frac{\phi}{2} & \text{if } \frac{\phi}{2} < 15 \cdot deg \\ 15 \cdot deg & \text{otherwise} \end{cases} = 15 \cdot deg$$

Coulomb theory

Earth pressure coefficients

$$K_a := \frac{\sin\left(\alpha_{wall} + \phi\right)^2}{\sin\left(\alpha_{wall}\right)^2 \cdot \sin\left(\alpha_{wall} - \delta_a\right) \cdot \left(1 + \sqrt{\frac{\sin\left(\phi + \delta_a\right) \cdot \sin(\phi - \beta)}{\sin\left(\alpha_{wall} - \delta_a\right) \cdot \sin\left(\alpha_{wall} + \beta\right)}}\right)^2} = 0.195$$

$$K_p := \frac{\sin\left(\alpha_{wall} - \phi\right)^2}{\sin\left(\alpha_{wall}\right)^2 \cdot \sin\left(\alpha_{wall} + \delta_p\right) \cdot \left(1 - \sqrt{\frac{\sin\left(\phi + \delta_p\right) \cdot \sin(\phi + \beta)}{\sin\left(\alpha_{wall} + \delta_p\right) \cdot \sin\left(\alpha_{wall} + \beta\right)}}\right)^2} = 9.231$$

Appendix C Mathcad – Boussinesq

$\gamma_{ballast} := 20 \cdot \frac{kN}{m^3}$

$\gamma_{fill} := 18 \cdot \frac{kN}{m^3}$

$\phi := 42 \cdot deg$ See table 5.2-4 TK GEO 11

$\delta_a := \frac{2 \cdot \phi}{3} = 28 \cdot deg$ Resultant friction angle to horizontal, active side.

$\delta_p := \frac{\phi}{2} = 21 \cdot deg$

Geometry

$H_{total} := 6.865 \cdot m$

$H_{slab} := 0.700 \cdot m$

$H_{wall} := H_{total} - H_{slab} = 6.165\,m$

$\alpha_{wall} := 1.85 \cdot deg$ Wall inclination to vertical

$W_{slab} := 6.600 \cdot m$

$W_{wall.bottom} := 0.600 \cdot m$

$W_{wall.top} := 0.400 \cdot m$

$L_{C.track1} := 3.438 \cdot m$ Center of track

$D_{ballast} := 0.510 \cdot m$

$W_{sleeper} := 2.5 \cdot m$ Assumed width for sleeper

$q_{train} := 44 \cdot kPa$ Assumed load, see Eurocode

$D_{sleeper} := 0.155 \cdot m$

K.a and K.p is derived from Table 10.1 from page 541 in Fethi Azizi book

Input data for the table is:

phi=42 degrees

beta=0 degrees

delta(wall friction)=2/3*phi

beta/phi=0

$$K_a := \frac{0.163 - 0.202}{5} \cdot 2 + 0.202 = 0.186$$

Linear interpolation of K.a from table

$$\sigma_h(z) := \sigma_v(z) \cdot K_a \cdot \cos(\delta_a)$$

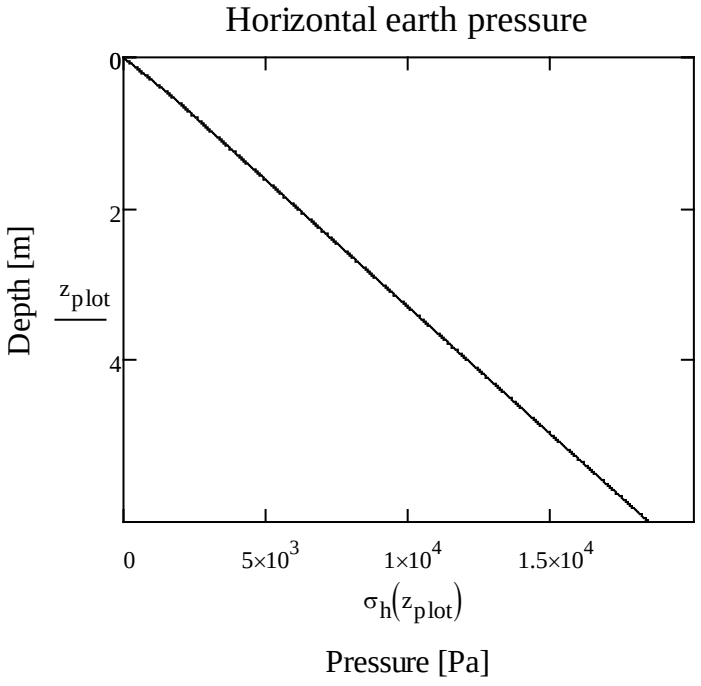

Appendix D Mathcad – Culmann

In this appendix calculations for the thrusts of segments number 2 to number 11 have been excluded. These segments are calculated in the same way as segments 1 and 12.

Material properties

$\gamma_{ballast} := 18 \cdot \frac{kN}{m^3}$

$\gamma_{fill} := 18 \cdot \frac{kN}{m^3}$

$\phi := 42 \cdot deg$ See table 5.2-4 TK GEO 11

Geometry

$H_{total} := 6.865 \cdot m$

$H_{slab} := 0.700 \cdot m$

$H_{wall} := H_{total} - H_{slab} = 6.165\,m$

$\alpha_{wall} := 90 \cdot deg - 1.85 \cdot deg = 88.15 \cdot deg$ Wall inclination to vertical

$W_{slab} := 6.600 \cdot m$

$W_{wall.bottom} := 0.600 \cdot m$

$W_{wall.top} := 0.400 \cdot m$

$L_{C.track1} := 3.438 \cdot m$ Center of track

$D_{ballast} := 0.510 \cdot m$ Layer thickness

$W_{sleeper} := 2.5 \cdot m$ Assumed width for sleeper

$q_{train} := 44 \cdot kPa$ Assumed load, see Eurocode

$D_{sleeper} := 0.155 \cdot m$

$\beta := 0 \cdot deg$ Ground inclination

Angles

$\delta_{assumed} := 0$ Assumed inclination, to get a perpendicular angle to the internal friction angle

$\alpha_{assumed} := 90 \cdot deg$ Assumed vertical wall

$\varphi_{increment} := 0 \cdot deg, 0.01 \cdot deg .. (90 \cdot deg - \phi)$

$L_{track.start} := L_{C.track1} - \frac{W_{sleeper}}{2}$

$L_{track.end} := L_{C.track1} + \frac{W_{sleeper}}{2}$

$\varphi_{load.start} := \operatorname{atan}\left(\frac{L_{track.start}}{H_{wall}}\right) = 19.54 \cdot deg$

$\varphi_{load.end} := \operatorname{atan}\left(\frac{L_{track.end}}{H_{wall}}\right) = 37.25 \cdot deg$

Wedges

$W_{max} := \frac{H_{wall}^{2} \cdot \tan(90 \cdot deg - \phi)}{2} \cdot \gamma_{ballast} + q_{train} \cdot W_{sleeper} = 489.902 \frac{1}{m} \cdot kN$

$L_{max} := \frac{H_{wall}}{\sin(\phi)} = 9.213\,m$

$$W(\varphi_{increment}) := \begin{cases} \left(\frac{H_{wall}^{2} \cdot \tan(\varphi_{increment})}{2} \cdot \gamma_{fill}\right) & \text{if } \varphi_{increment} < \varphi_{load.start} \\ \left[\begin{array}{l} \frac{H_{wall}^{2} \cdot \tan(\varphi_{increment})}{2} \cdot \gamma_{fill} \cdots \\ + q_{train} \cdot \left(H_{wall} \cdot \tan(\varphi_{increment}) \cdots \right. \\ \left. + -L_{track.start}\right) \end{array}\right] & \text{if } \varphi_{load.start} \le \varphi_{increment} < \varphi_{load.end} \\ \left(\frac{H_{wall}^{2} \cdot \tan(\varphi_{increment})}{2} \cdot \gamma_{fill} + q_{train} \cdot W_{sleeper}\right) & \text{otherwise} \end{cases}$$

$$L(\varphi_{increment}) := L_{max} \cdot \frac{W(\varphi_{increment})}{W_{max}}$$

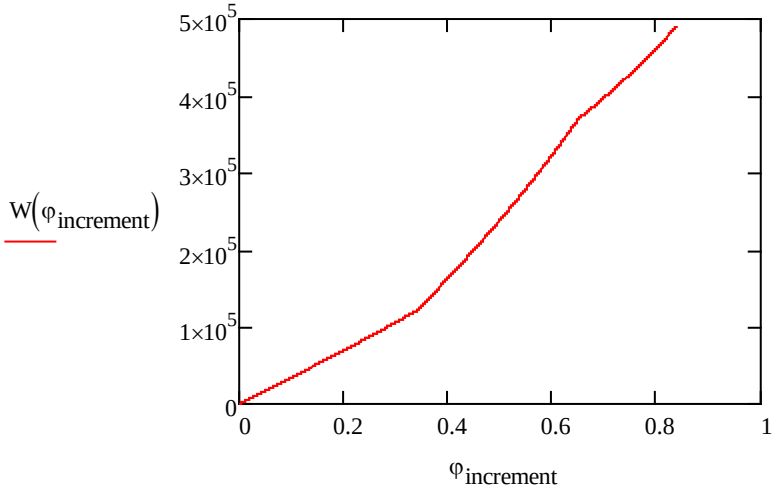

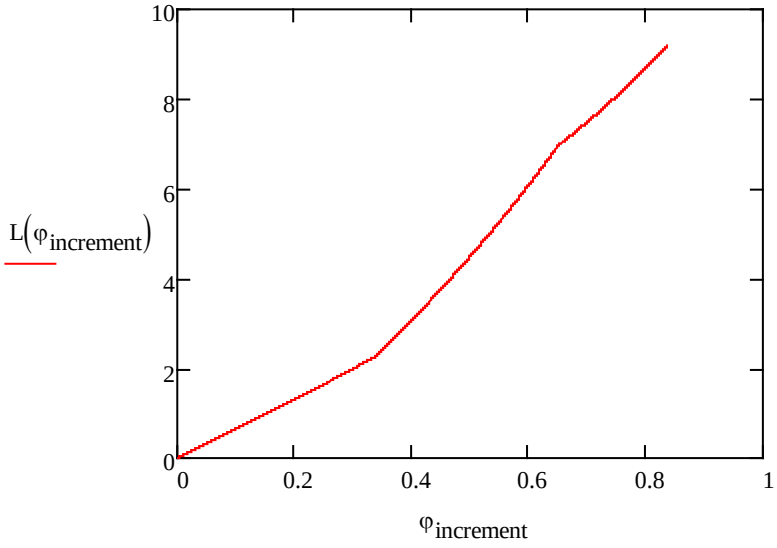

Thrust by wedges

$$F_{factor} := \frac{W_{max}}{L_{max}} = 5.317 \times 10^{4}\,Pa$$

$$F(\varphi_{increment}) := \frac{L(\varphi_{increment})}{\tan(\varphi_{increment} + \phi)} \cdot F_{factor}$$

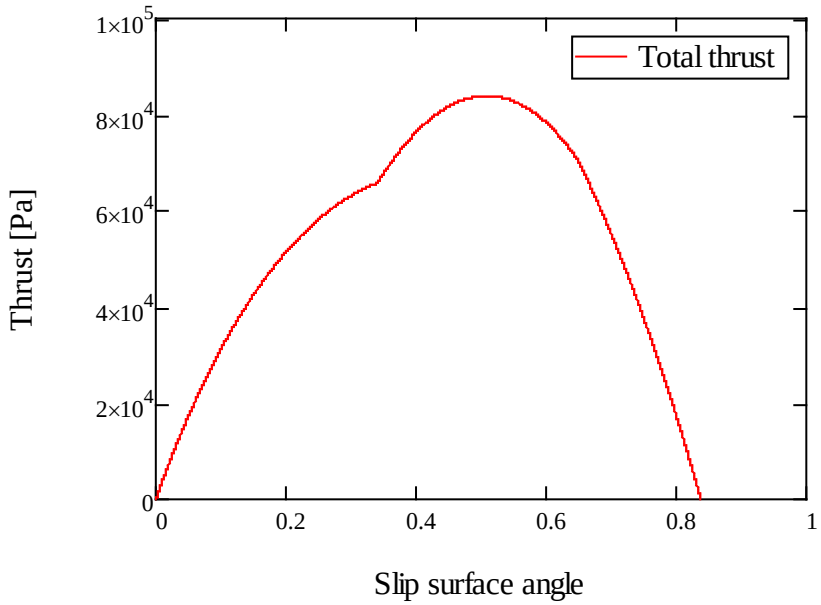

Given

$$\varphi_{increment} := 0.4$$

$$\varphi_{max} := Maximize(F, \varphi_{increment}) = 29.153 \cdot deg$$

$$F_0 := F(\varphi_{max}) = 83.917 \frac{1}{m} \cdot kN$$ **Maximum thrust**

Thrust by wedges when no load is applied

$\varphi_{increment} := 0 \cdot deg, 0.01 \cdot deg .. (90 \cdot deg - \phi)$

$$W_{max.noload} := \frac{H_{wall}^{2} \cdot \tan(90 \cdot deg - \phi)}{2} \cdot \gamma_{ballast} = 379.902 \frac{1}{m} \cdot kN$$

$$W_{noload}(\varphi_{increment}) := \frac{H_{wall}^{2} \cdot \tan(\varphi_{increment})}{2} \cdot \gamma_{ballast}$$

$$L_{noload}(\varphi_{increment}) := L_{max} \cdot \frac{W_{noload}(\varphi_{increment})}{W_{max.noload}}$$

$$F_{factor.noload} := \frac{W_{max.noload}}{L_{max}} = 4.123 \times 10^{4} \, Pa$$

$$F_{noload}(\varphi_{increment}) := \frac{L_{noload}(\varphi_{increment})}{\tan(\varphi_{increment} + \phi)} \cdot F_{factor.noload}$$

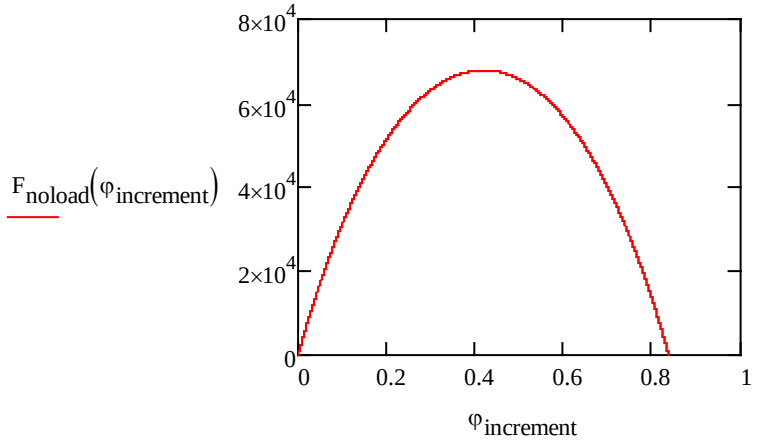

Given

$\varphi_{increment} := 0.4$

$\varphi_{max} := Maximize(F_{noload}, \varphi_{increment}) = 24 \cdot deg$

$F_{noload}(\varphi_{max}) = 67.807 \frac{1}{m} \cdot kN$ **Maximum thrust without surcharge**

Multiple sections to find position of resultant

A number of different sections are used to be able to find the load distribution on the cantilever wall.

$z_1 := 0.5 \cdot m$ $\Delta z := 0.5 \cdot m$

$z_2 := 1 \cdot m$

$z_3 := 1.5 \cdot m$

$z_4 := 2 \cdot m$

$z_5 := 2.5 \cdot m$

$z_6 := 3 \cdot m$

$z_7 := 3.5 \cdot m$

$z_8 := 4 \cdot m$

$z_9 := 4.5 \cdot m$

$z_{10} := 5 \cdot m$

$z_{11} := 5.5 \cdot m$

$z_{12} := 6 \cdot m$

Angles

1

$\varphi_{increment} := 0 \cdot deg, 0.01 \cdot deg .. (90 \cdot deg - \phi)$

$\varphi_{load.start} := \operatorname{atan}\left(\frac{L_{track.start}}{H_{wall} - z_1}\right) = 21.118 \cdot deg$

$\varphi_{load.end} := \operatorname{atan}\left(\frac{L_{track.end}}{H_{wall} - z_1}\right) = 39.609 \cdot deg$

Wedges

$W_{max} := \frac{(H_{wall} - z_1)^2 \cdot \tan(90 \cdot deg - \phi)}{2} \cdot \gamma_{ballast} + q_{train} \cdot W_{sleeper} = 430.778 \frac{1}{m} \cdot kN$

$L_{max} := \frac{H_{wall} - z_1}{\sin(\phi)} = 8.466\,m$

$$W(\varphi_{increment}) := \begin{cases} \left[\frac{(H_{wall} - z_1)^2 \cdot \tan(\varphi_{increment})}{2} \cdot \gamma_{fill}\right] & \text{if } \varphi_{increment} < \varphi_{load.start} \\ \left[\begin{array}{l} \frac{(H_{wall} - z_1)^2 \cdot \tan(\varphi_{increment})}{2} \cdot \gamma_{fill} \ldots \\ + q_{train} \cdot \left[(H_{wall} - z_1) \cdot \tan(\varphi_{increment}) \ldots \right. \\ \left. \quad + -L_{track.start}\right] \end{array}\right] & \text{if } \varphi_{load.start} \le \varphi_{increment} < \varphi_{load.end} \\ \left[\frac{(H_{wall} - z_1)^2 \cdot \tan(\varphi_{increment})}{2} \cdot \gamma_{fill} + q_{train} \cdot W_{sleeper}\right] & \text{otherwise} \end{cases}$$

$L(\varphi_{increment}) := L_{max} \cdot \frac{W(\varphi_{increment})}{W_{max}}$

Thrust by wedges

$$F_{factor} := \frac{W_{max}}{L_{max}} = 5.088 \times 10^4\ \text{Pa}$$

$$F(\varphi_{increment}) := \frac{L(\varphi_{increment})}{\tan(\varphi_{increment} + \phi)} \cdot F_{factor}$$

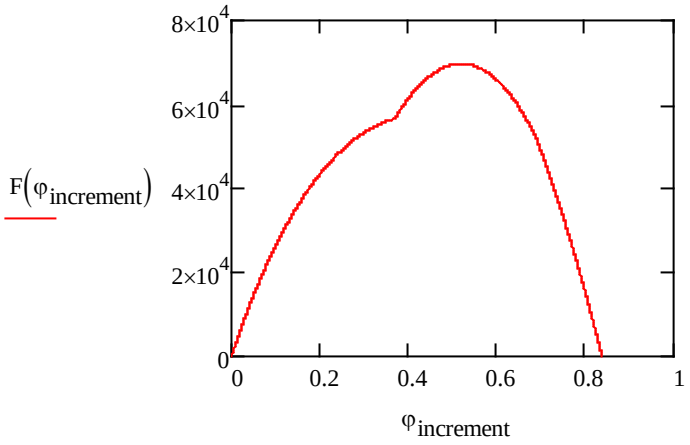

Given

$$\varphi_{increment} := 0.6$$

$$\varphi_{max} := \text{Maximize}(F, \varphi_{increment}) = 29.807 \cdot \text{deg}$$

$$F_1 := F(\varphi_{max}) = 69.668 \frac{1}{\text{m}} \cdot \text{kN}$$

Maximum thrust

12

Angles

$\varphi_{increment} := 0 \cdot deg, 0.01 \cdot deg .. (90 \cdot deg - \phi)$

$\varphi_{load.start} := \operatorname{atan}\left(\frac{L_{track.start}}{H_{wall} - z_{12}}\right) = 85.687 \cdot deg$

$\varphi_{load.end} := \operatorname{atan}\left(\frac{L_{track.end}}{H_{wall} - z_{12}}\right) = 87.984 \cdot deg$

Wedges

$W_{max} := \frac{(H_{wall} - z_{12})^2 \cdot \tan(90 \cdot deg - \phi)}{2} \cdot \gamma_{ballast} + q_{train} \cdot W_{sleeper} = 110.272 \frac{1}{m} \cdot kN$

$L_{max} := \frac{H_{wall} - z_{12}}{\sin(\phi)} = 0.247\,m$

$$W(\varphi_{increment}) := \begin{cases} \left[\frac{(H_{wall} - z_{12})^2 \cdot \tan(\varphi_{increment})}{2} \cdot \gamma_{fill}\right] & \text{if } \varphi_{increment} < \varphi_{load.start} \\ \left[\begin{array}{l} \frac{(H_{wall} - z_{12})^2 \cdot \tan(\varphi_{increment})}{2} \cdot \gamma_{fill} \cdots \\ + q_{train} \cdot \left[\begin{array}{l} (H_{wall} - z_{12}) \cdot \tan(\varphi_{increment}) \cdots \\ + -L_{track.start} \end{array}\right] \end{array}\right] & \text{if } \varphi_{load.start} \le \varphi_{increment} < \varphi_{load.end} \\ \left[\frac{(H_{wall} - z_{12})^2 \cdot \tan(\varphi_{increment})}{2} \cdot \gamma_{fill} + q_{train} \cdot W_{sleeper}\right] & \text{otherwise} \end{cases}$$

$L(\varphi_{increment}) := L_{max} \cdot \frac{W(\varphi_{increment})}{W_{max}}$

Thrust by wedges

$$F_{factor} := \frac{W_{max}}{L_{max}} = 4.472 \times 10^{5}\,Pa$$

$$F(\varphi_{increment}) := \frac{L(\varphi_{increment})}{\tan(\varphi_{increment} + \phi)} \cdot F_{factor}$$

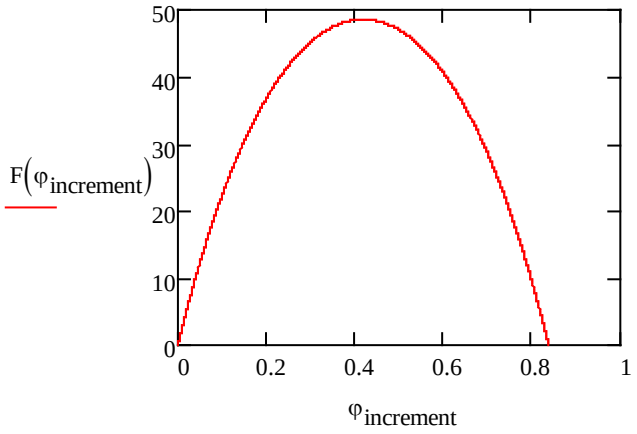

Given

$$\varphi_{increment} := 0.4$$

$$\varphi_{max} := Maximize(F, \varphi_{increment}) = 24 \cdot deg$$

$$F_{12} := F(\varphi_{max}) = 0.049 \frac{1}{m} \cdot kN$$

Maximum thrust

Medium pressure on wall for every section

$$P_1 := \frac{F_0 - F_1}{\Delta z} = 2.85 \times 10^4\,\text{Pa} \qquad f_1 := P_1 \cdot \Delta z = 14.25\,\frac{1}{\text{m}}\cdot\text{kN}$$

$$P_2 := \frac{F_1 - F_2}{\Delta z} = 2.644 \times 10^4\,\text{Pa} \qquad f_2 := P_2 \cdot \Delta z = 13.221\,\frac{1}{\text{m}}\cdot\text{kN}$$

$$P_3 := \frac{F_2 - F_3}{\Delta z} = 2.43 \times 10^4\,\text{Pa} \qquad f_3 := P_3 \cdot \Delta z = 12.152\,\frac{1}{\text{m}}\cdot\text{kN}$$

$$P_4 := \frac{F_3 - F_4}{\Delta z} = 2.205 \times 10^4\,\text{Pa} \qquad f_4 := P_4 \cdot \Delta z = 11.026\,\frac{1}{\text{m}}\cdot\text{kN}$$

$$P_5 := \frac{F_4 - F_5}{\Delta z} = 1.861 \times 10^4\,\text{Pa} \qquad f_5 := P_5 \cdot \Delta z = 9.305\,\frac{1}{\text{m}}\cdot\text{kN}$$

$$P_6 := \frac{F_5 - F_6}{\Delta z} = 1.219 \times 10^4\,\text{Pa} \qquad f_6 := P_6 \cdot \Delta z = 6.093\,\frac{1}{\text{m}}\cdot\text{kN}$$

$$P_7 := \frac{F_6 - F_7}{\Delta z} = 1.04 \times 10^4\,\text{Pa} \qquad f_7 := P_7 \cdot \Delta z = 5.201\,\frac{1}{\text{m}}\cdot\text{kN}$$

$$P_8 := \frac{F_7 - F_8}{\Delta z} = 8.617 \times 10^3\,\text{Pa} \qquad f_8 := P_8 \cdot \Delta z = 4.308\,\frac{1}{\text{m}}\cdot\text{kN}$$

$$P_9 := \frac{F_8 - F_9}{\Delta z} = 6.833 \times 10^3\,\text{Pa} \qquad f_9 := P_9 \cdot \Delta z = 3.416\,\frac{1}{\text{m}}\cdot\text{kN}$$

$$P_{10} := \frac{F_9 - F_{10}}{\Delta z} = 5.049 \times 10^3\,\text{Pa} \qquad f_{10} := P_{10} \cdot \Delta z = 2.524\,\frac{1}{\text{m}}\cdot\text{kN}$$

$$P_{11} := \frac{F_{10} - F_{11}}{\Delta z} = 3.265 \times 10^3\,\text{Pa} \qquad f_{11} := P_{11} \cdot \Delta z = 1.632\,\frac{1}{\text{m}}\cdot\text{kN}$$

$$P_{12} := \frac{F_{11} - F_{12}}{\Delta z} = 1.481 \times 10^3\,\text{Pa} \qquad f_{12} := P_{12} \cdot \Delta z = 0.74\,\frac{1}{\text{m}}\cdot\text{kN}$$

$$P_{13} := \frac{F_{12}}{H_{wall} - z_{12}} = 294.369\,\text{Pa} \qquad f_{13} := P_{13} \cdot \left(H_{wall} - z_{12}\right) = 0.049\,\frac{1}{\text{m}}\cdot\text{kN}$$

$$f_1 + f_2 + f_3 + f_4 + f_5 + f_6 + f_7 + f_8 + f_9 + f_{10} + f_{11} + f_{12} + f_{13} = 83.917 \frac{1}{m} \cdot kN$$

$$F_0 = 83.917 \frac{1}{m} \cdot kN$$

$$x_{cm2} := \frac{\begin{bmatrix} f_1 \cdot 0.5 \cdot z_1 + f_2 \cdot (0.5 \cdot z_1 + z_1) + f_3 \cdot (0.5 \cdot z_1 + 2z_1) + f_4 \cdot (0.5 \cdot z_1 + 3z_1) \dots \\ + f_5 \cdot (0.5 \cdot z_1 + 4z_1) + f_6 \cdot (0.5 \cdot z_1 + 5z_1) \dots \\ + f_7 \cdot (0.5 \cdot z_1 + 6z_1) + f_8 \cdot (0.5 \cdot z_1 + 7z_1) \dots \\ + f_9 \cdot (0.5 \cdot z_1 + 8z_1) \dots \\ + f_{10} \cdot (0.5 \cdot z_1 + 9z_1) \dots \\ + f_{11} \cdot (0.5 \cdot z_1 + 10z_1) \dots \\ + f_{12} \cdot (0.5 \cdot z_1 + 11z_1) \dots \\ + f_{13} \cdot [0.5 \cdot (H_{wall} - z_{12}) + 12z_1] \end{bmatrix}}{f_1 + f_2 + f_3 + f_4 + f_5 + f_6 + f_7 + f_8 + f_9 + f_{10} + f_{11} + f_{12} + f_{13}} = 1.887\,m$$

Trend lines from Excel

Trend line from Excel when making a single equation represent the entire stress profile

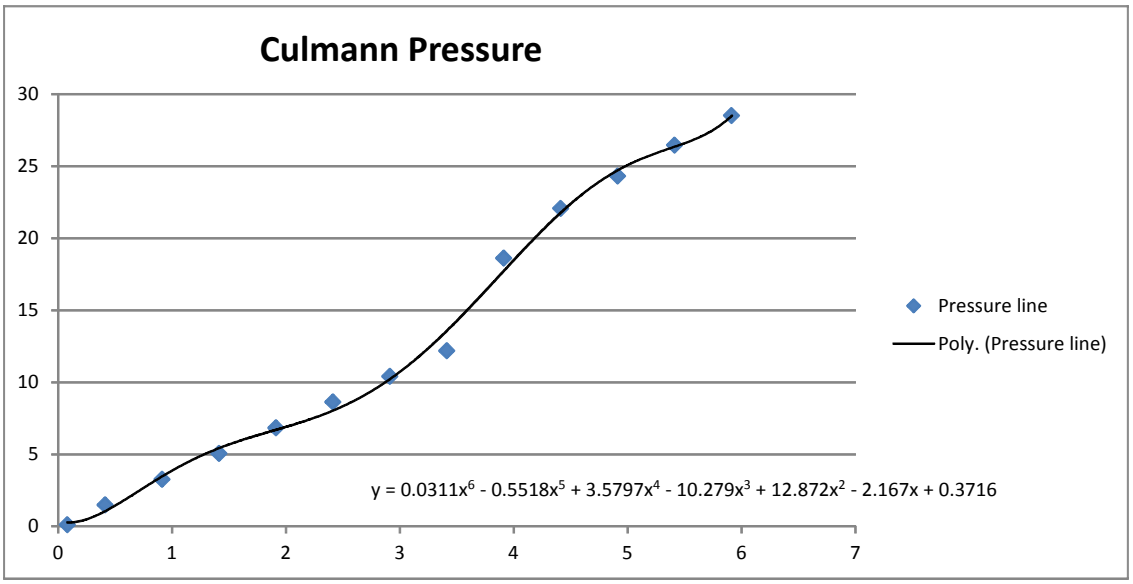

Trend lines using two equations and splitting the profile in two

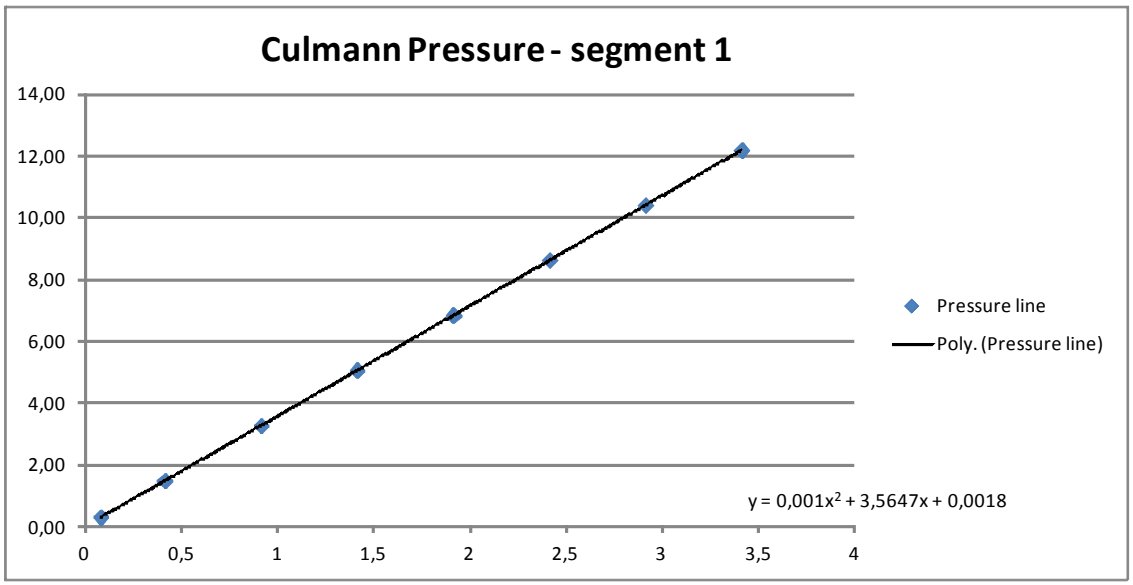

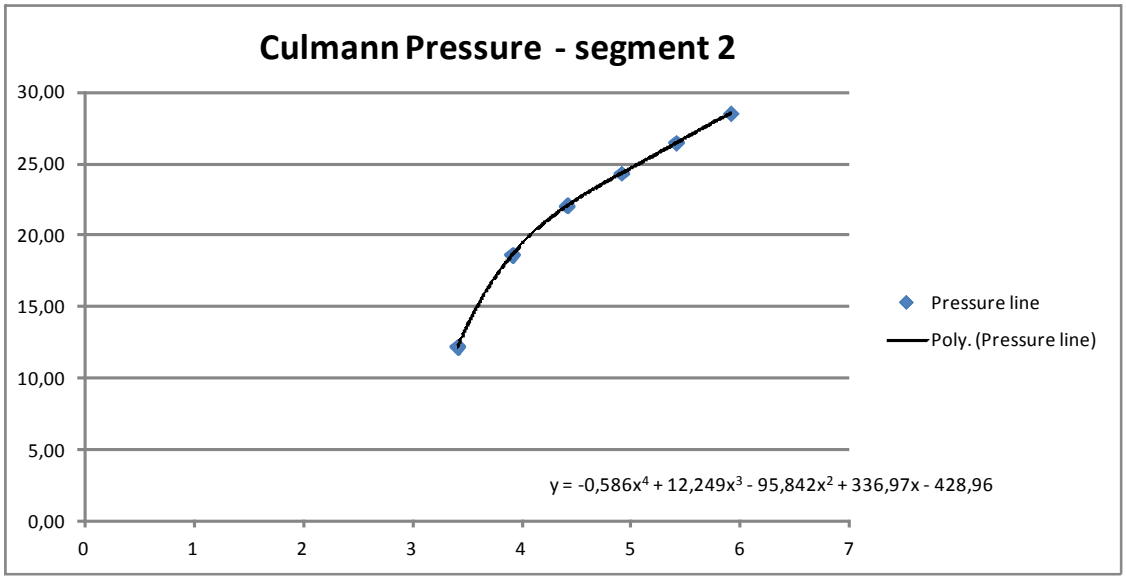

$$z_{plot} := 0, 0.01 .. \frac{H_{wall}}{m}$$

Since the equation for the pressure (F and F.new) is unitless H.wall

is divided by meter

$$F(z_{plot}) := 0.0311 \cdot (z_{plot})^6 - 0.5518 (z_{plot})^5 \ldots + 3.5797 (z_{plot})^4 - 10.279 \cdot (z_{plot})^3 + 12.872 \cdot (z_{plot})^2 - 2.167 (z_{plot}) + 0.3716$$

$$F_{new}(z_{plot}) := \begin{cases} \left(-0.0324 z_{plot}^{\ 2} + 3.7118 \cdot z_{plot}\right) & \text{if } 0 \le z_{plot} \le 3.415 \\ \left(-0.586 \cdot z_{plot}^{\ 4} + 12.249 \cdot z_{plot}^{\ 3} - 95.842 \cdot z_{plot}^{\ 2} + 336.97 \cdot z_{plot} - 428.96\right) & \text{otherwise} \end{cases}$$

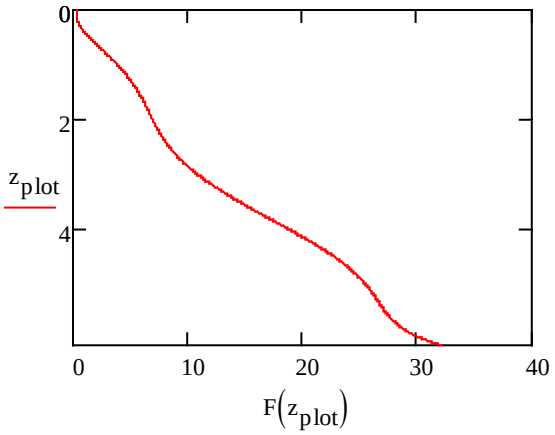

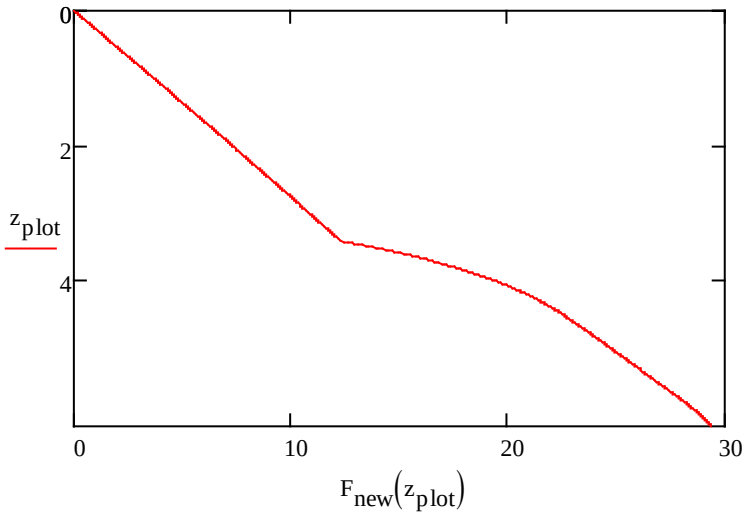

$$P_{tot} := \int_0^{\frac{H_{wall}}{m}} F(z_{plot})\, dz_{plot} = 84.793 \qquad P_{tot2} := \int_0^{\frac{H_{wall}}{m}} F_{new}(z_{plot})\, dz_{plot} = 84.713$$

$$F_0 = 83.917 \frac{1}{m} \cdot kN$$ Error due to trendline

$$x_{cm} := \int_0^{\frac{H_{wall}}{m}} \frac{F(z_{plot}) \cdot z_{plot}}{P_{tot}}\, dz_{plot} = 4.301 \qquad x_{cm3} := \int_0^{\frac{H_{wall}}{m}} \frac{F_{new}(z_{plot}) \cdot z_{plot}}{P_{tot2}}\, dz_{plot} = 4.271$$

x.cm is the center of concentration for the single equation trend line

x.cm2 is for the segmented way of calculating

x.cm3 is from the multi equation trend line

$H_{wall} - x_{cm} \cdot m = 1.864\,m$

$(H_{wall} - x_{cm} \cdot m) - x_{cm2} = -0.023\,m$ Difference between concentration point method

$H_{wall} - x_{cm3} \cdot m = 1.894\,m$

$\frac{H_{wall} \cdot 2}{3 \cdot m} - x_{cm} = -0.191$ Center of mass is 0.191 m below H/3 method

$\frac{H_{wall}}{3} - x_{cm2} = 0.168\,m$ Center of mass is 0.168 m below H/3 method

$\frac{H_{wall} \cdot 2}{3 \cdot m} - x_{cm3} = -0.161$ Center of mass is 0.161 m below H/3 method